Magnetotelluric constraints on lithospheric structures

Dr. Kristina Tietze, Helmholtz Centre Potsdam – German Research Centre for Geosciences (GFZ)

ICTP Workshop on the Lithosphere, 10 October 2024, Trieste

Overview of todays program

9-10.30

Theory

- Electrical conductivity of Earth's materials
- A very short introduction to MT theory

11-12.30

14-15.30

MT workflow

- **MT surveying**: Site setup and data processing
- **MT data**: What do they already tell us?
- **Modelling and Inversion**: How to get from data to an underground image?
- **(Interpretation** of electrical conductivity models)

16-17.30

MT case studies: Constraints on the lithosphere from MT

- Attempt of a review in ~60-90 minutes

What is Magnetotellurics?

Magnetotellurics (MT)?

magnet,
magnetic field

tellus
"concerning Earth"
Electric currents in the Earth

"MT is an electromagnetic **geophysical** method

for inferring the earth's subsurface **electric conductivity**

from measurements of **natural geomagnetic and geoelectric field variation**

at the Earth's **surface**."

Source: Wikipedia

Cagniard 1951, Tikhonov 1950

MT setup

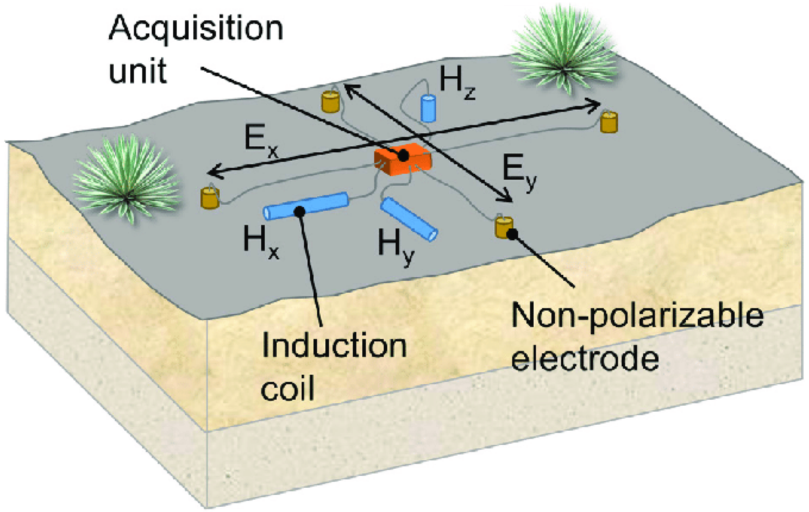

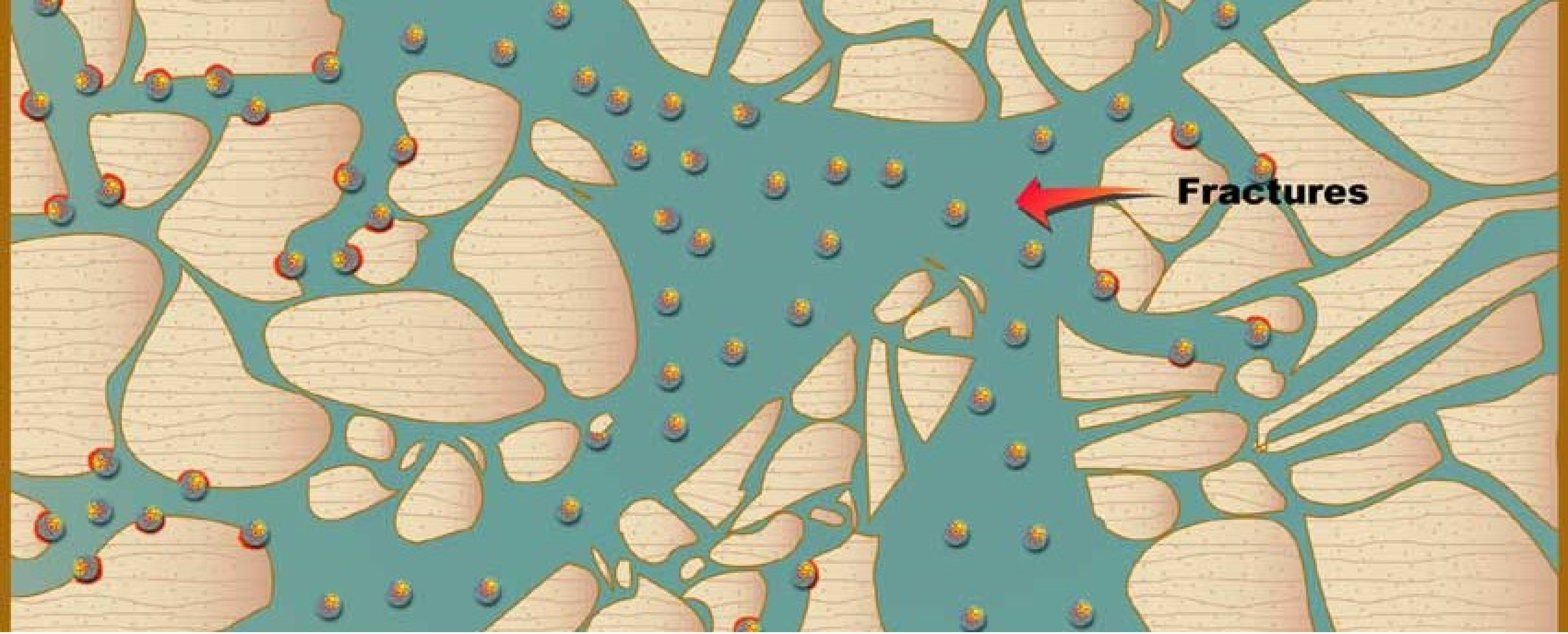

Electrical conductivity of Earth’s materials

What is electrical conductivity and electrical resistivity?

ELECTRICAL CONDUCTIVITY

The electrical **conductivity** describes the degree to which a specified material can transport electrical charges.

Definition of the the electrical conductivity **σ** of a material:

$$j = \sigma \cdot E \quad \textit{(Generalized Ohm's Law)}$$

Electical current density j *[A/m²]*

Electric field strength E *[V/m]*

SI Unit of **σ**: A/(V m) = 1/(Ω m) = **S/m** *„Siemens per metre"*

ELECTRICAL RESISTIVITY

The electric resistivity **ρ** is the inverse of the electrical conductivity **σ**.

$$\rho = 1/\sigma$$

SI Unit of **ρ**: Ω m *„Ohm metre"*

Copper wire

Copper wires

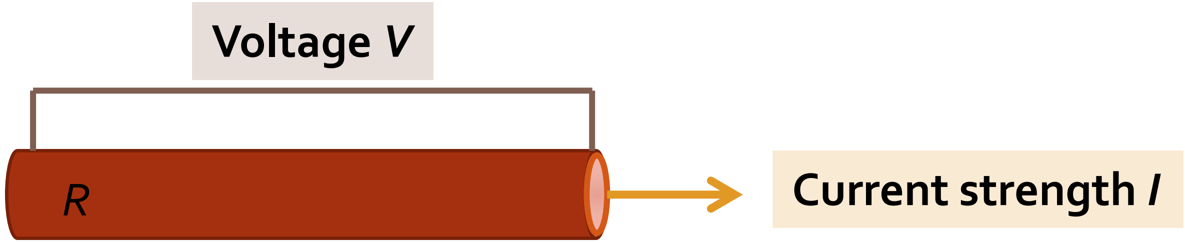

Resistance *R*,
Inverse of conductance S = 1/R
Specific to body material (+ shape)
e.g. copper

If we know the voltage across the copper wire and the current which flows through it, we can calculated the resistance the copper wire.

The result is specific to the material copper.

Ohm’s Law:

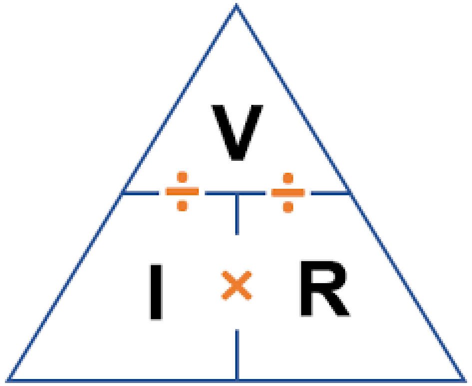

Power cable

Insulated copper cable

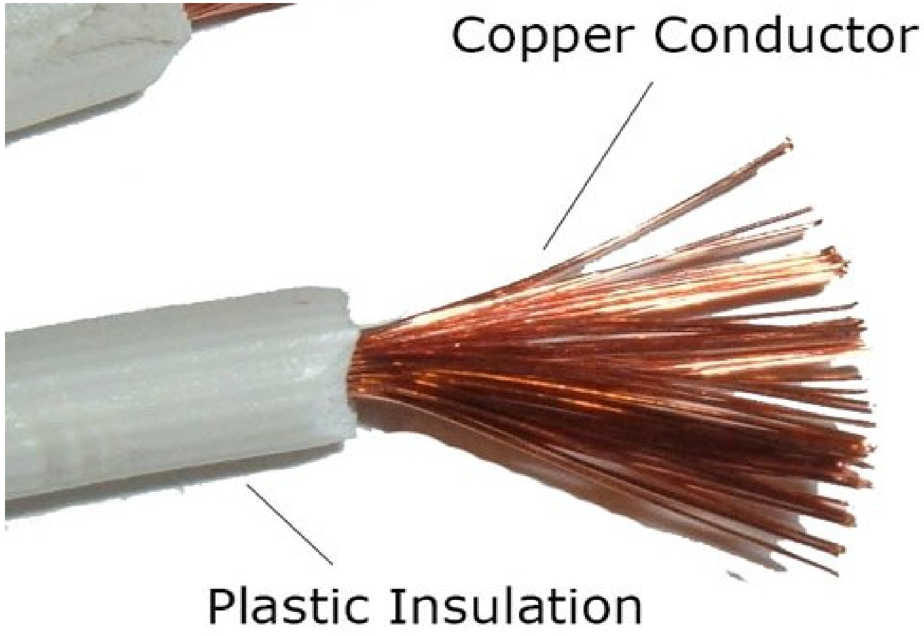

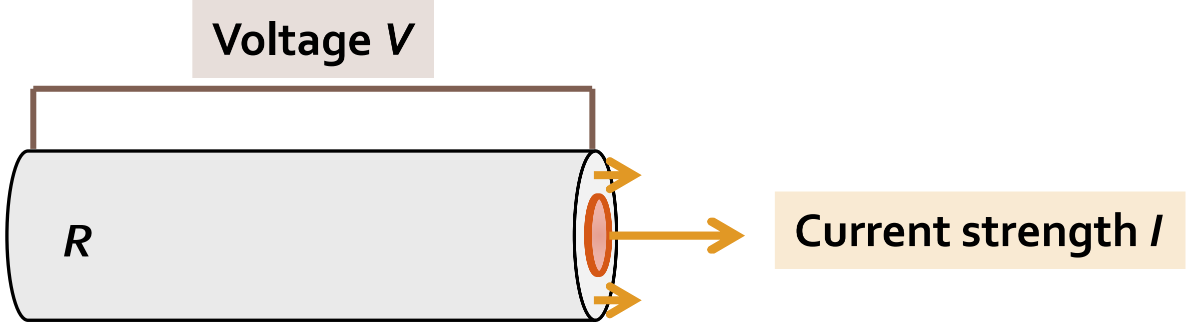

Resistance *R*,
Inverse of conductance S = 1/R
Specific to body material (+ shape)

Ohm's Law:

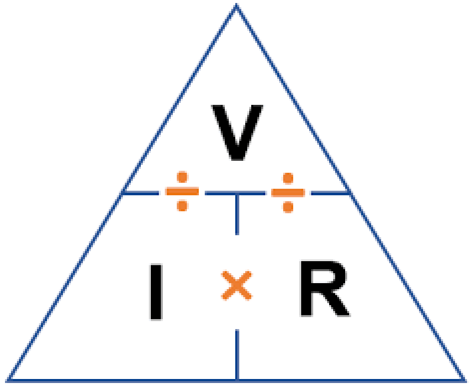

Nearly all current will flow through the copper part of the cable because the copper is much more electrically conductive than the insulation (that's why the insulation works!). Yet, a small fraction of current will flow through the insulation as well.

The resistance of the entire cable depends mainly on the copper, but to a small part also on the resistance of the insulation.

What can we learn from the cable idea?

Electric current flows mainly through the electrically conductive part

- Copper has much higher electrical conductivity than the insulation
- The copper wire is a throughgoing structure, it is not broken, has no gaps, no corrosion etc.

The result of resistance measurements on the wire will be determined mainly by the conductivity of the copper, and to a lesser extent by the conductivity of the insulation. In return, we can learn mainly something about the conductive (copper) part of the material, it is harder to get information on the insulation out of the measurement.

How does this translate to the magnetotelluric world?

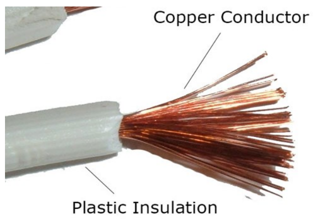

- Electric currents in the Earth flow through electrically conductive material.
- With MT we can image the 3D distribution of electric conductivity in the subsurface

Resistivity / conductivity of Earth’s materials

←
Copper
~ $6 \cdot 10^{-7}$ Ωm

conductive

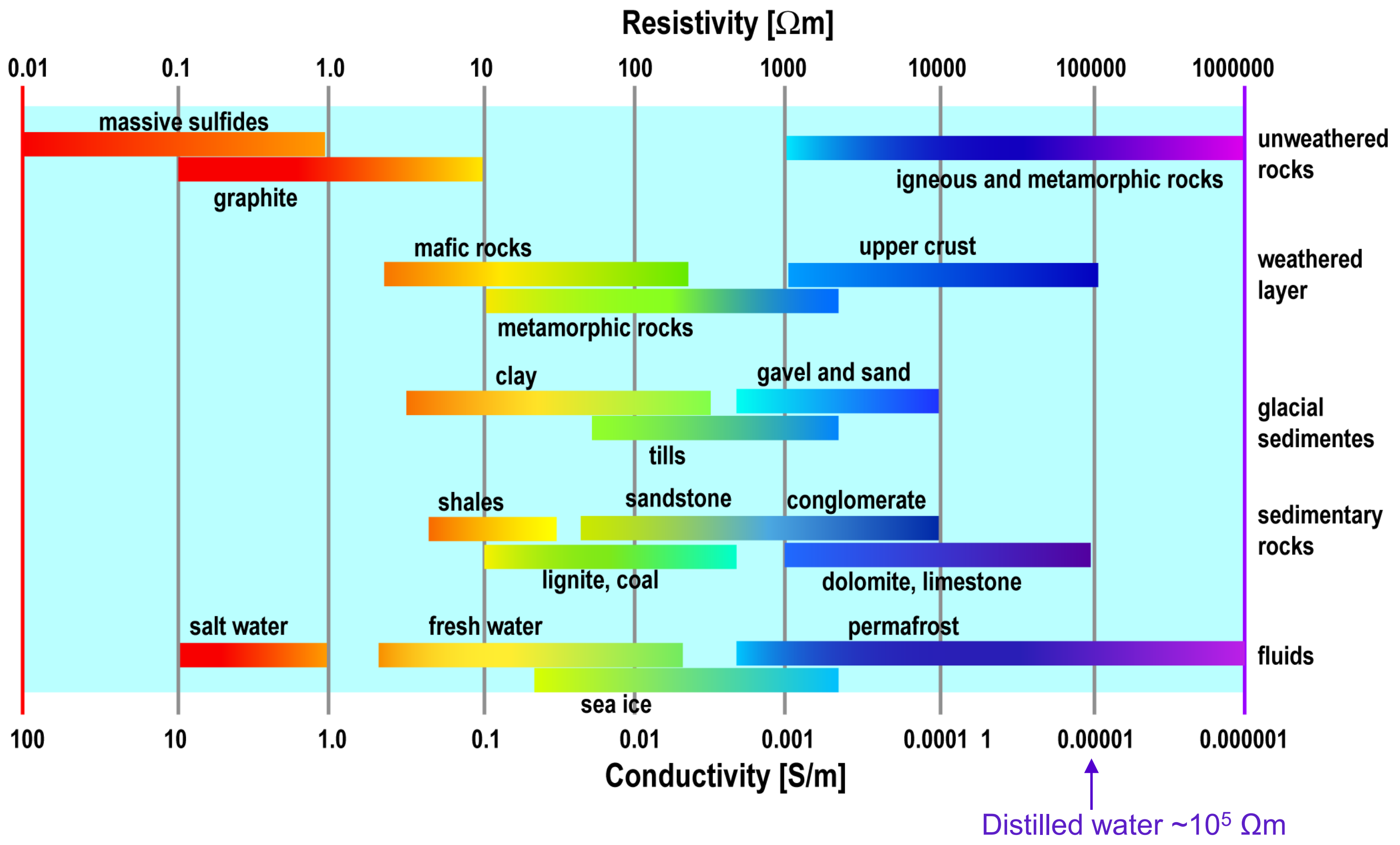

→
Polypropylen (PP)
Polyethylen (PE)
~ 10^8 Ωm

Air ~ 10^9 Ωm

Quartz ~ 10^{17} Ωm

resistive

- Electric conductivity of materials is extremely different spanning numerous decades.
- Electric conductivity of Earth’s materials mostly ranges between 100 and 10^{-6} S/m (resistivity: 0.01 to 10^6 Ωm).

What causes the wide span of conductivities of Earth’s materials?

Simplistic: Earth materials consist of

- **rock matrix** and
  - ➡ very resistive
- **pores / fractures** filled with other material, e.g.
  - fluids (gas, aqueous fluids, …)
  - melts
  - ores
  - graphite
  - sulfide
  - ➡ conductive

Simplified structure of a rock sample

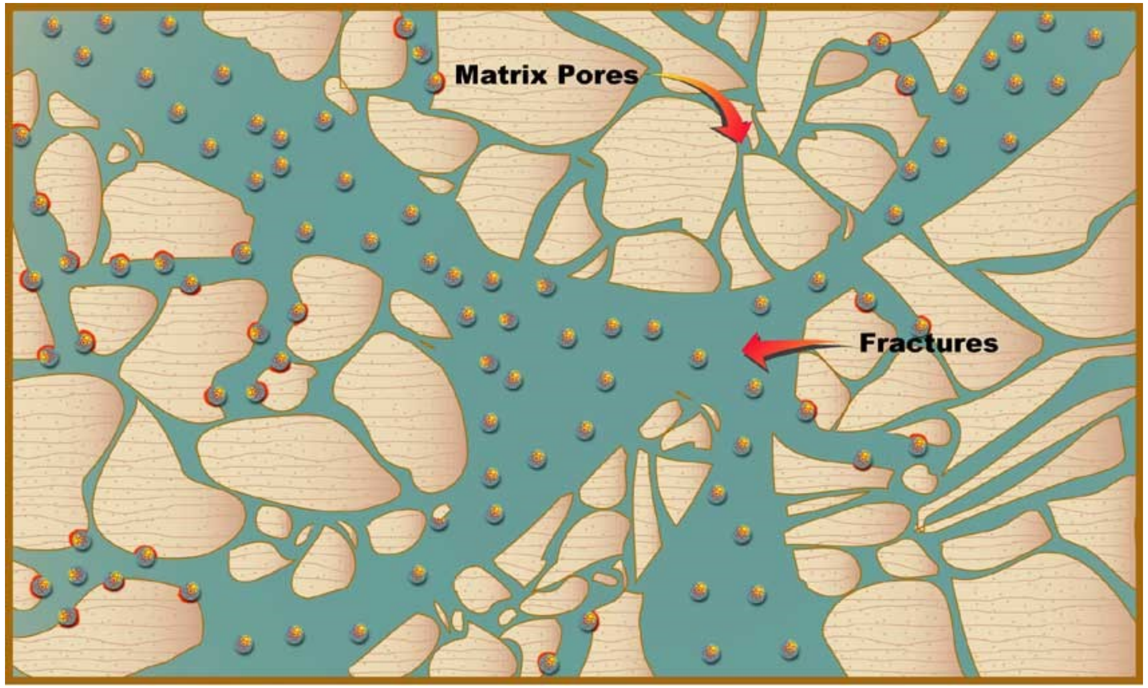

Mixing laws: Archie's Law

Valid for porous, fluid filled rocks

$$\rho_{ROCK} = \rho_{FLUID} \; A \; \phi^{-m}$$

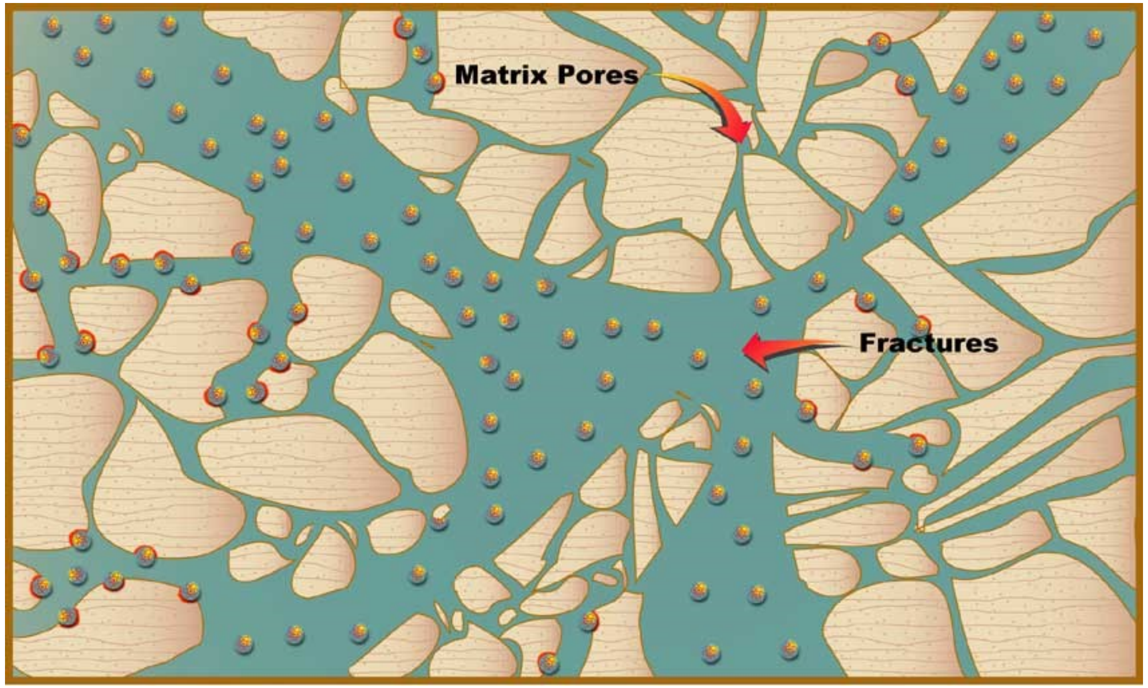

ρ_{rock}	overall resistivity of the rock
ρ_{fluid}	resistivity of the pore fill (e.g. water)
A	fluid saturation (rate of pores which are filled with fluid)
Φ	porosity
m	Geometry factor, determined empirically For most rocks *m* ranges between 1 and 2.

Mixing laws: Archie‘s Law

Valid for porous, fluid filled rocks

$$\rho_{ROCK} = \rho_{FLUID} \; A \; \phi^{-m}$$

ρ_{rock}	overall resistivity of the rock
ρ_{fluid}	resistivity of the pore fill (e.g. water)
A	fluid saturation (rate of pores which are filled with fluid)
Φ	porosity
m	Geometry factor, determined empirically For most rocks *m* ranges between 1 and 2.

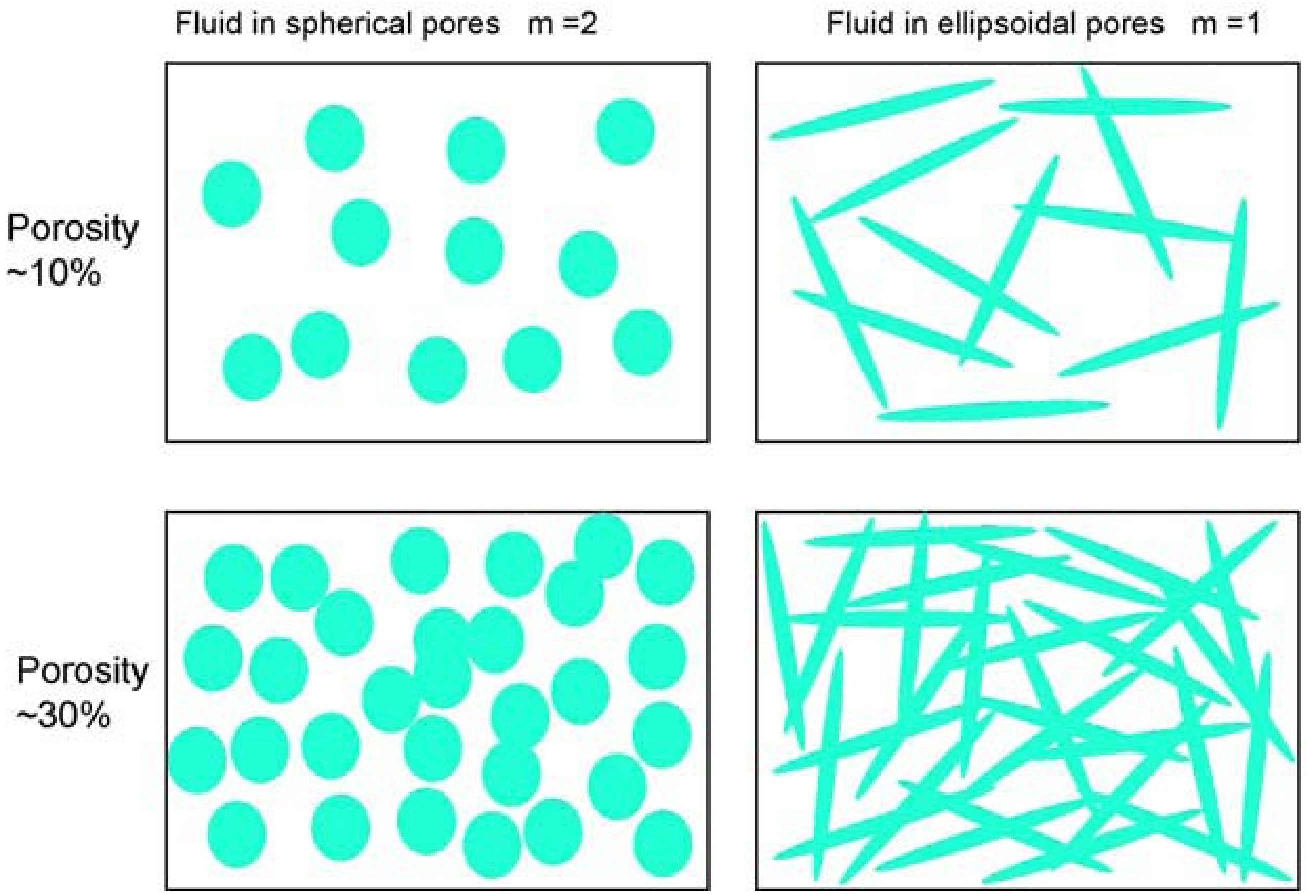

Hands on: Exercise 01 – Archie’s Law

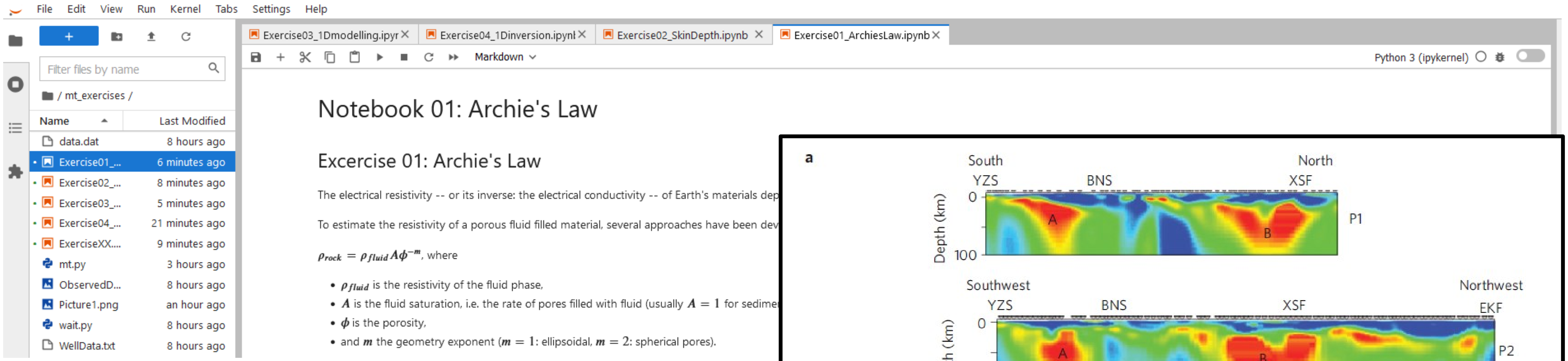

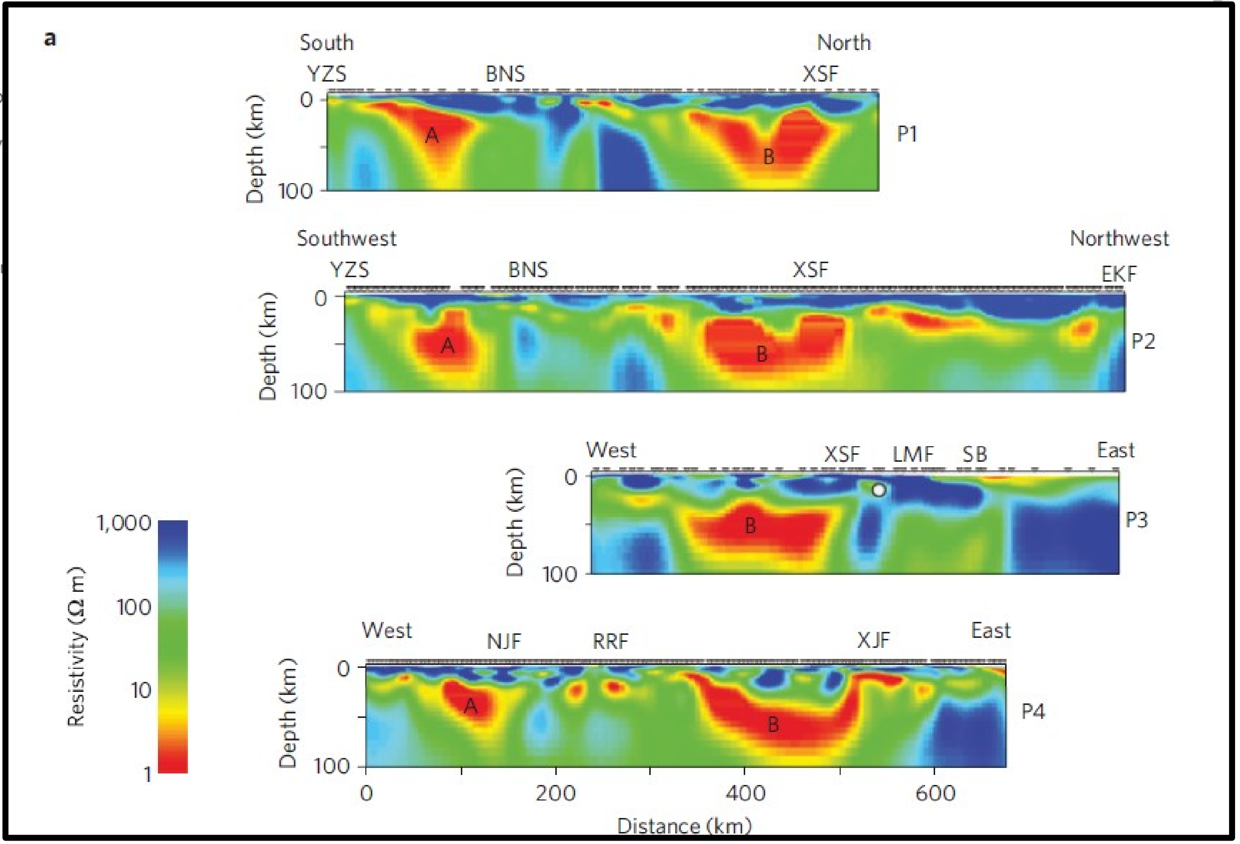

Bai et al. 2010

Zones A and B:

- Bulk resistivity: 1 Ωm
- Let‘s assume a melt resistivity of 0.01 Ωm.
- We also assume that melt is well connected (m=1).
- How much melt do we need? How much porosity?

Archie‘s Law is only valid for pores filled with aqeuous fluids.

Other „mixing laws“ have to be used for e.g.

- Graphite cover (can be highly anisotropic)
- Iron ore, metal sulfides
- (Partial melts)

Hashin-Shtrikman upper and lower bounds

Archie's Law is only valid for pores filled with aqeuous fluids.

Hashin-Shtrikman upper and lower bounds can be used for e.g.

- Graphite cover (can be highly anisotropic)
- Iron ore, metal sulfides
- (Partial melts)

Porosity host rock !

$$\sigma_{HS^+} = \sigma_{II}\left(1 + \frac{3x_I \partial\sigma}{3\sigma_{II} + (1-x_I)\partial\sigma}\right)$$

Conductivity of fill

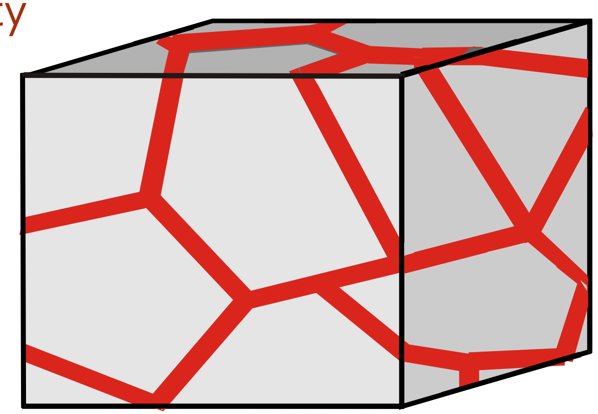

Upper bound

Conductivity difference (between host rock and fill)

$$\sigma_{HS^-} = \sigma_I\left(1 - \frac{3(1-x_I)\partial\sigma}{3\sigma_I - x_I\partial\sigma}\right)$$

Conductivity of host rock !

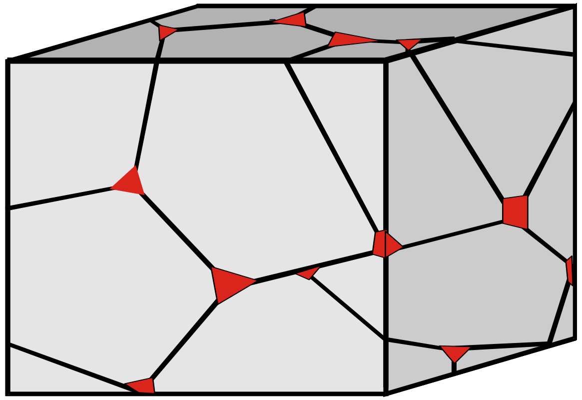

Lower bound

$$\partial\sigma = \sigma_I - \sigma_{II}$$

$$\sigma_{II} >> \sigma_I$$

Hashin & Shtrikman 1962

Hashin-Shtrikman upper and lower bounds

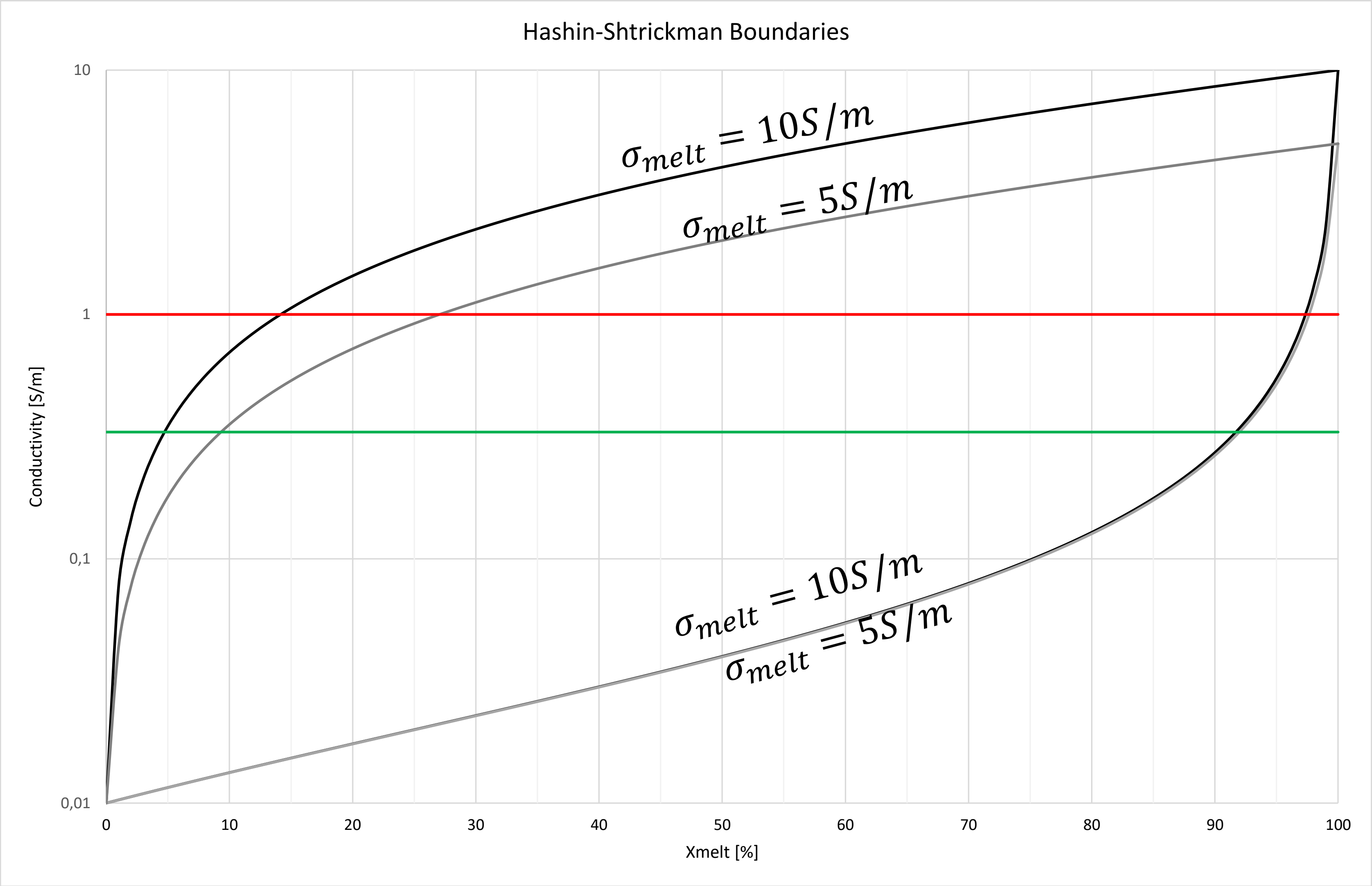

Sensitivity of electrical resistivity and P-wave velocity to gas saturation

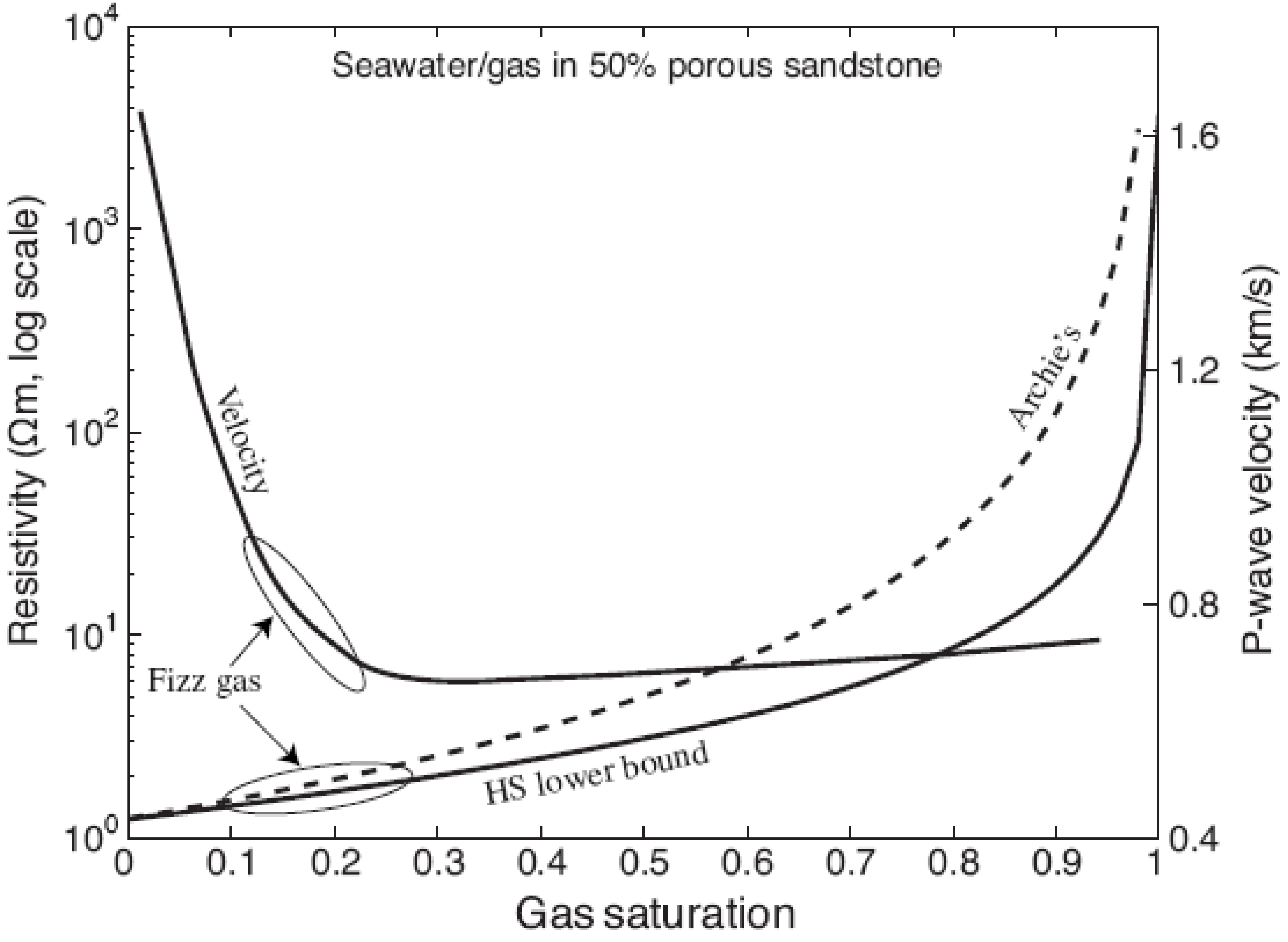

Constable (2010)

Generalized distribution of electrical resistivity in the Earth

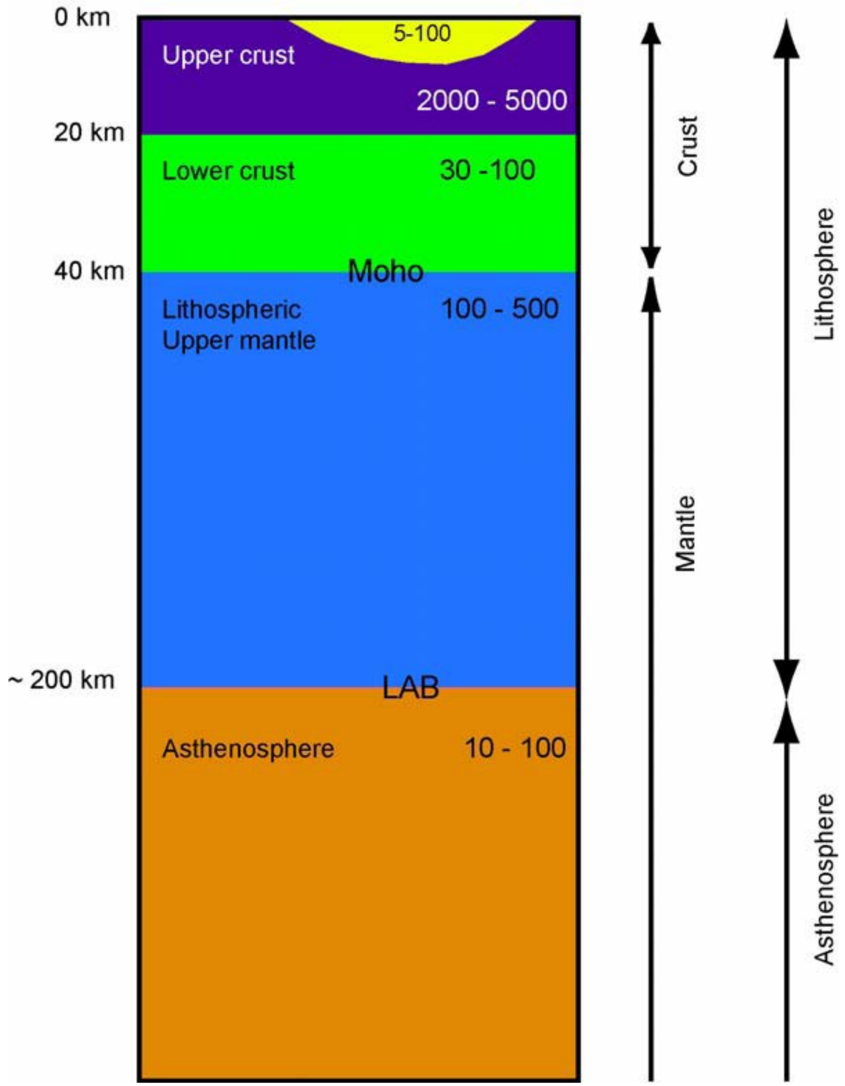

Unsworth, 2015

High spatial variability
broad range

More uniform

Different geologic
settings

Summary

- Electrical conductivity of rocks spans a wide range.
- Electrical resistivity is the inverse of the electric conductivity. Both terms are used regularly, depending of which end of the spectrum we are talking about.
- The rock matrix is usually very resistive.
- Electrical conductivity is mainly determined by the pore / crack fill:
  - Amount of the conductive phase (fluid, ore, graphite, sulphide, clay)
  - Conductivity of the conductive phase
  - Spatial distribution of the conductive phase in the rock
- Factors which increase the conductivity:
  - Increase in pore volume
  - Increase in conductivity of the fluid, e.g. higher salinity
  - Increase in permeability = connectivity of pores
  - Cracks, faults

You get high electrical conductivities (low resistivities) where fluids are and where they were.

A very short story of MT theory

Frequency spectrum of the geomagnetic field

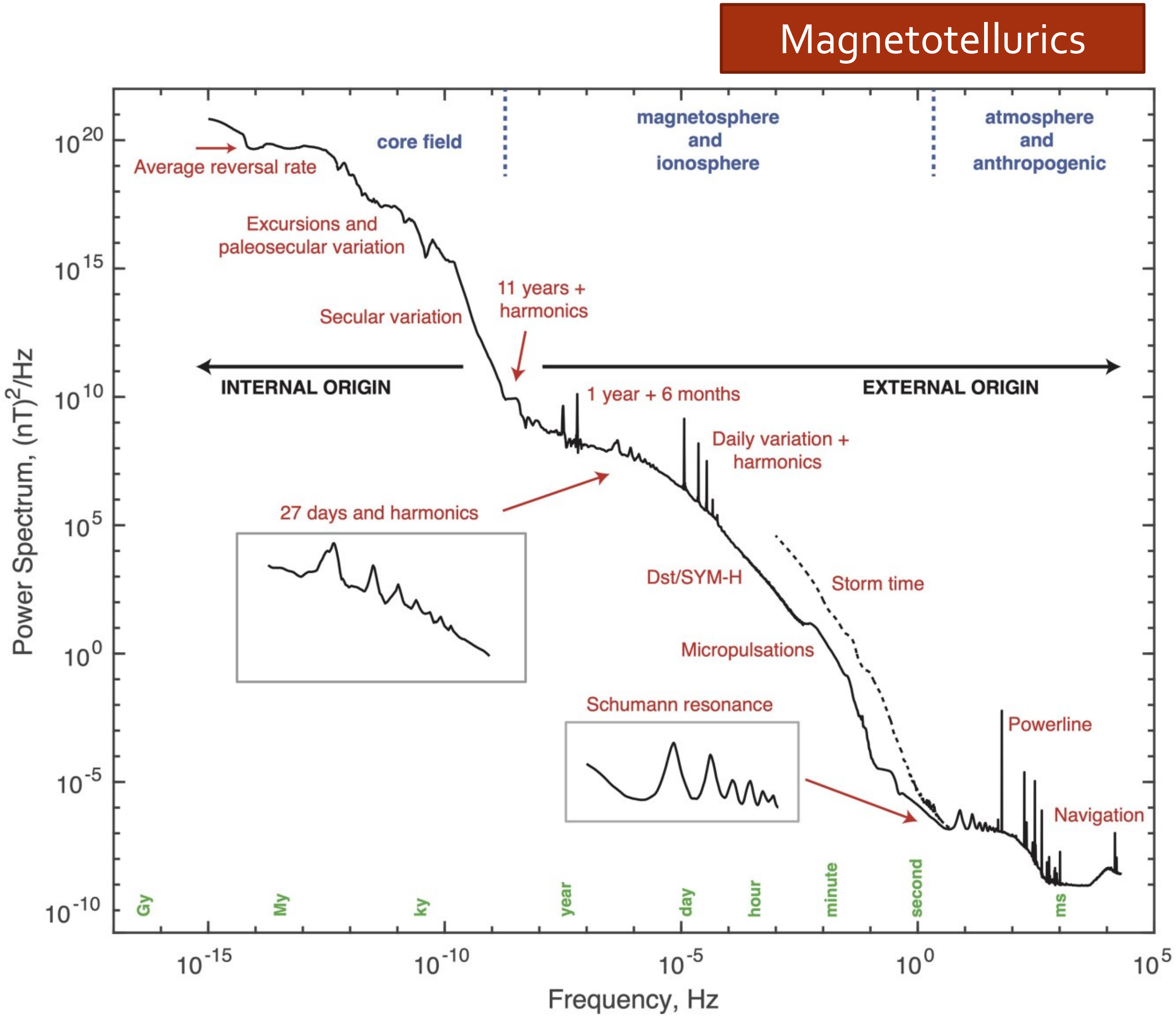

The Grand Spectrum of the geomagnetic field, based on global observations of the geomagnetic dipole at periods greater than one minute and local observations of the horizontal field at shorter periods.

Constable & Constable 2023
A grand spectrum of the geomagnetic field, PEPI

Sources of natural electromagnetic fields

Solar activity

Lightning

Ionospheric current Systems (60 -300 km above the Earth's surface)

Global lightning activity

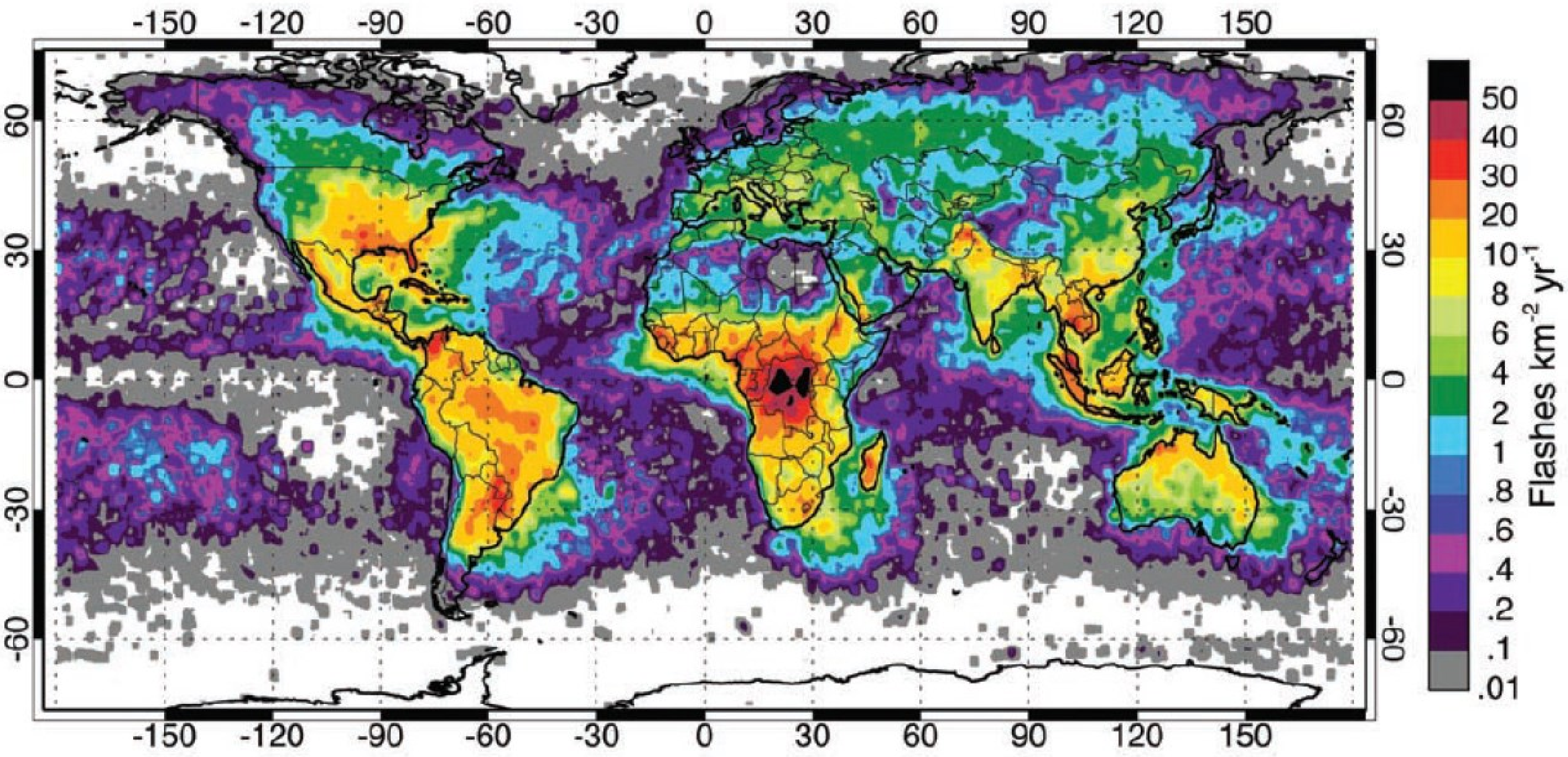

Fig. 2: **Global lightning activity** exhibits a distinct maximum in the Congo basin. Most lightnings in Europe occur over Albania and Italy (Christian (2003)).

The heart of electromagnetic theory: Maxwell's equations (with most simplifications for MT already applied)

Frequency domain: $F \sim e^{i\omega t}$

All MT modelling and interpretation is performed in frequency domain.

$$\nabla \cdot \vec{\mathrm{B}} = 0$$

There is no magnetic "sources", i.e. monopoles in the Earth.

$$\nabla \cdot \vec{\mathrm{E}} = 0$$

There are no free charges, i.e. no electric sources in the surveying domain. *Electric currents of the ionosphere or lightnings are far away. We do not need to know the exact source geometry, currents etc. to solve the MT problem.*

$$\nabla \times \vec{\mathrm{E}} = -\boldsymbol{i\omega}\vec{\mathrm{B}}$$

A time varying magnetic field excites an electric field (dynamo).

$$\nabla \times \vec{\mathrm{B}} = \boldsymbol{i\omega}\mu_0\varepsilon_0\vec{E} + \mu_0\vec{\mathrm{J}}$$

A time varying electric field excites a magnetic field, e.g. around a wire with current. That's how electromagnets work.

Ohm's law $$\vec{J} = \sigma\vec{E} = \frac{1}{\rho}\vec{E}$$

Some Considerations on (4)

Frequencies normally considered for the magnetotelluric method are $< 10^5 Hz$, so some more simplifications can be made:

μ_r: relative permeability

ε_r: relative permittivity

(4) $\nabla \times \vec{B} = i\omega\mu_0\varepsilon_0\vec{E} + \mu_0\vec{J}$ correctly: $\nabla \times \vec{B} = i\omega\mu_0\mu_r\varepsilon_0\varepsilon_r\vec{E} + \mu_0\vec{J}$

- BUT: For most Earth's materials and frequencies < 10^5 Hz μ_r and ε_r are ~1 and can be neglected.

- The term $\varepsilon_0\vec{E}$ << $\vec{J}$

wave part
Radar (GPR)
~ seismics

diffusion of electric currents
e.g. MT

- All we need is: (4) $\nabla \times \vec{B} = \mu_0\vec{J}$

The heart of electromagnetic theory: Maxwell's equations (with all simplifications for MT already applied)

Frequency domain: $F \sim e^{i\omega t}$

$$\nabla \times \vec{\mathrm{E}} = -i\omega\vec{\mathrm{B}}$$

$$\nabla \times \vec{\mathrm{B}} = \mu_0\vec{\mathrm{J}} \quad = \mu_0\sigma\vec{E}$$

$$\nabla \cdot \vec{\mathrm{B}} = 0$$

$$\nabla \cdot \vec{\mathrm{E}} = 0$$

Ohm's law $\vec{J} = \sigma\vec{E} = \frac{1}{\rho}\vec{E}$

- Only terms of the electric and magnetic fields $(\vec{E}, \vec{B})$.
- Left hand sides describe spatial variation of the fields
- Right hand sides describe time dependence.
- σ appears in the equations.

Do some algebra to solve the equations...

The skin depth (sounding depth)

A very useful result solving the MT problem:

$$p = \sqrt{\frac{2}{\omega\mu_0\sigma}} \approx \frac{1}{2}\sqrt{\rho T}\ [km]$$

ρ: electric resistivity $[\Omega m]$

T: period [s]

The skin depth is used as a rule of thumb to estimate the sounding depth of an electromagnetic field into the subsurface. Strictly speaking, it is only valid for a homogeneous half-space.

This formula is very useful (worthwhile to ~~know by heart~~ write down for today).

The skin depth (sounding depth)

$$p = \sqrt{\frac{2}{\omega\mu_0\sigma}} \approx \frac{1}{2}\sqrt{\rho T}\ [km]$$

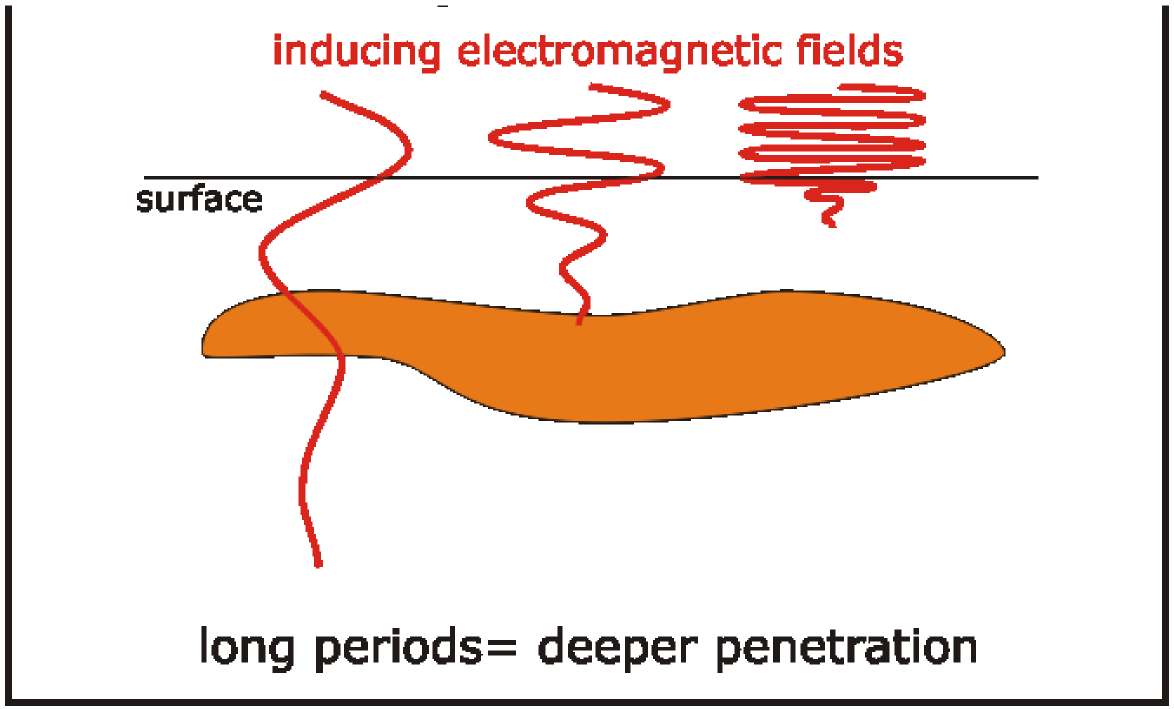

The sounding depth depends on the subsurface conductivity and the period contents of the induced fields (skin effect).

The „true“ conductivity distribution of the subsurface is found by modelling.

Hands on: Python exercise 02 – The skin depth

Excercise 02: The skin depth

The skin depth is the distance at which the electromagnetic field has decayed to 1/e (~33 %) of it's initial value at surface. The skin depth is often used as a rule of thumb to estimate the approximate sounding depth of a given period. In fact, it is actually a rough number of the relevant subsurface volume, i.e. a half sphere with the radius of the skin depth.

The skin depth is calculated from the **resistivity of the underground** ρ and the **period length of the MT signal** T in the following way:

$$p = 0.5\sqrt{\rho * T}$$

Here is the code:

```
rho = 100 # resistivity of the subsurface in Ohm*m
T = 10 # period length of the MT signal in seconds

# ---- calculate skin depth, round to 2 decimals and display result: ----- #
#------ DO NOT EDIT BELOW ------#
import numpy as np
p = 0.5*np.sqrt(rho*T) # skin depth in km
p = np.round(p, 2)
print(f"The skin depth for a resistivity of {rho} Ohmm and a period length of {T} s is: \n{p} km.")
```

```
The skin depth for a resistivity of 100 Ohmm and a period length of 10 s is:
15.81 km.
```

Now it is your task:

Modify the resistivity and period length in the code box above and complete *one column* of the following table:

	$\rho = 1\Omega m$	$\rho = 10\Omega m$	$\rho = 100\Omega m$	$\rho = 300\Omega m$	$\rho = 1000\Omega m$
$T = 0.01s$					
$T = 0.1s$					
$T = 1s$					
$T = 10s$					
$T = 10,000s$					

MT and other electromagnetic methods

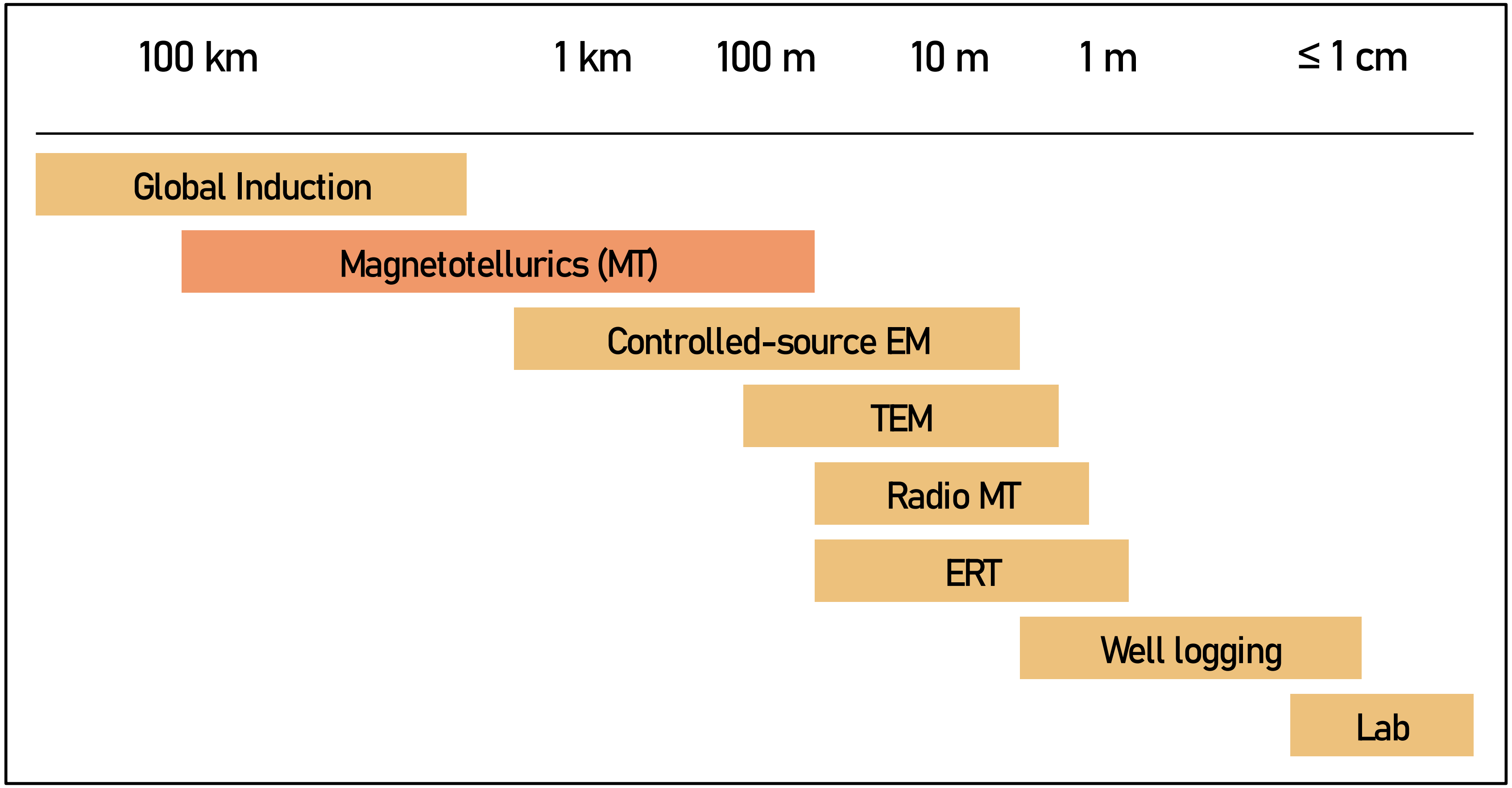

TEM Time-domain EM, e.g. Lotem
ERT Electrical resistivity tomography

Summary

- Sources of MT signals are natural. Major source are currents in the ionosphere and global lightning.
- Maxwell’s equations describe the relation between magnetic & electric fields and the electric conductivity of Earth.
- Sounding depth (skin depth) depends on the period length of the MT signal:

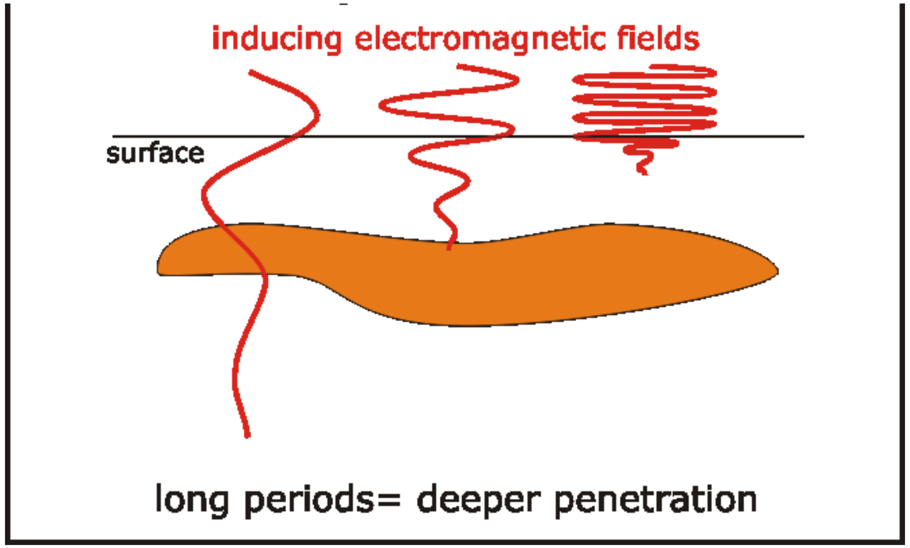

$$p = \sqrt{\frac{2}{\omega\mu_0\sigma}} \approx \frac{1}{2}\sqrt{\rho T}\ [km]$$

Literature: Good overviews of the Magnetotelluric Method (books)

- Chave, A., Jones, A., The Magnetotelluric Method: Theory and Practice, 1st Edition, Cambridge University Press, 2012.
- Nabighian, M.N., Electromagnetic Methods in Applied Geophysics, Society of Exploration Geophysicists, Volume 1 & 2, 1987.
- Berdichevsky, M.N., Dmitriev, V. I., Models and Methods of Magnetotellurics, Springer, 2008.
- Telford, W.M., Geldart, L.P. & Sheriff, R.E., Applied Geophysics, 2nd edition, Cambridge University Press, 1990.
- Simpson, F., Bahr, K., Practical Magnetotellurics, University Press, Cambridge, 2005.

MT field work and data processing

Wanted: Remote areas without EM noise

Setup of an MT site

Electric and magnetic field sensors are usually aligned parallel and perpendicular to the static geomagnetic main field (**declination!**).

MT coordinate system

X mag. North

Y mag. East

Z Downwards

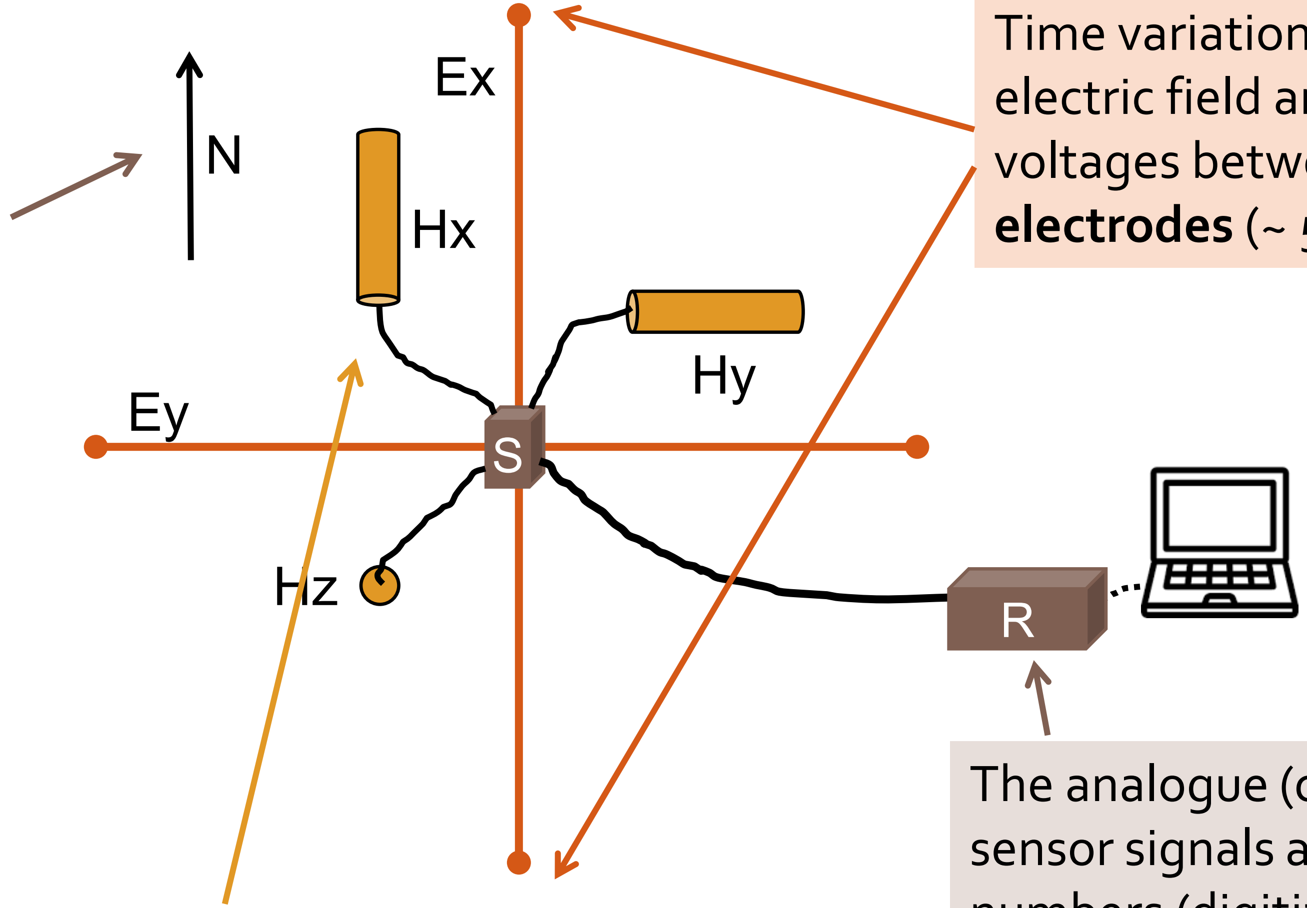

Time variations of the electric field are measured as voltages between pairs of **electrodes** (~ 50 m distance).

The analogue (continuous) sensor signals are converted to numbers (digitized) and stored on computer hard disk.

S Sensor box **R** Recorder

Induction coils can measure magnetic field variations in the range 1000(0)Hz – 0.001Hz.

Electrodes, type Ag-AgCl

Installation of induction coils (magnetic field sensors)

Induction coil magnetometers measure **time variations of the magnetic field**.

Recording data...

View of complete MT site

Some notes on resources

Set-up time per site	~ 1-3 h with 2 people
MT sites per survey	20-200 sites
Site distances	depends on target
Most critical factor	time to access site

Typical surveys require 6-8 people for several weeks.

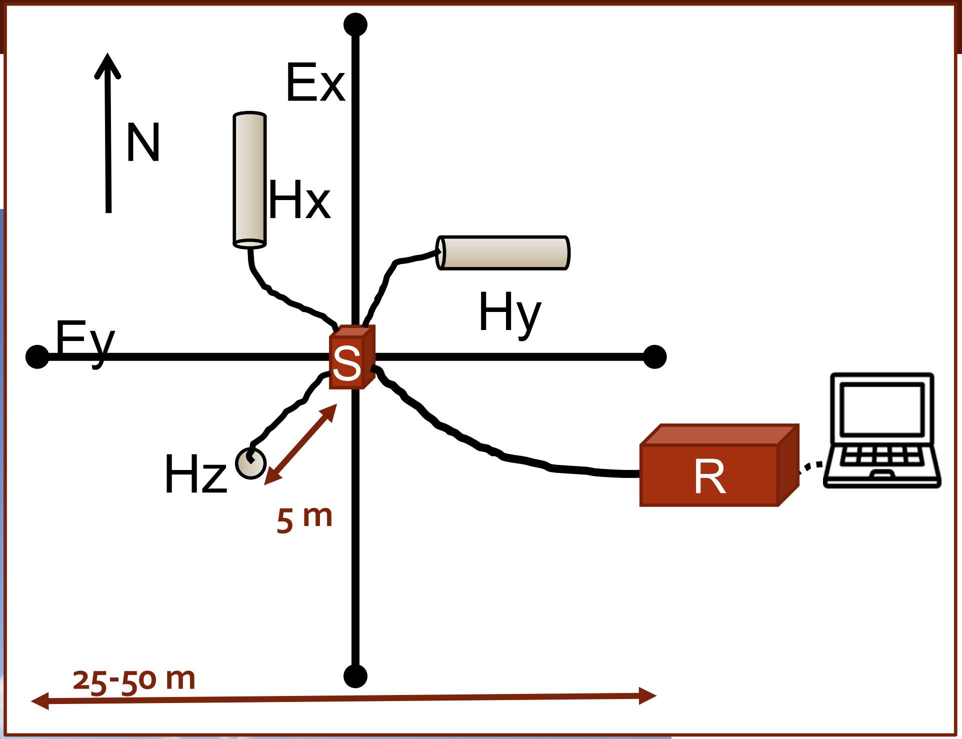

Time series example

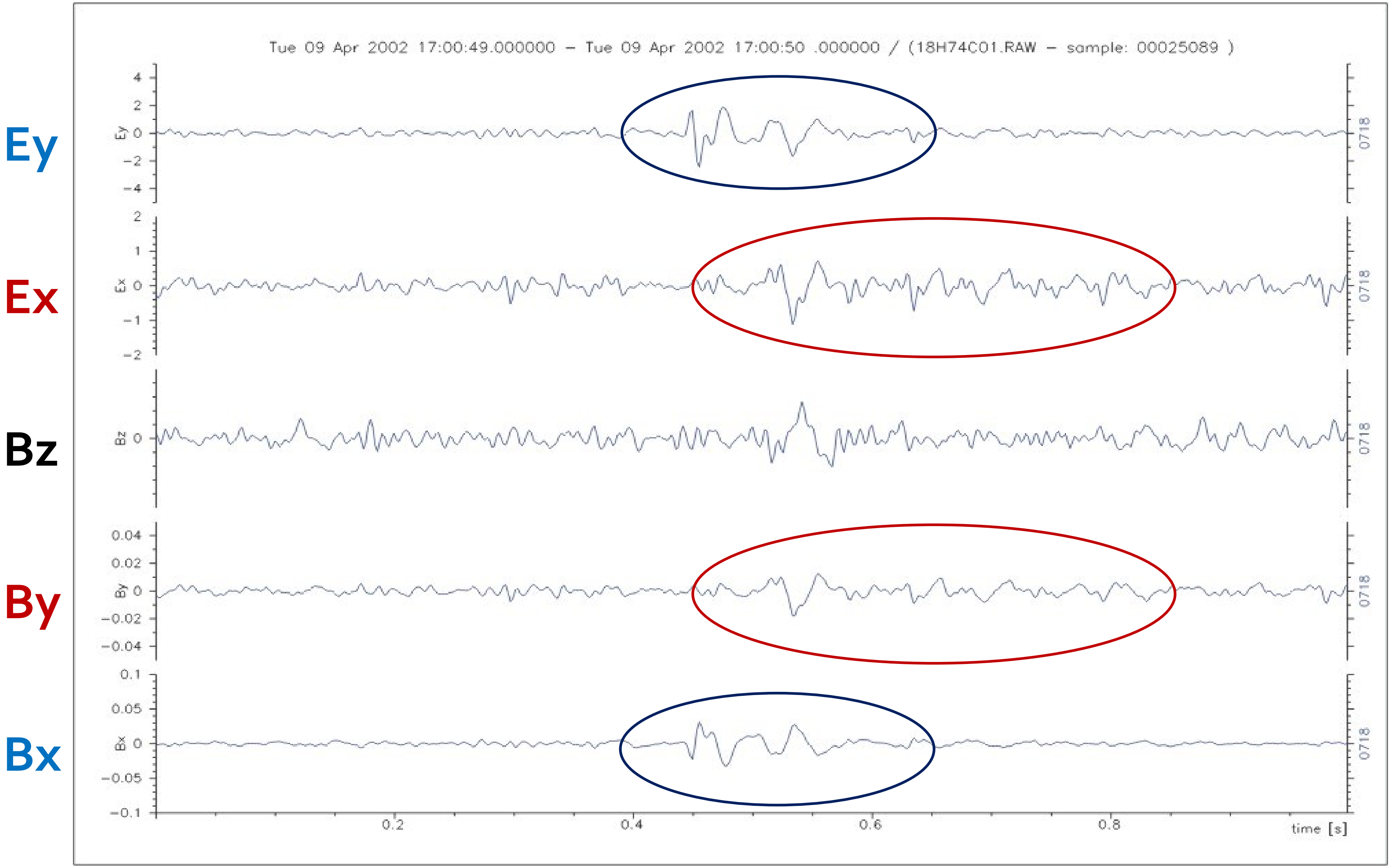

MT data processing (simplified)

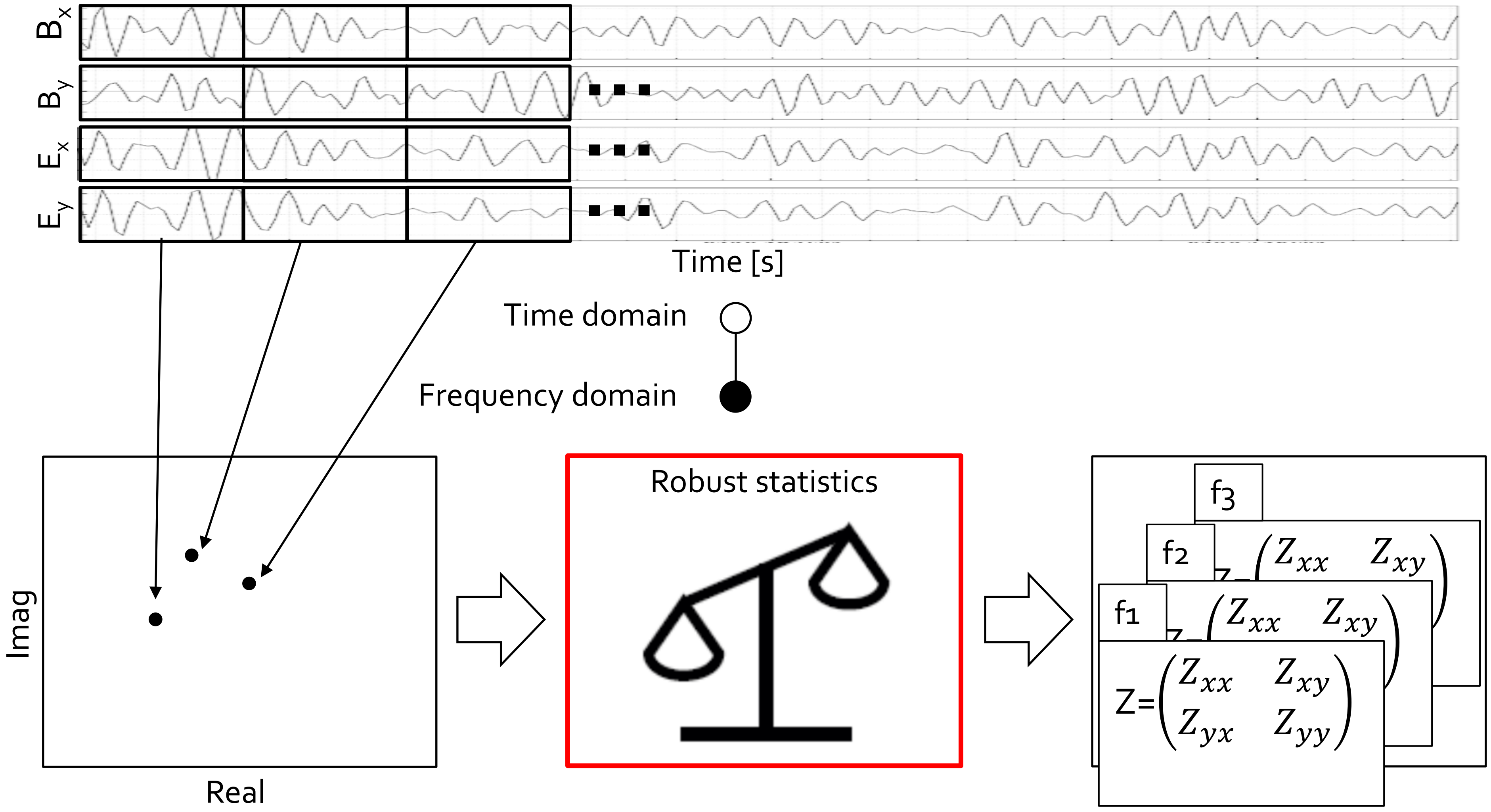

MT transfer functions

Impedance: Z

$$\begin{pmatrix} E_x \\ E_y \end{pmatrix} = \begin{pmatrix} Z_{xx} & Z_{xy} \\ Z_{yx} & Z_{yy} \end{pmatrix} \begin{pmatrix} B_x \\ B_y \end{pmatrix}$$

Z and T depend on conductivity and period.

Vertical magnetic transfer function: T**

$$B_z = \begin{pmatrix} T_x & T_y \end{pmatrix} \begin{pmatrix} B_x \\ B_y \end{pmatrix}$$

The impedance *Z* is usually displayed as apparent resistivity (~ magnitude of Z)

$$\rho_{a,ij} = \frac{\mu_0}{\omega} |Z_{ij}|^2$$

and phase vs. period (~ phase of Z)

$$\phi_{ij} = \arctan \frac{Y_{ij}}{X_{ij}}$$

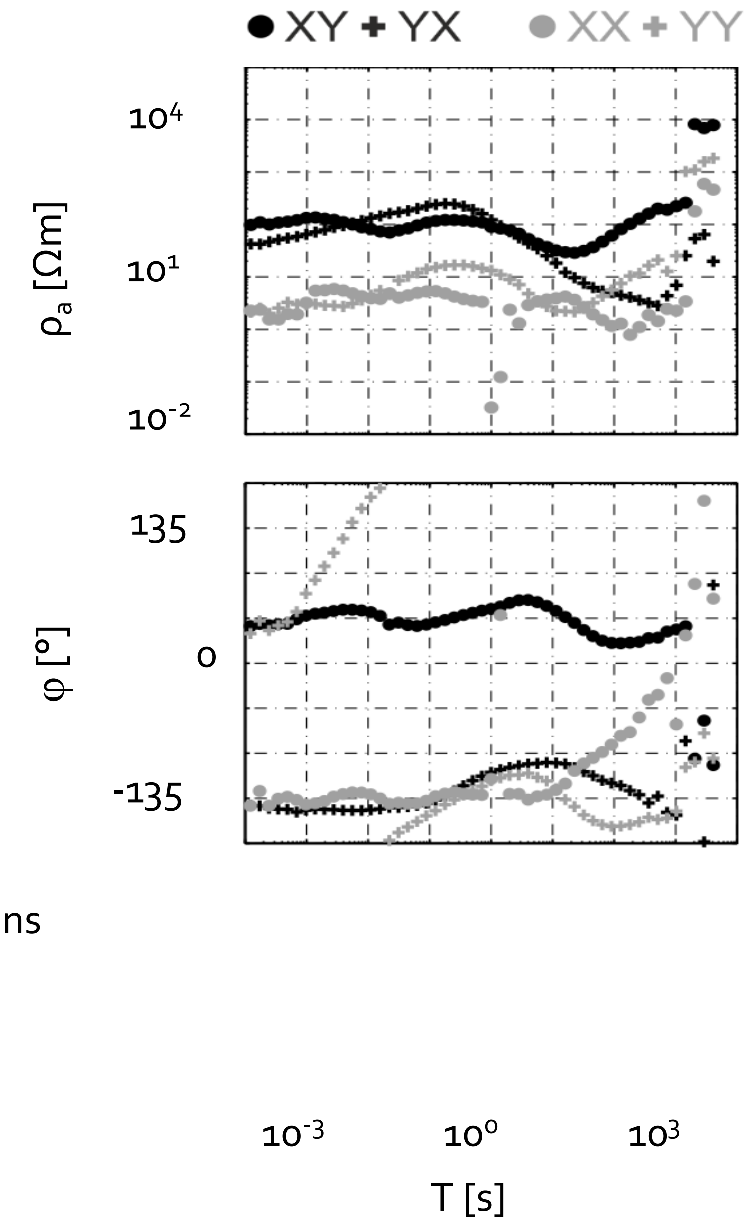

Vertical magnetic transfer functions are often displayed as arrows

*** In a strict sense, vertical magnetic transfer functions do not belong to classic MT which considers only the horizontal magnetic and electric fields, but is a method of its own referred to as Geomagnetic Depth Sounding (GDS).*
But in most MT campaigns, Bz is measured as well and T is be used.

Principle of magnetotelluric sounding

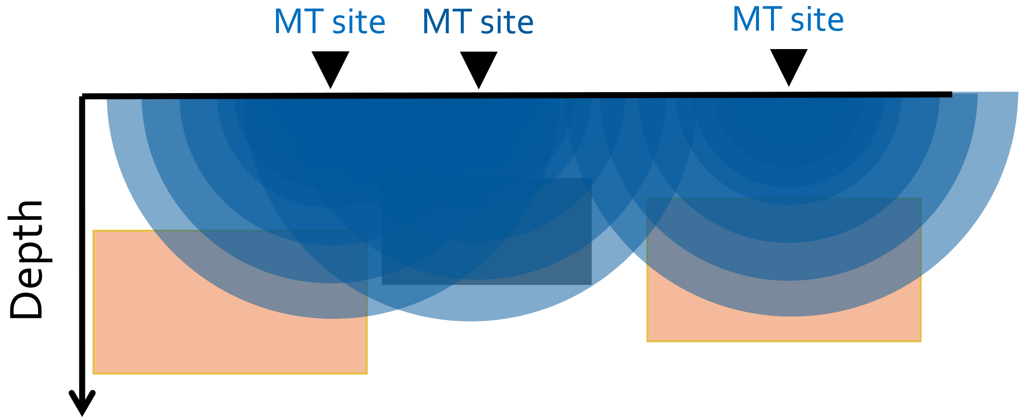

Electric field

Magnetic field

$$\mathbf{E}(\omega) = \underline{\mathbf{Z}}(\omega) \cdot \mathbf{B}(\omega)$$

Impedance

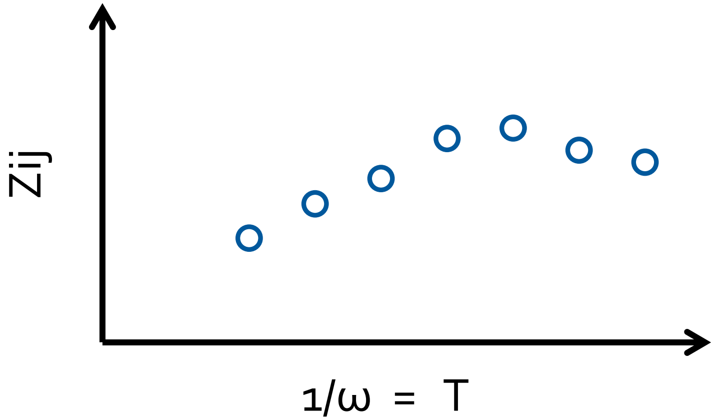

Impedance tensor

$$\underline{\mathbf{Z}} = \begin{pmatrix} Z_{xx} & Z_{xy} \\ Z_{yx} & Z_{yy} \end{pmatrix}$$

Skin depth

$$p = \sqrt{\frac{2}{\omega \mu_0 \sigma}} \approx \frac{1}{2}\sqrt{\rho T}\ [km]$$

Sources of man-made electromagnetic noise

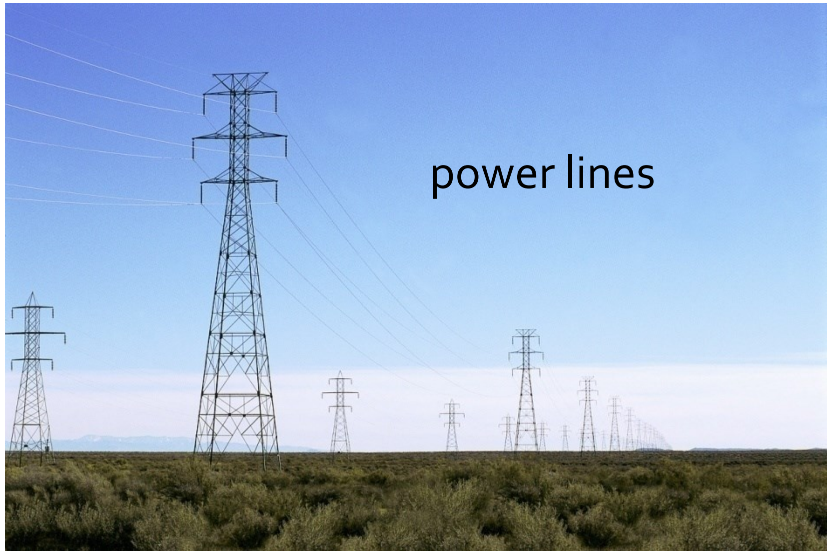

Sources of man-made electromagnetic noise

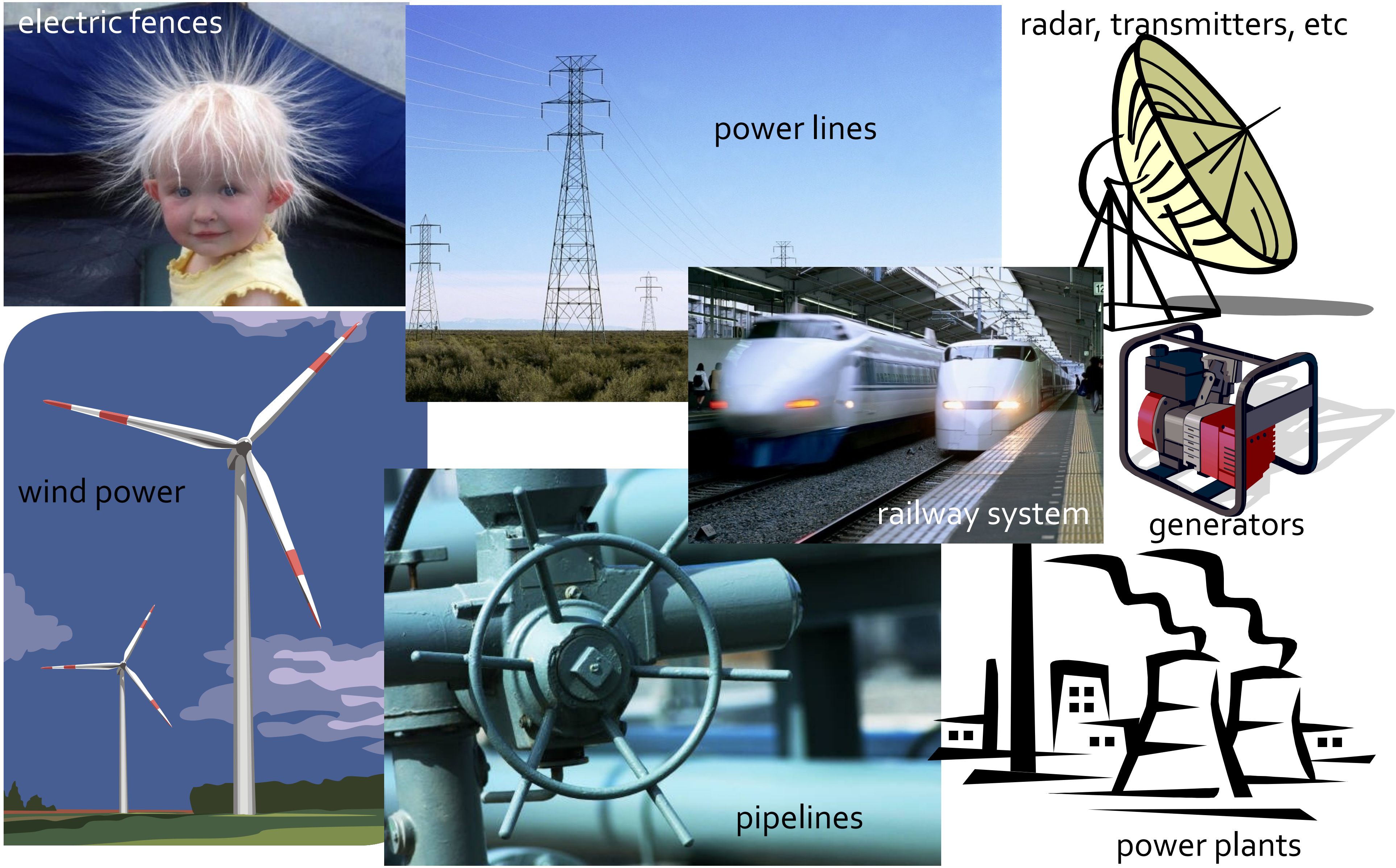

Advanced processing features – there is ways to get rid of (most of) the noise!

Robust statistics

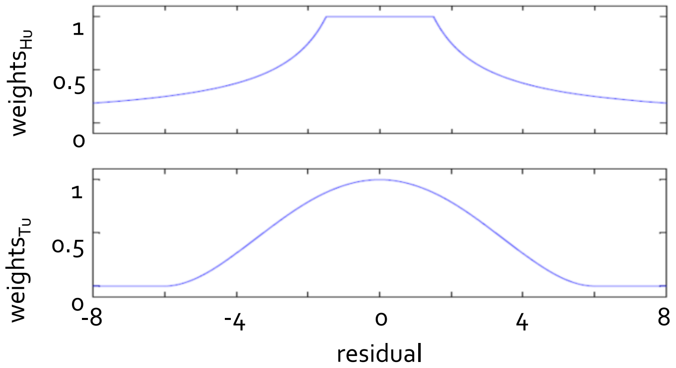

Remote reference processing

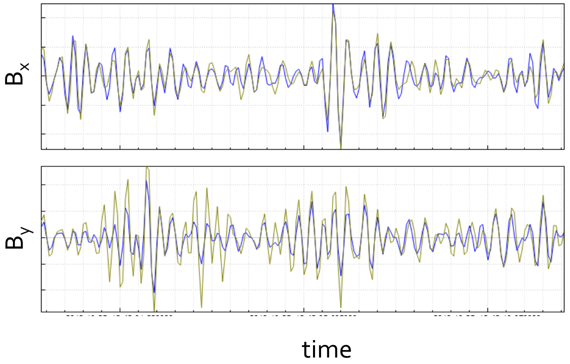

Preselection criteria

- Coherence
- Mahalanobis distance
- Magnetic polarisation
- …

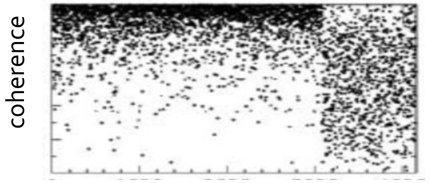

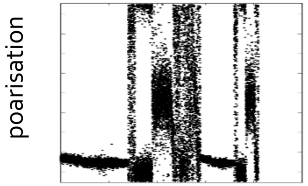

Time-domain filter for noise removal

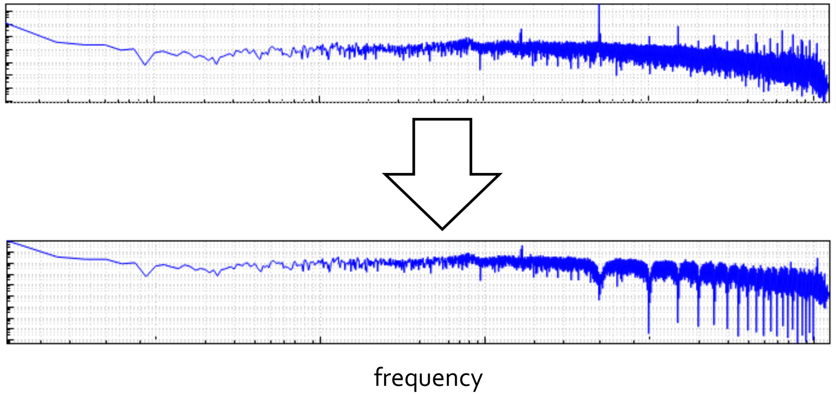

Transfer functions from a densely populated area in Germany

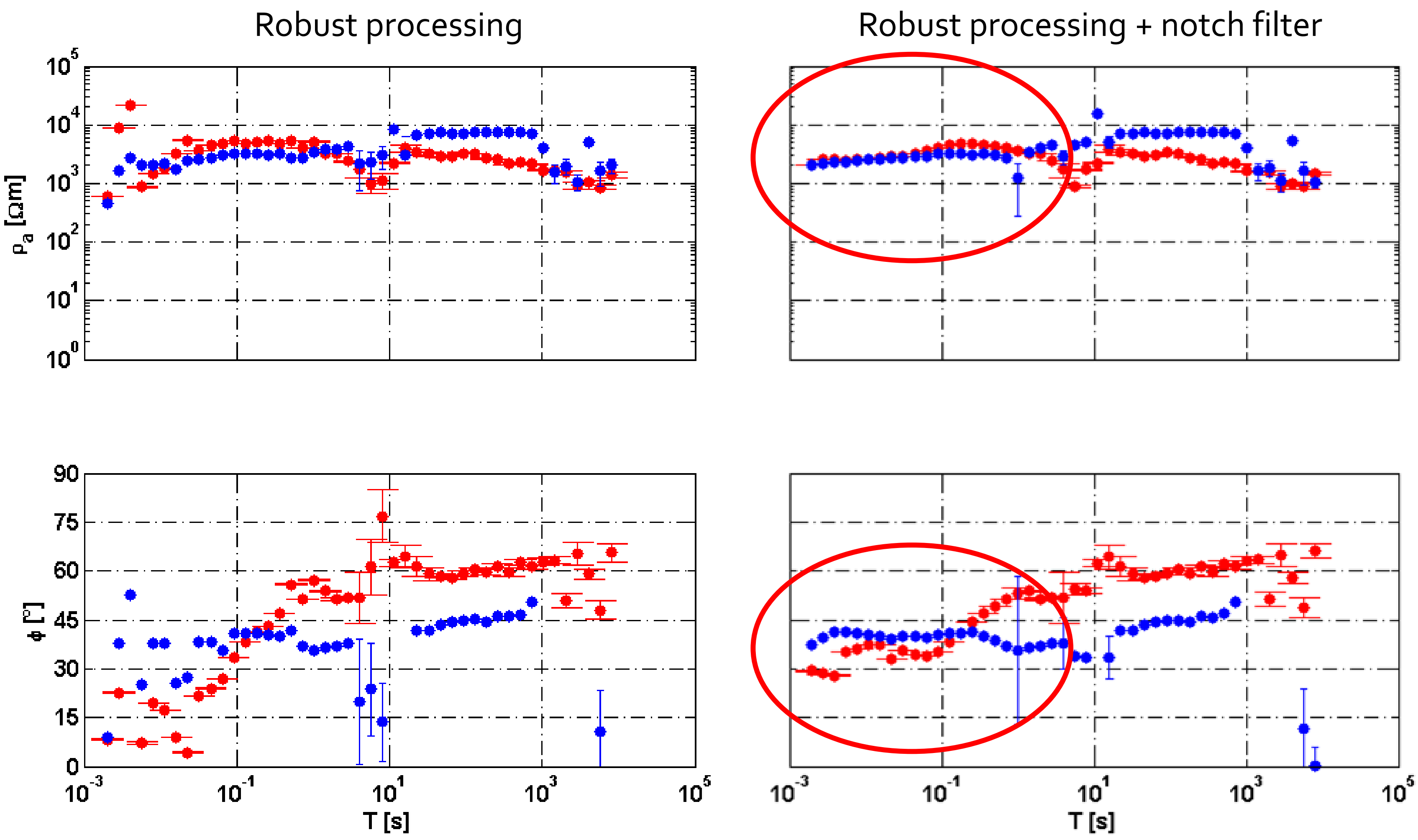

Surveying in industrialised, populated areas is viable.

Summary

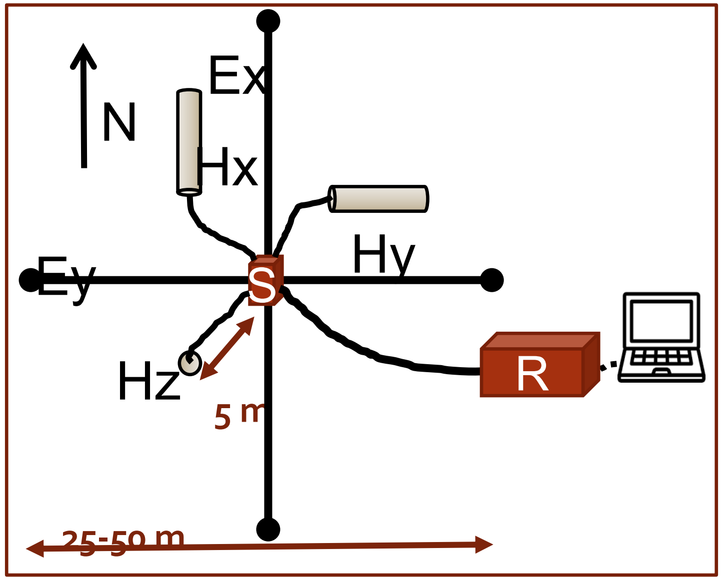

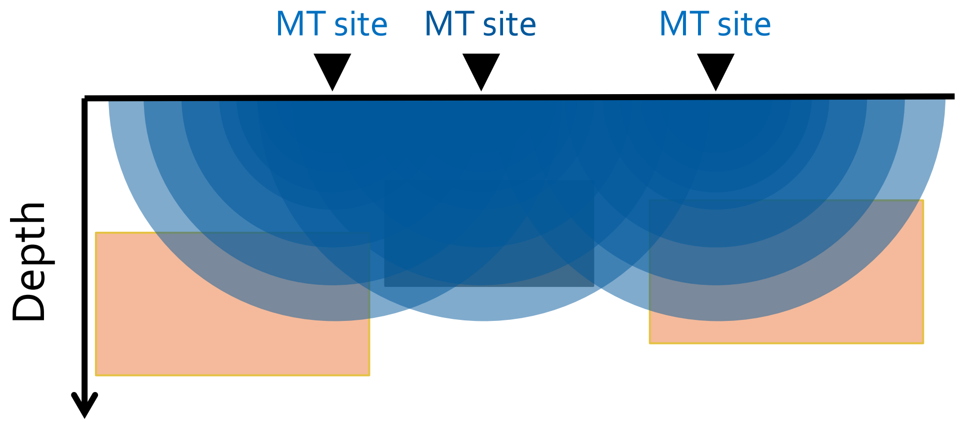

- Electric and magnetic fields are measured at Earth's surface.
- Data are transferred to and processed in frequency domain → transfer functions.
- Transfer functions contain information about subsurface conductivity
  - Period length is a proxy for depth.
  - Lateral resolution is provided by MT site distribution
- MT can be done nearly everywhere on the world, maybe not in the middle of a city of millions.
- MT can be applied at the ocean bottom (no examples shown today).
  - But conductive seawater above stations reduces MT signal strength
- MT sites can be measured sequentially
  - No active source, no dependence of data between sites, i.e. no need that all stations run at the same time.
  - Allows adding sites in surveys years later.

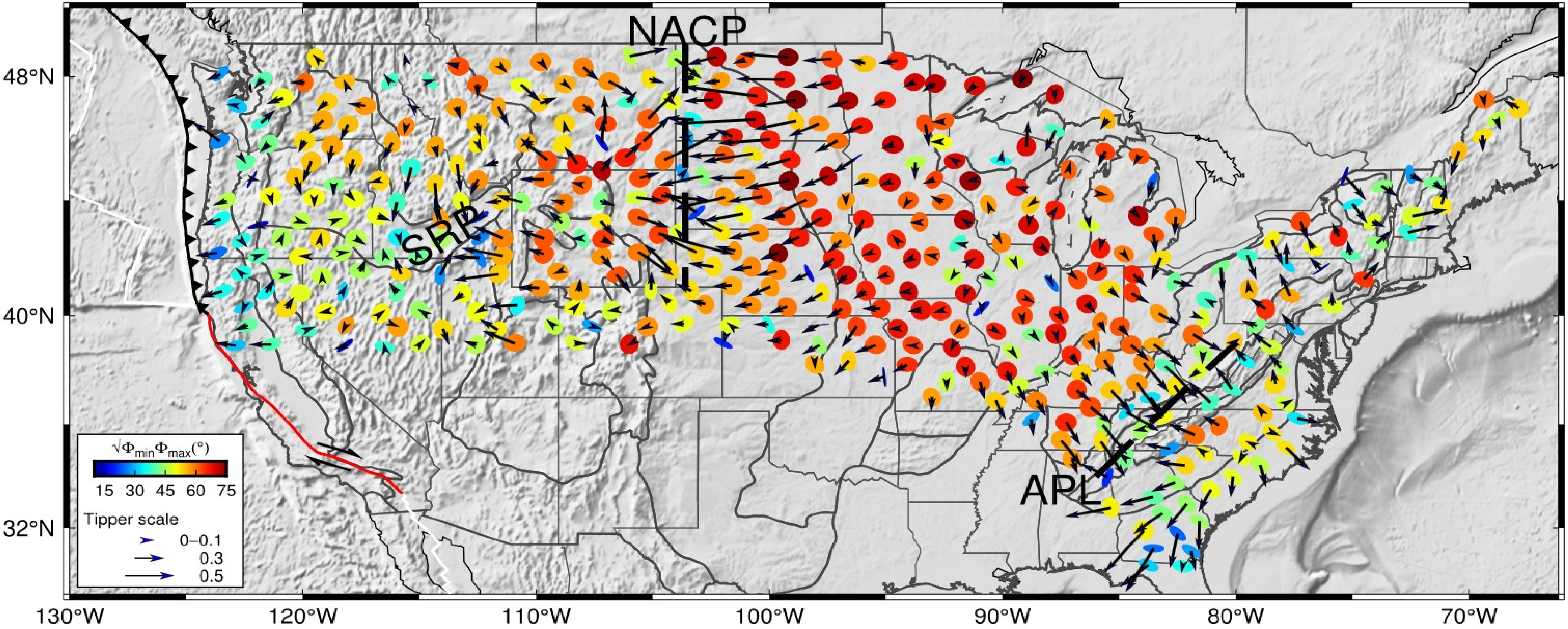

What can I learn from looking at MT data?

Dimensionality of the subsurface

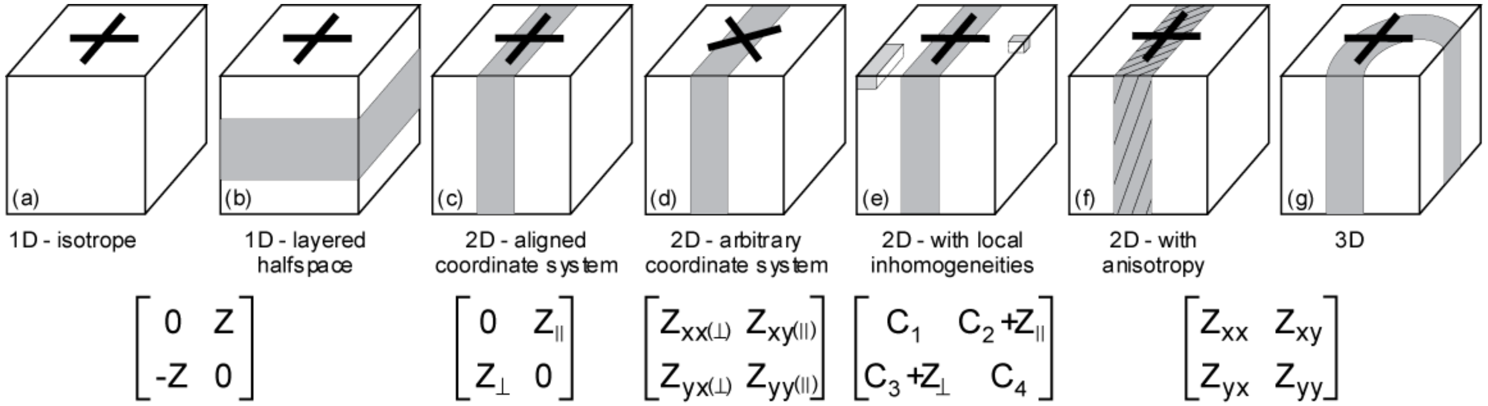

Dimensionality of the subsurface and geoelectric strike directions (2D) can be mathematically determined from the observed impedance tensor (and the induction vectors).

This is particularly relevant if 2D modelling and inversion approaches are going to be used.

Most relevant approaches:

- Bahr 1988, 1991 (telluric vectors)
- Groom & Bailey 1988; McNeice & Jones 2001 (multisite, multi-frequency tensor decomposition of magnetotelluric data)
- Becken et al., 2004 (ellipticity of impedance tensor)
- Caldwell et al. 2004 (phase tensor), most commonly used nowadays

Alternative representations of the magnetotelluric impedance

Impedance

$$\mathbf{Z} = \mathbf{X} + i\mathbf{Y}$$

X – real part of Z

Y – imaginary part of Z

Apparent resistivity and phase

$$\rho_{a,ij} = \frac{\mu_0}{\omega}|Z_{ij}|^2 \qquad \phi_{ij} = \arctan\frac{Y_{ij}}{X_{ij}}$$

Phase tensor (Caldwell et al., 2004)

$$\mathbf{\Phi} = \mathbf{X}^{-1}\mathbf{Y}$$

$$\begin{pmatrix} \Phi_{11} & \Phi_{12} \\ \Phi_{21} & \Phi_{22} \end{pmatrix} = \frac{1}{\det \mathbf{X}} \begin{pmatrix} X_{22}Y_{11} - X_{12}Y_{21} & X_{22}Y_{12} - X_{12}Y_{22} \\ X_{11}Y_{21} - X_{21}Y_{11} & X_{11}Y_{22} - X_{21}Y_{12} \end{pmatrix}$$

The phase tensor is a real tensor of rank 2.

What can I learn from looking at MT data?

Phase tensor skew angle – a dimensionality criterion

$$\beta = \frac{1}{2}\arctan\left(\frac{\Phi_{xy} - \Phi_{yx}}{\Phi_{xx} + \Phi_{yy}}\right)$$

Skew angle, rotationally invariant

The phase tensor can be imaged as ellipse and actually tell us something about the underground structure if displayed e.g. on a map.

Here: Colour of fill is the skew angle β

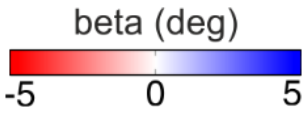

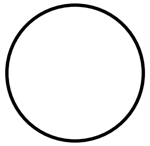

1D: Circular, beta = 0 (in practice, beta < ±3 deg)
size can vary and tell something about vertical conductivity variations)

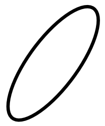

2D: Elliptic, beta = 0 (in practice, beta < ±3 deg)
Major and minor axis aligned with current flows
parallel / perpendicular to geologic strike

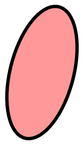

3D: Elliptic, beta > 0 (in practice, beta > ±3 deg)

What can I learn from looking at MT data?

Parkfield MT array, central California

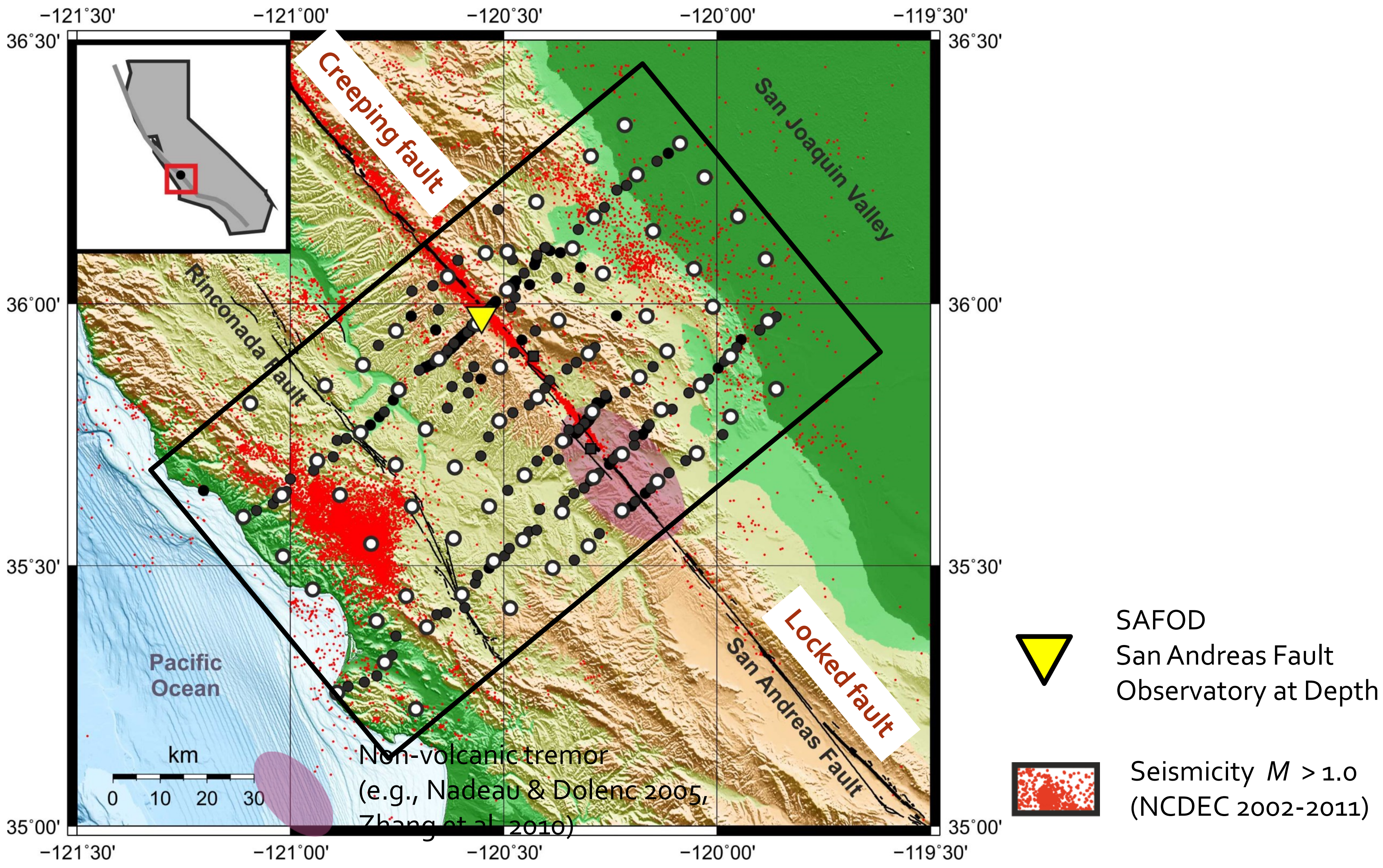

Parkfield MT array – Phase tensors

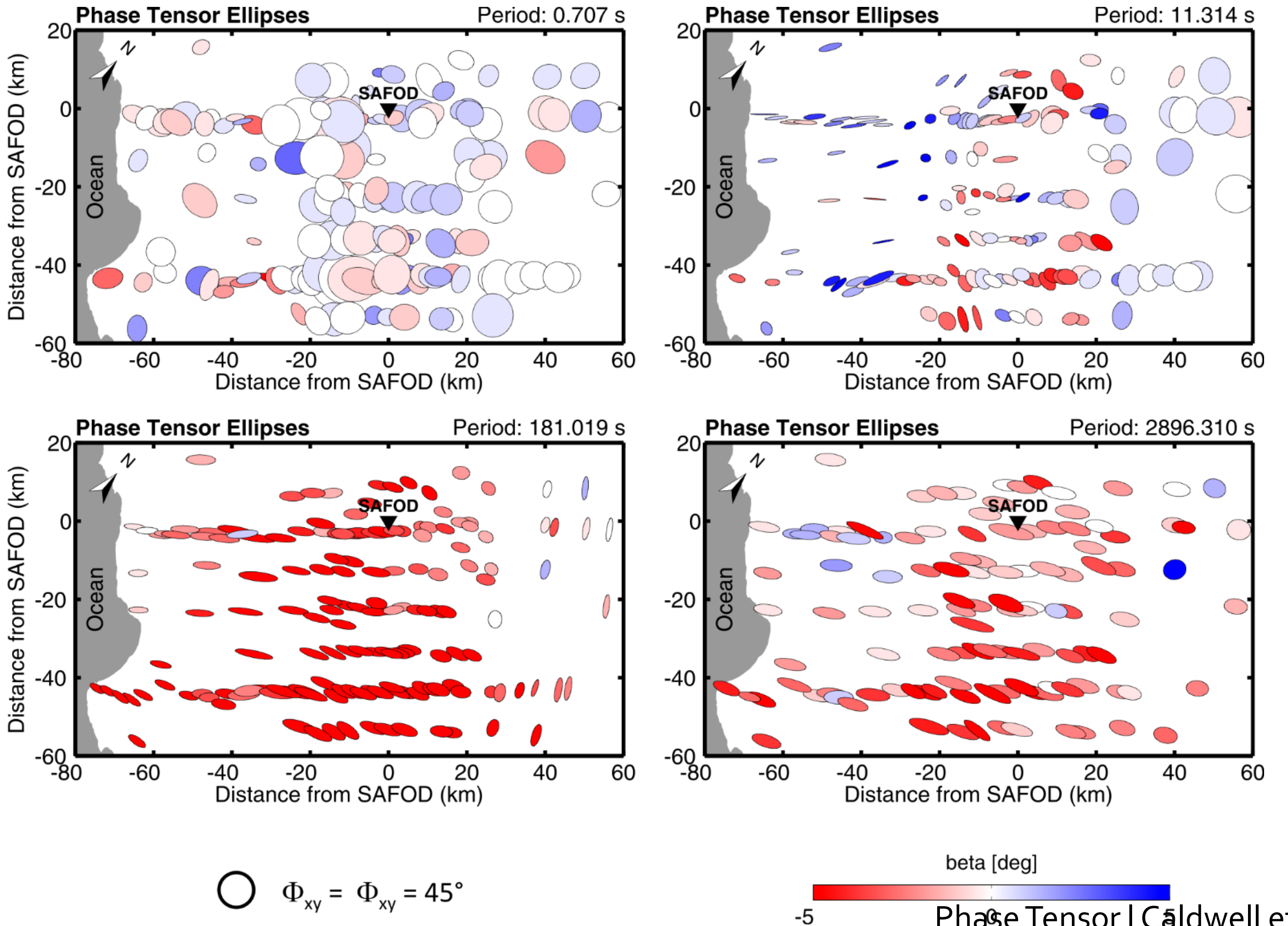

Phase Tensor | Caldwell et al. (2004)

Parkfield MT array – Phase tensors

~ 1D

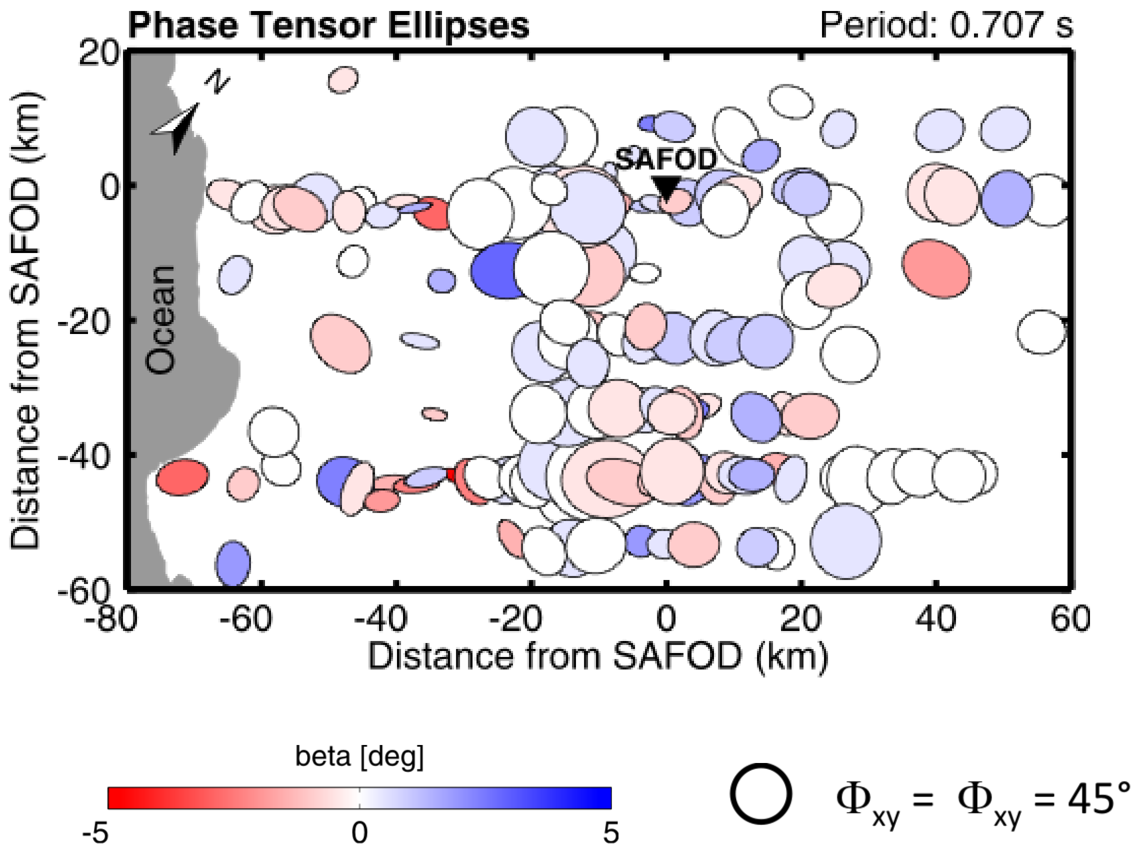

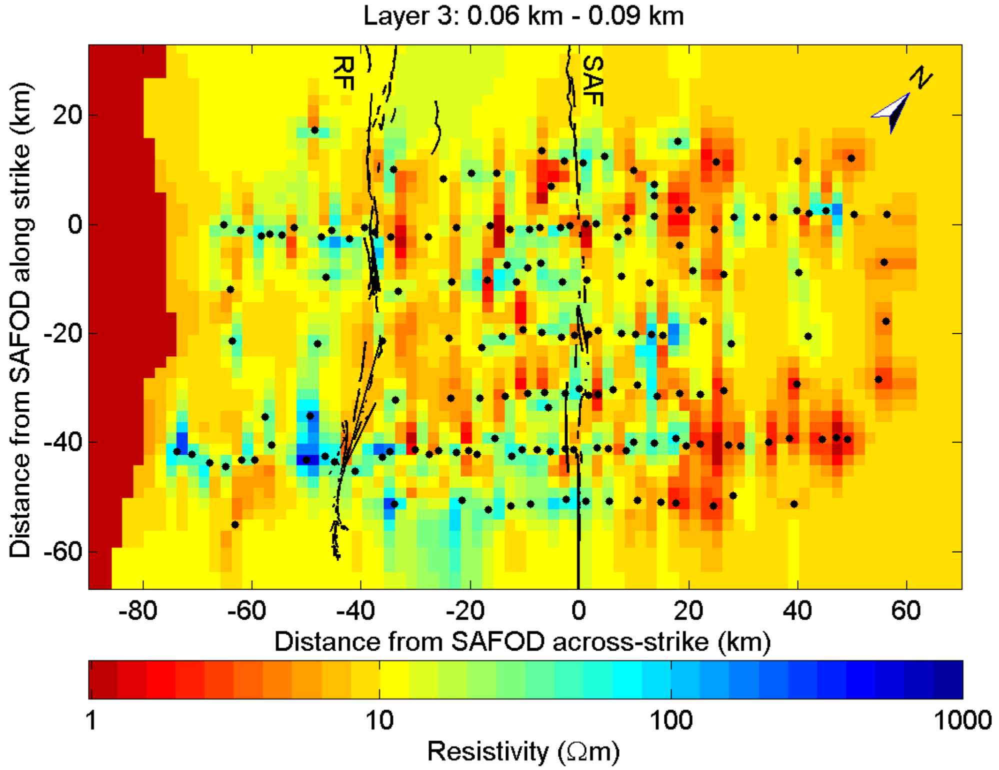

Parkfield MT array – Phase tensors

~ 2D ~ 1D

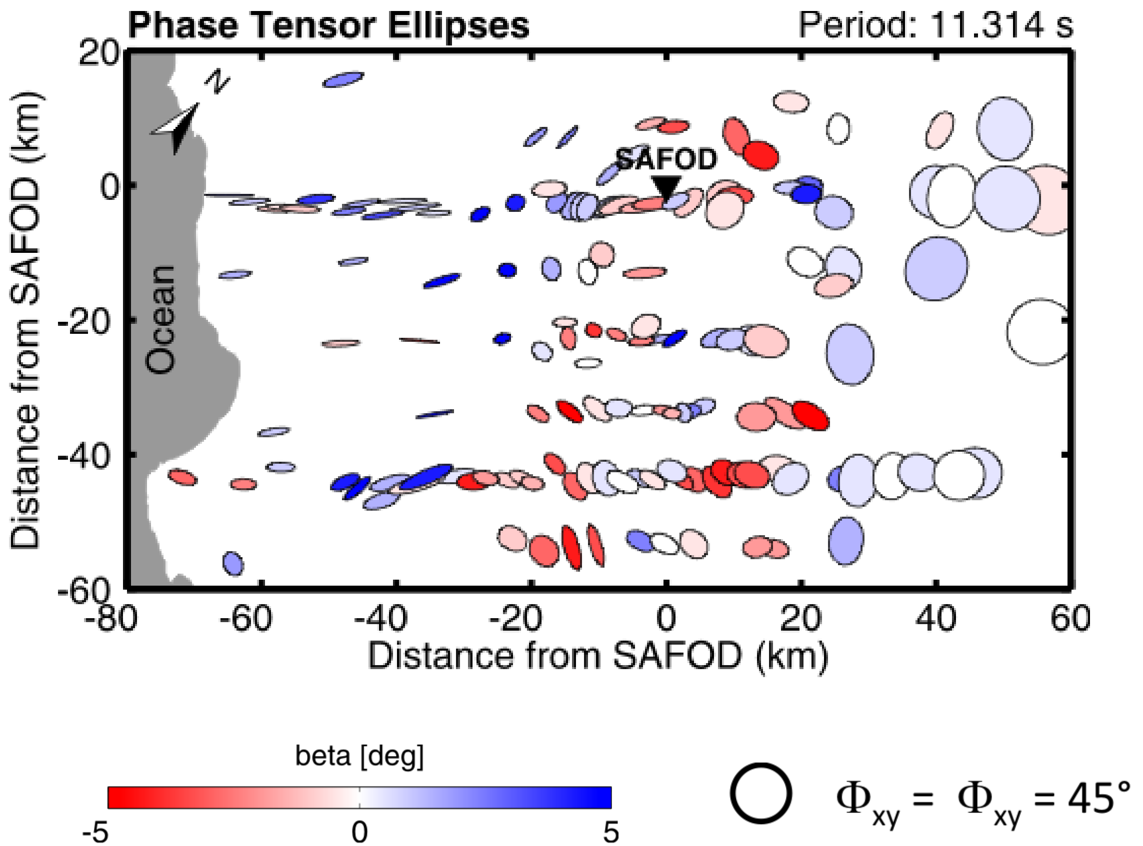

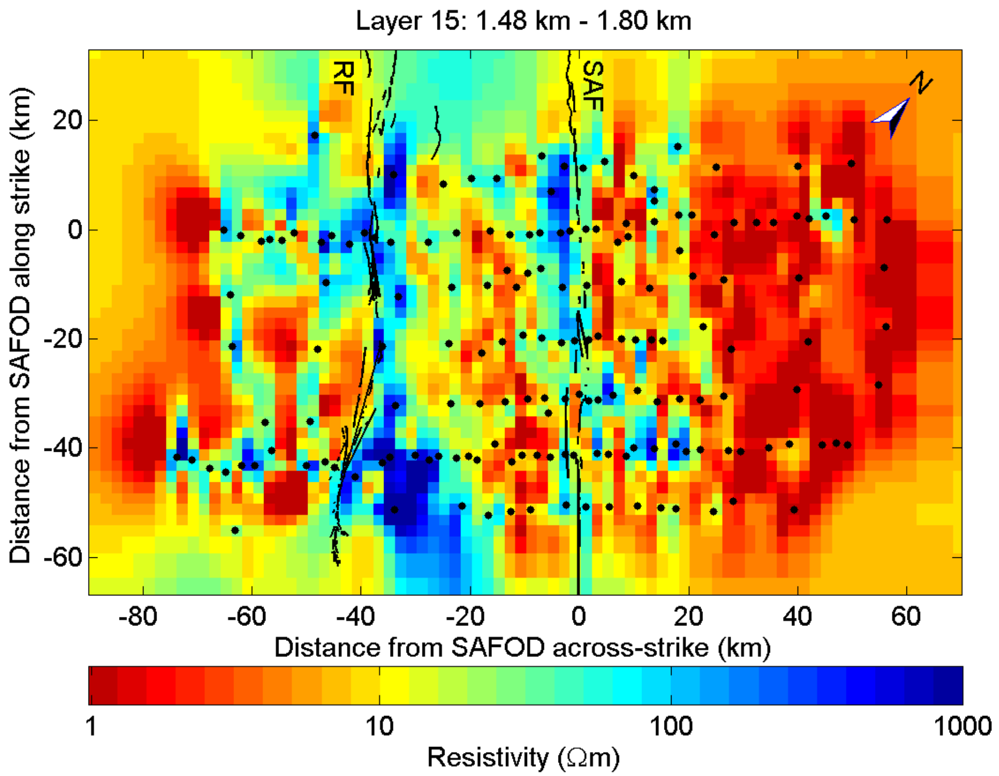

Parkfield MT array – Phase tensors

~ 3D ~ 2D

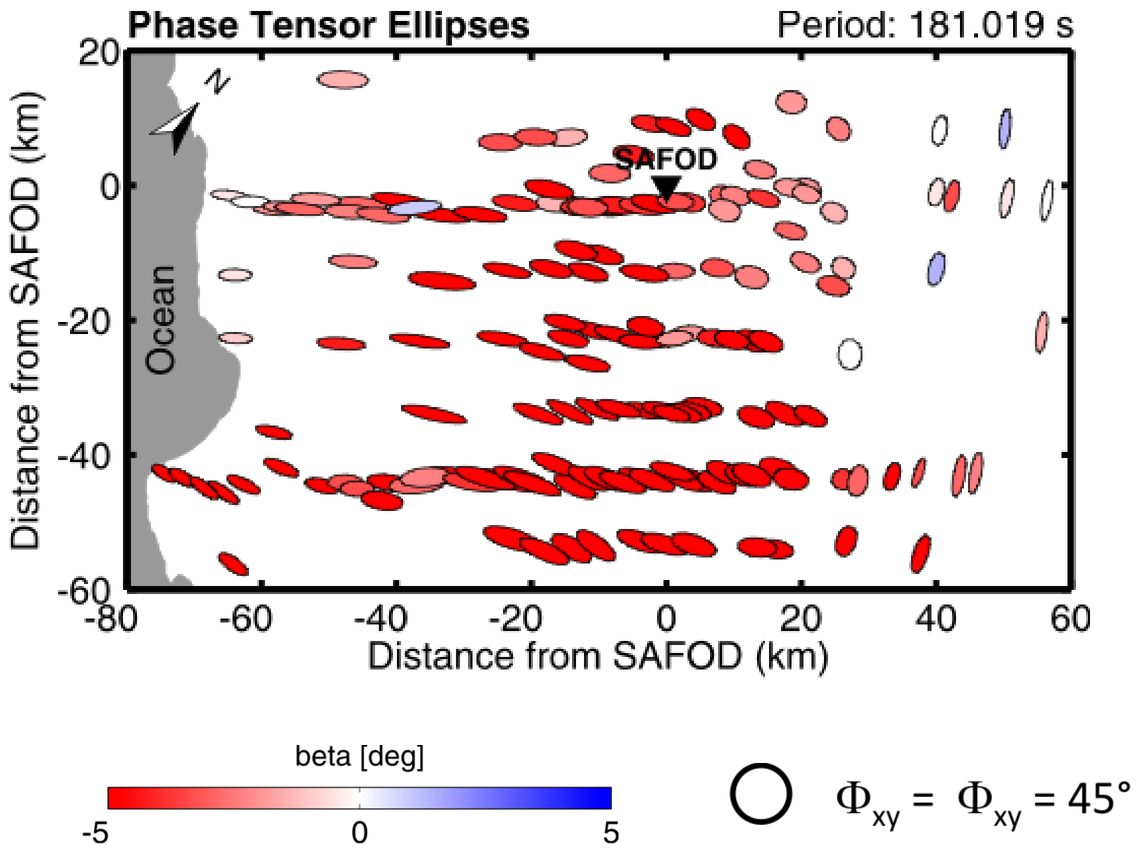

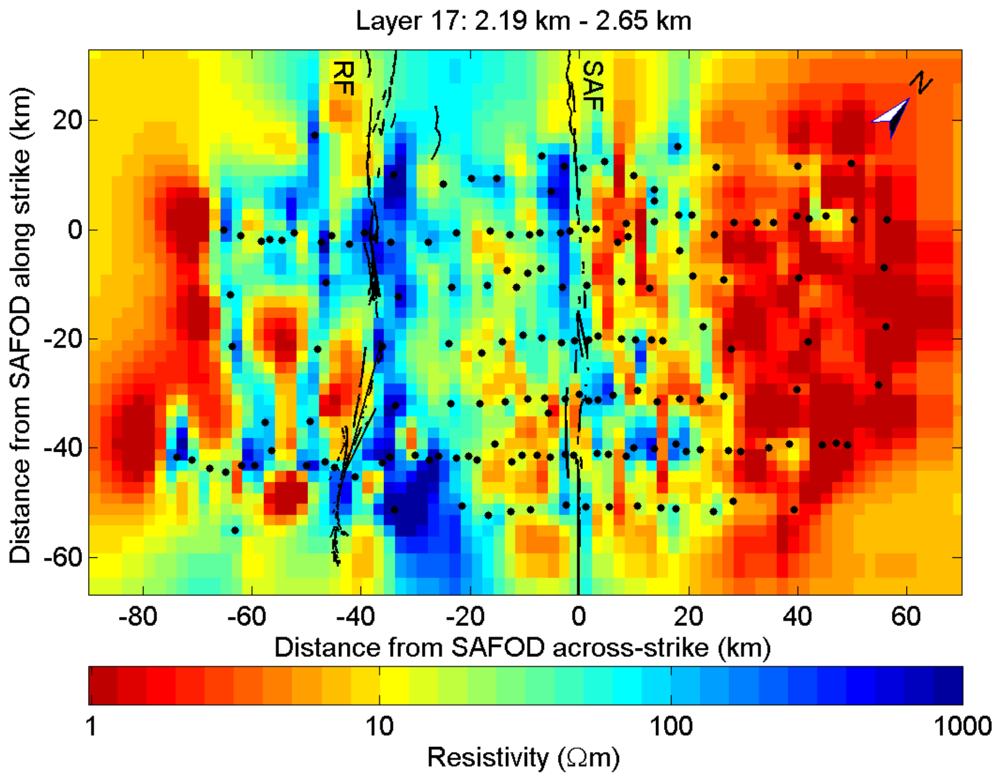

Parkfield MT array – Phase tensors

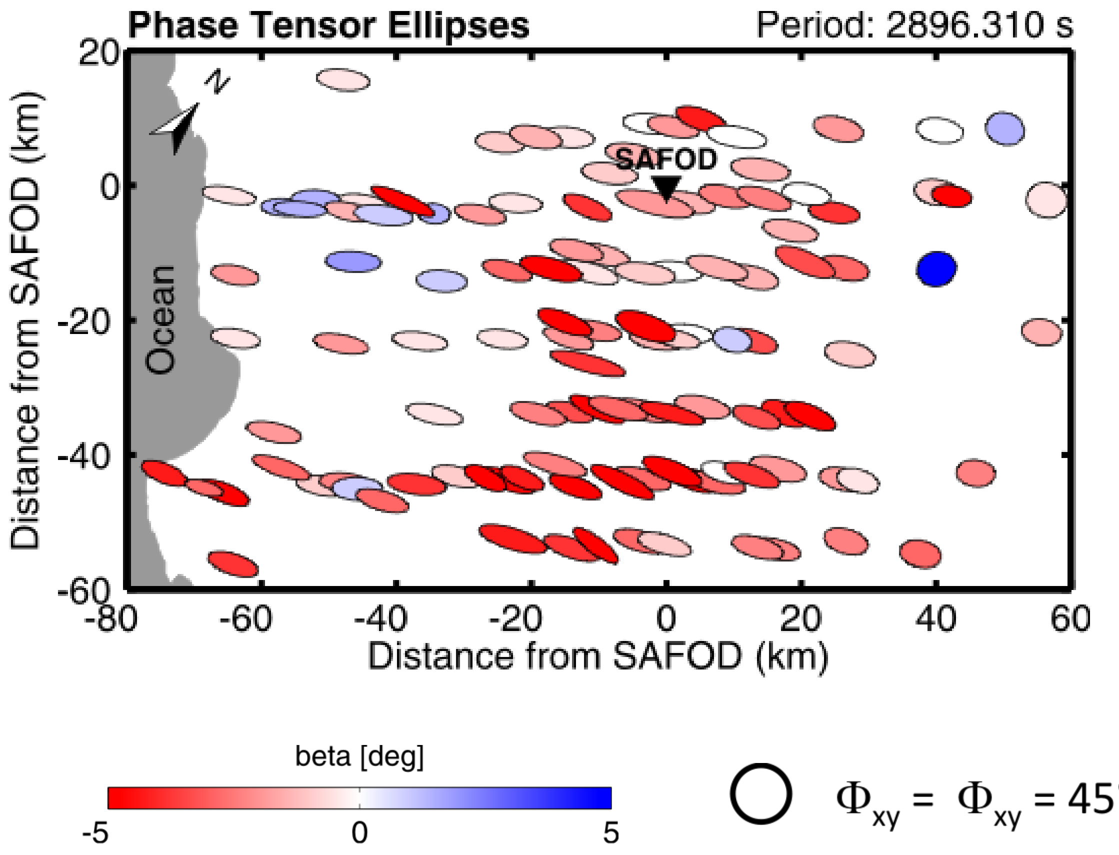

$\Phi_{xy} = \Phi_{xy} = 45°$

~ 3D (2D)

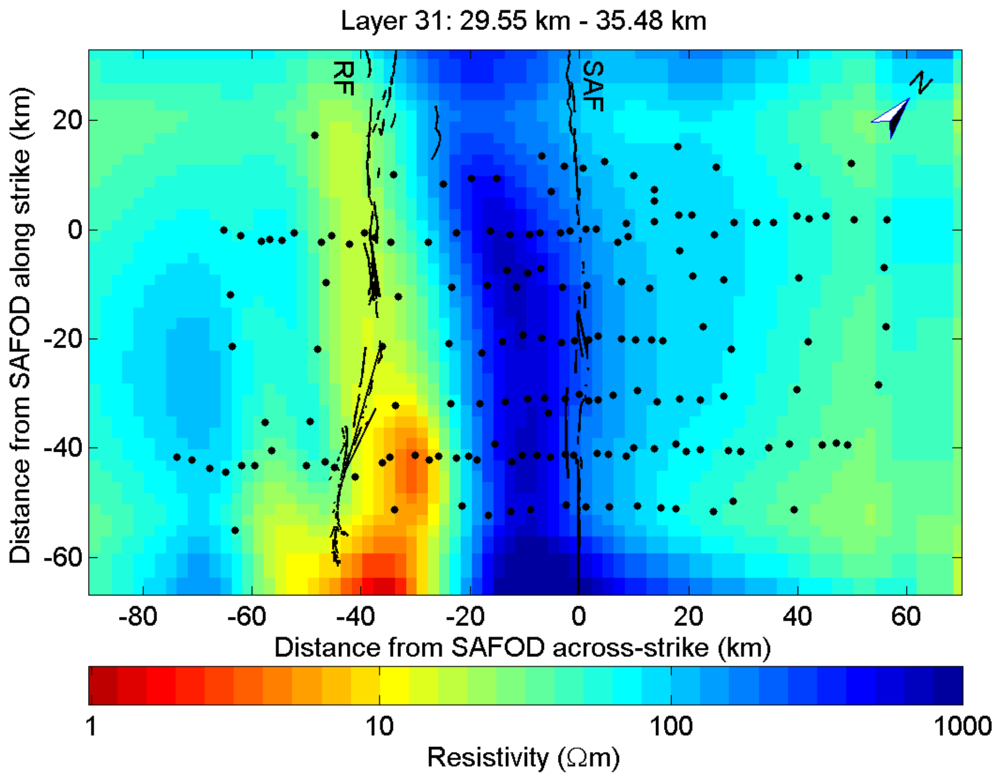

Parkfield MT array – Phase tensors

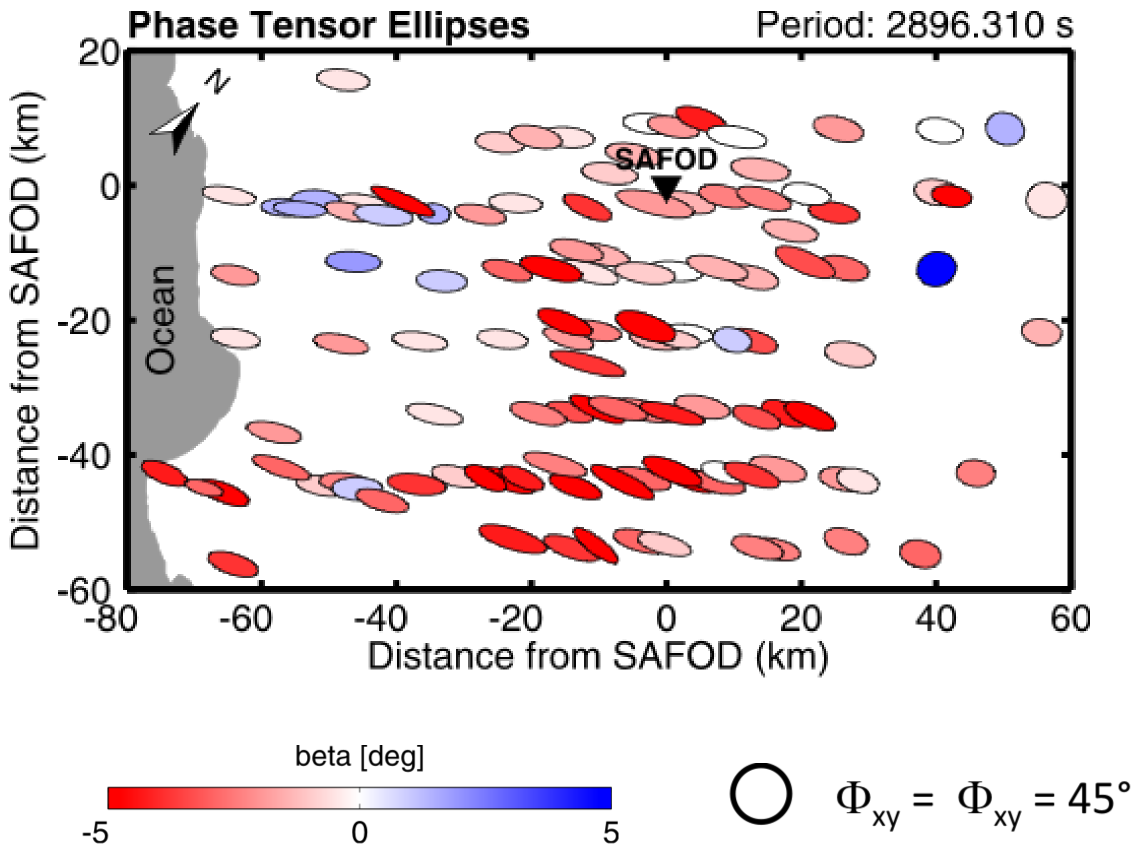

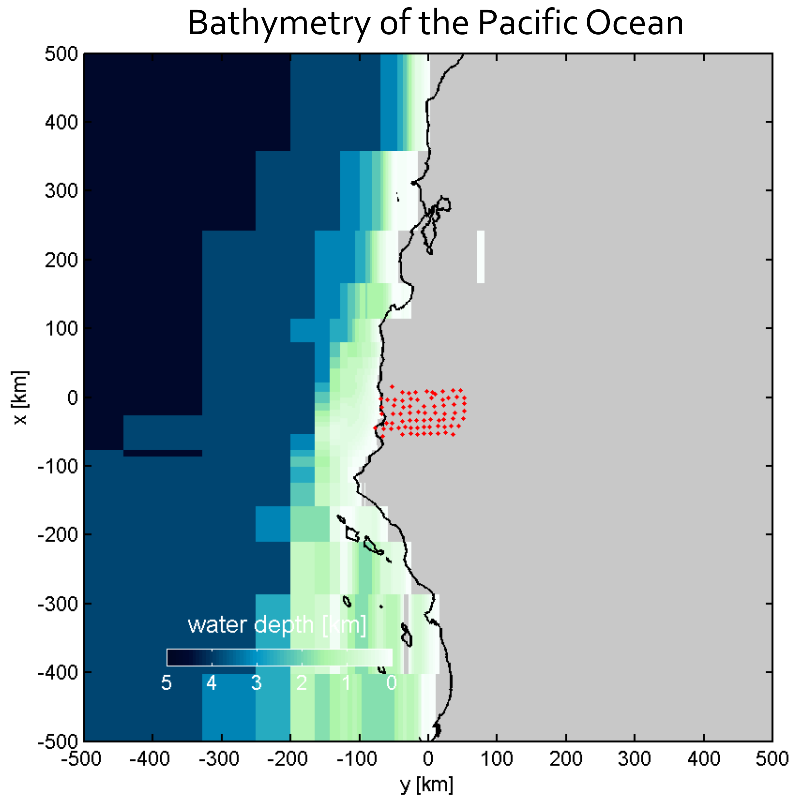

Sea water is electrically very conductive (~ 3 S/m) because of the high salt content.

The ocean has a strong influence on MT data and has to be considered as a priori information in MT modelling.

Induction vectors

Vertical magnetic transfer function: **T****

$$B_z = \begin{pmatrix} T_x & T_y \end{pmatrix} \begin{pmatrix} B_x \\ B_y \end{pmatrix}$$

$$l = \sqrt{T_{xr}^2 + T_{yr}^2} \qquad \theta = \tan^{-1}\left(\frac{T_{yr}}{T_{xr}}\right)$$

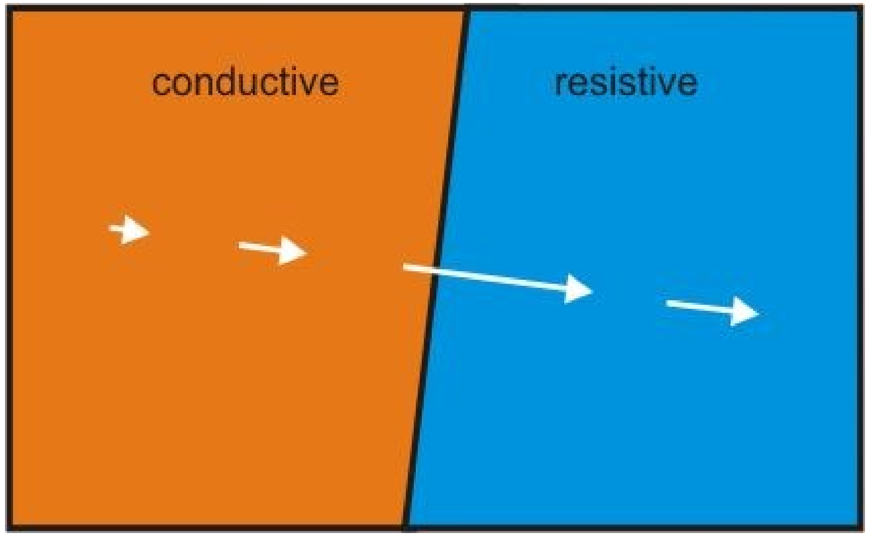

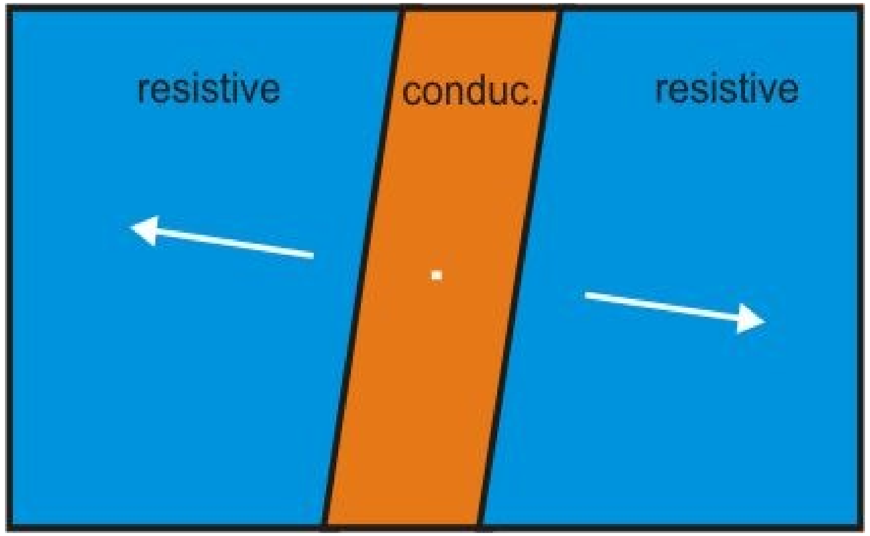

Induction vectors are useful to map lateral changes in conductivity:

- They (tend to) point away from the conductive side of a contrast**.
- The largest induction vectors are found across the boundary.
- Induction vectors diminish less rapidly on the resistive side.
- In 2D real and imaginary induction vectors are (anti-)parallel (or zero).

** Wiese convention, found in European papers. Parkinson convention makes the arrows point towards conductors, mainly used by US and Asian authors.

Induction vectors (and phase tensor ellipses) for ~400 sites of the USArray (Parkinson convention).

Sign reversals of induction arrows at black dashed lines point to massive conductive features below.

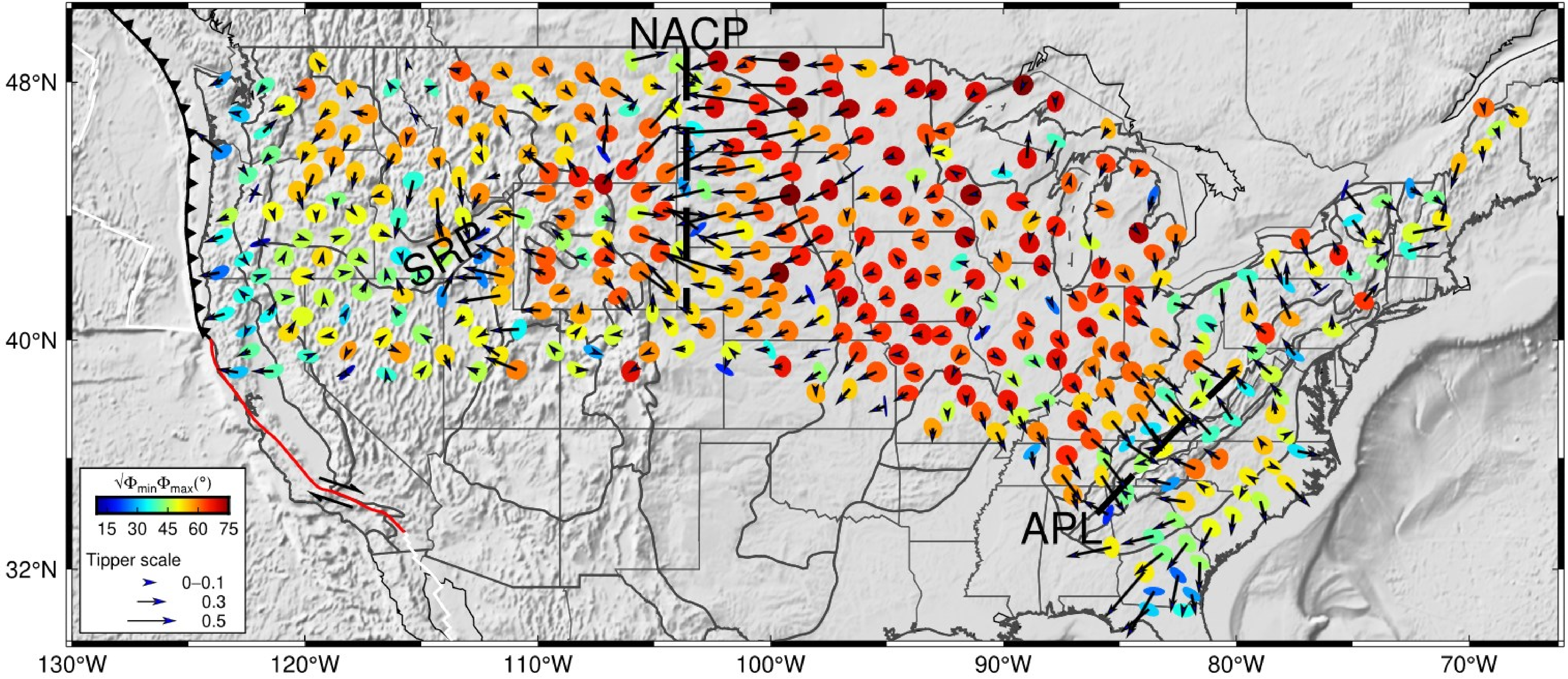

T = 12,000 s (here ~lower lithosphere to upper asthenosphere)

Yang et al. 2021

Summary

- Dimensionality can be estimated from the observed data, no need to know this before the survey.
- 2D: Geoelectric (usually ~geological) strike direction can also be estimated from the measured data.
  Ideally, sites are distributed along a profile perpendicular to strike for subsequent modelling and interpretation.
- Maps of phase tensors (calculated from the impedance tensor) and induction vectors can be instructive w.r.t. location of major features or contrasts.

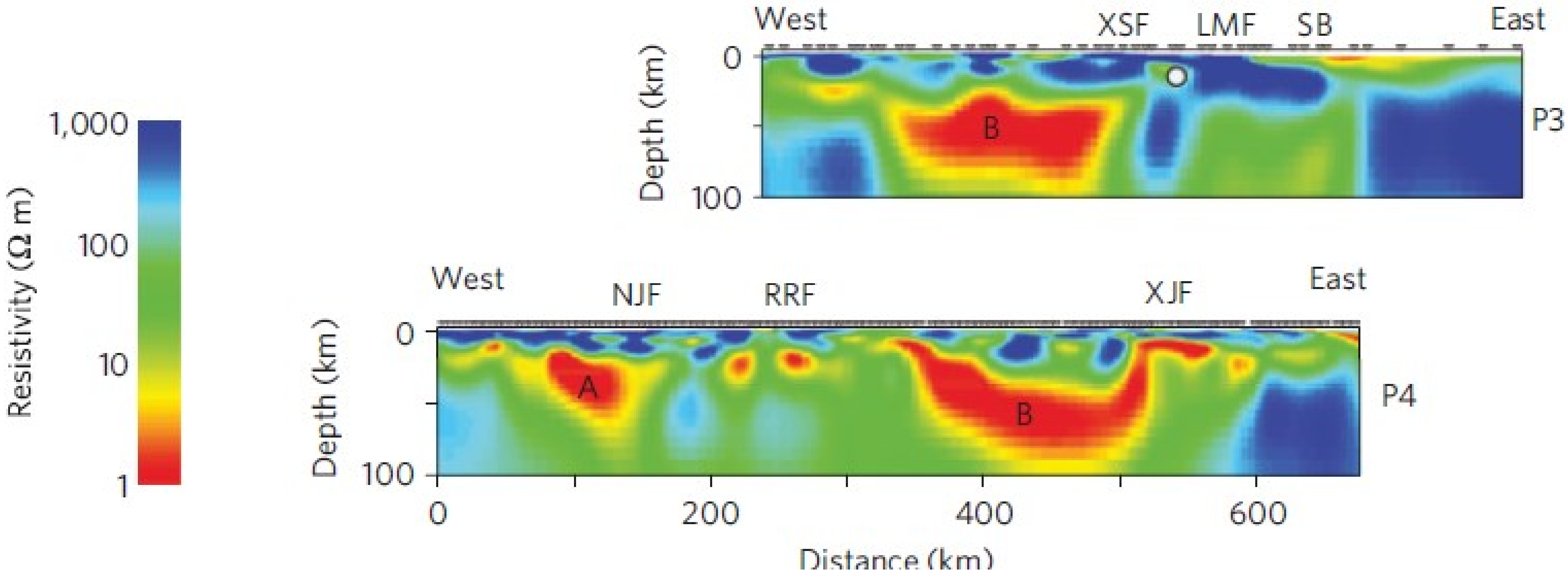

Modelling and inversion of MT data

Forward modelling and inversion

Model space
Model parameter *m*

Data are calculated for a given distribution of the electrical resistivity in the subsurface.

Forward modelling

Forward operator
d = f(m),
describes physics.

Data space
Data *d*

MT curves

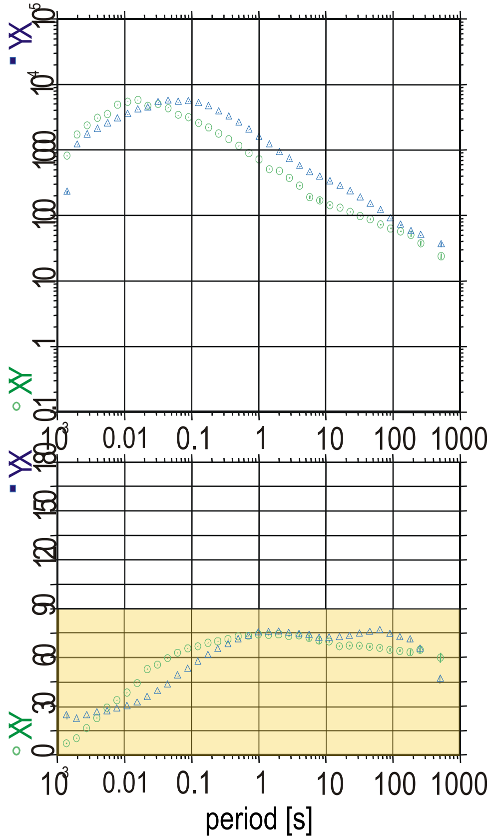

Resistivity model

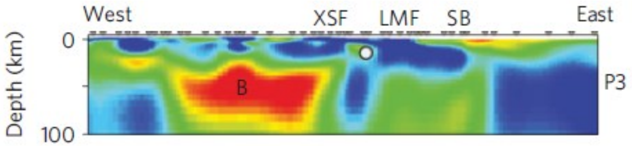

A model is sought from observed data.

Inversion

Inverse operator
$m = f^{-1}(d)$

How to transform measured data to a subsurface resistivity distribution?

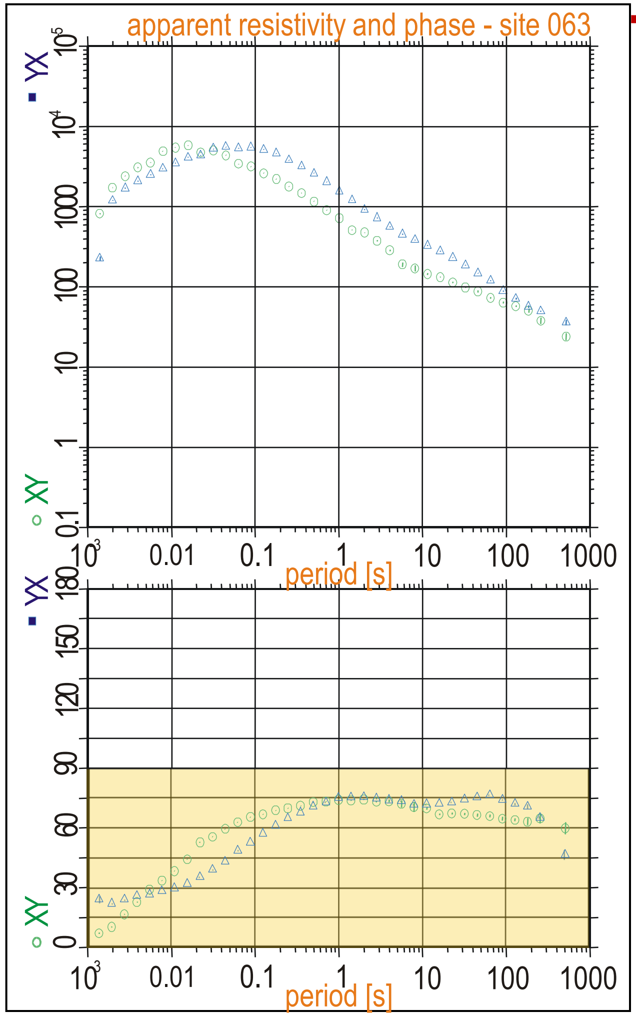

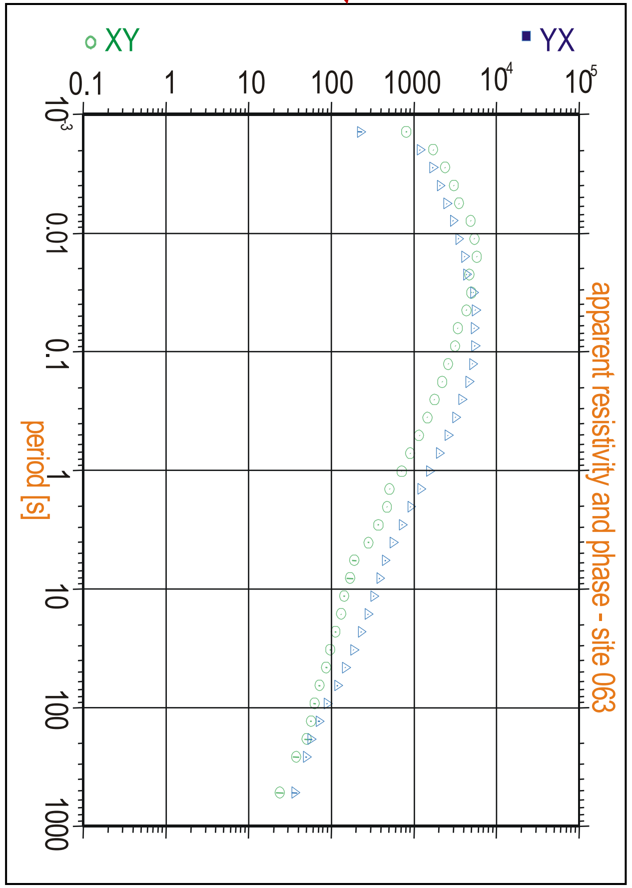

How to transform measured data to a subsurface resistivity distribution?

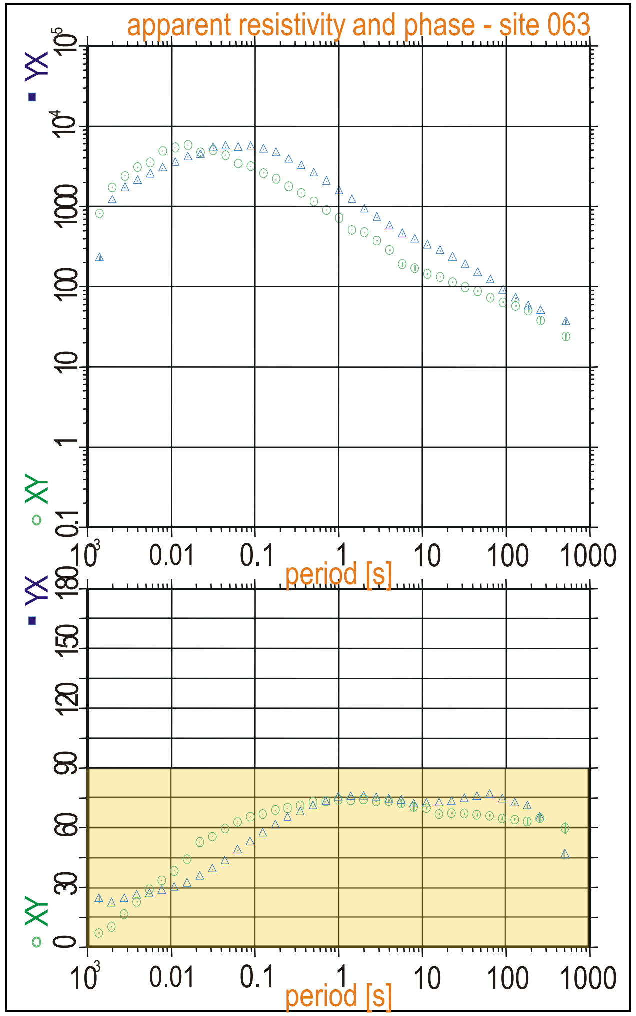

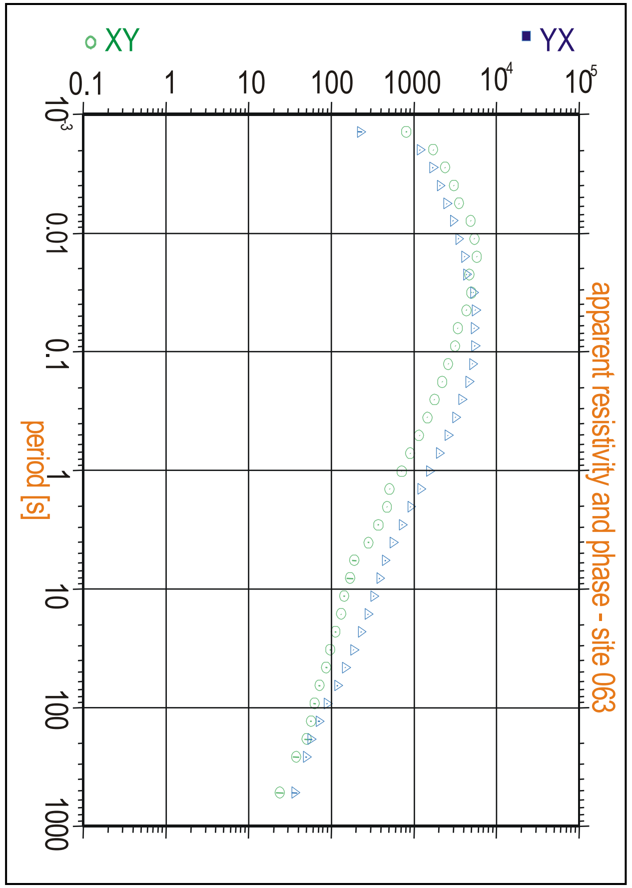

Inversion problem of MT

It is not easy to find $\mathbf{m} = \mathbf{f}^{-1}(\mathbf{d})$

- Analytical solution exists only for 1D problems
  → Numerical methods for 2D/3D problems
- The problem is non-linear
  → Linearisation (Taylor approximation)
- More model parameters than data points
  → System of equations is underdetermined, regularisation required
  → The solution is non-unique
- Iterative algorithms
  → Cycles of forward and inverse calculations

Iterative inversion scheme

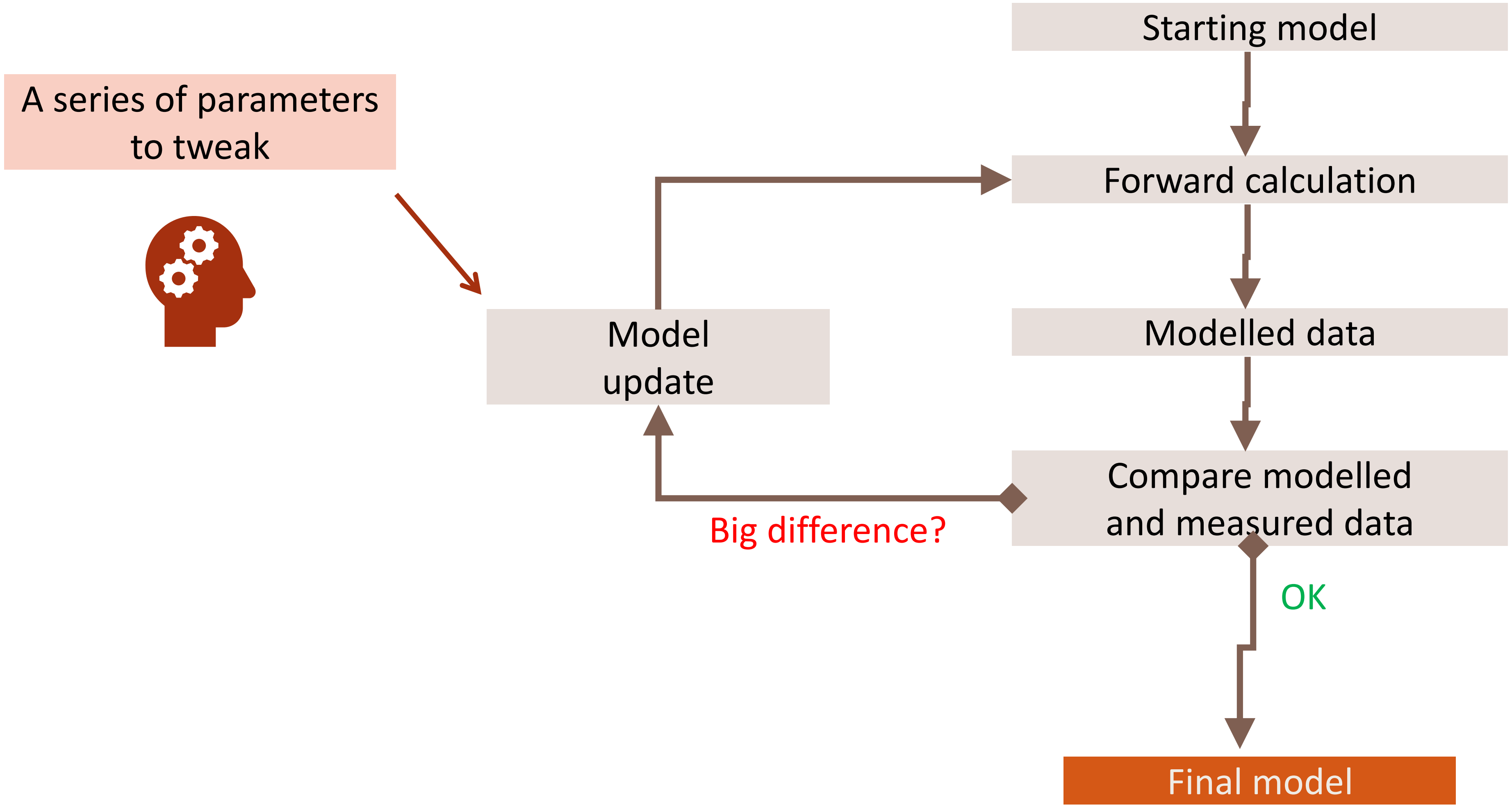

Representation of the electric conductivity in a model → discretisation

FINITE DIFFERENCE

Advantages

- Mathematically easy
- Fast, easy to parallelize

Disadvantages

- Discretisation not representative of true world geometries
- May require large number of cells (unknowns)

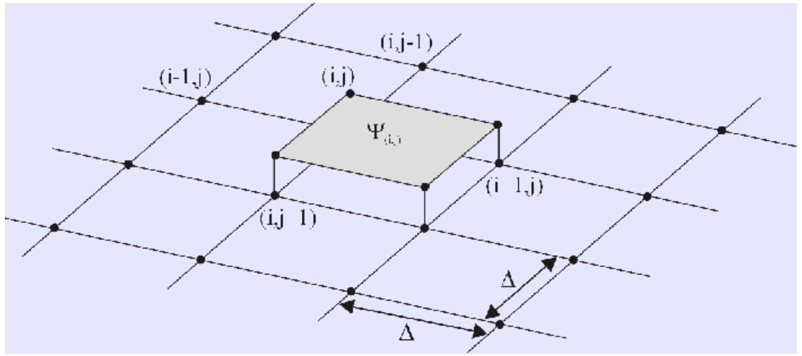

FINITE ELEMENT

Advantages

- Good representation of subsurface geometries; mesh can reflect resolution potential of MT (fine at surface, coarser at depth)
- Good representation of topography/bathymetry

Disadvantages

- Numerically expensive

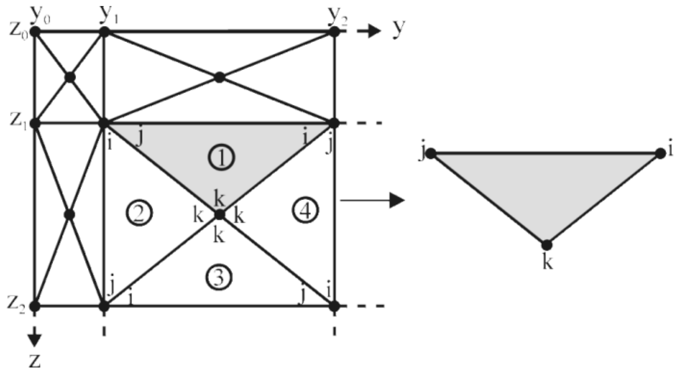

Modelling and inversion

inversion

f(X, m) *forward operator, data kernel*

m model parameter (geometry of model cells and resistivity values)

X independent variables (location, period, ...)

d observed data (MT response of the subsurface)

e data uncertainties, measurment errors

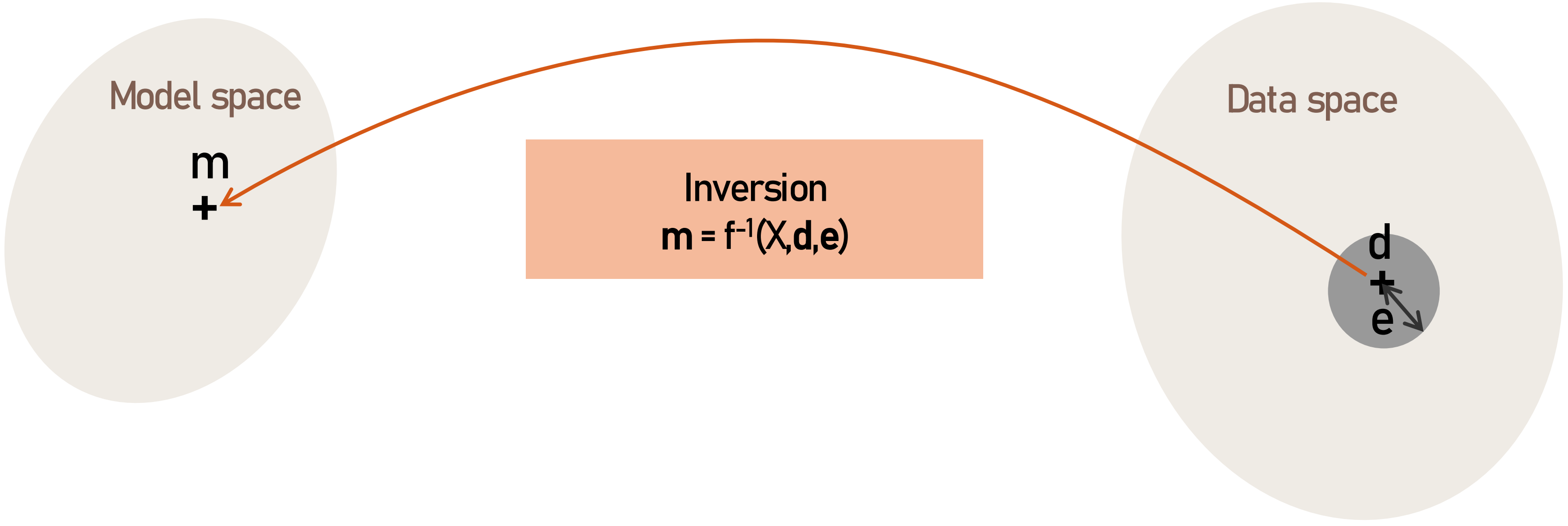

objective function

$\Phi(\mathbf{m})$ be reduced to a minimum

trade-off parameter

$$\Phi(\mathbf{m}) = \Phi_{data}(\mathbf{m}) + \lambda\Phi_{reg}(\mathbf{m})$$

data misfit

model regularisation

Usually some kind of smoothness request is imposed on the distribution of conductivity.

Modelling and inversion

inversion

$f(X, m)$ *forward operator, data kernel*

m model parameter (geometry of model cells and resistivity values)

X independent variables (location, period, …)

d observed data (MT response of the subsurface)

e data uncertainties, measurment errors

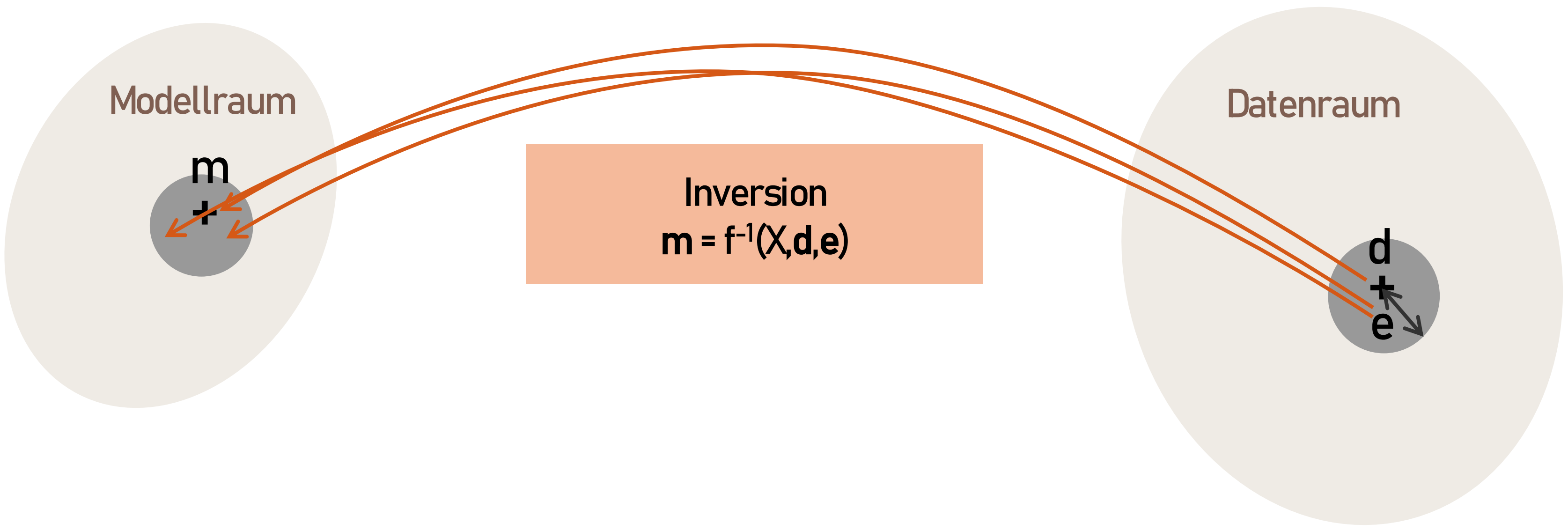

In MT (as in a lot of other methods), the inversion problem is non-unique because

… measured data are erroneous.

… the problem is underdetermined (more unknowns than knowns).

… there are alternative models which explain data similarly well.

… representation of the parameters does not match reality.

Let's talk numbers: Parkfield MT array

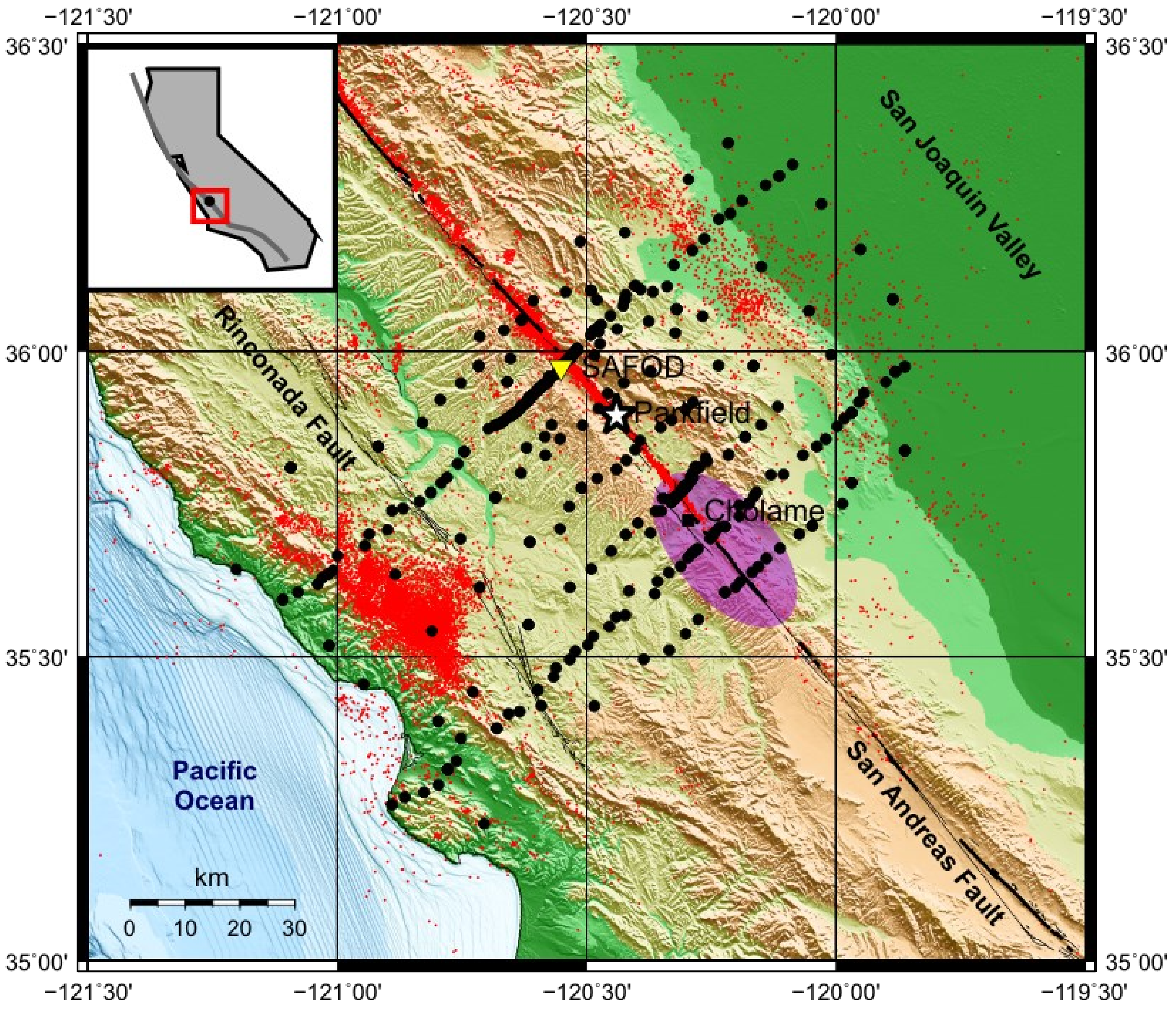

Number of data points used for 3D modelling:

- 220 stations (out of 350 sites in total)
  30 periods
  6 components (real + imaginary part)
  → 220 x 30 x 6 x 2 = 79,200 data points (knowns)
- data points are not completely independent of each other

3D finite difference model

- 130 x 65 x 55 = 464,750 model cells (unknowns)
- Run time for 1 inversion model
  ~140 iterations x 90 minutes = 12,600 minutes
  = 210 h
  = 8.75 days
  on a high performance cluster, 61 processors
- For my PhD, I ran ~2000 inversions with different parameter settings (that was really a lot, maybe 100 is enough for "normal studies").

Python exercise 03: 1D forward modelling

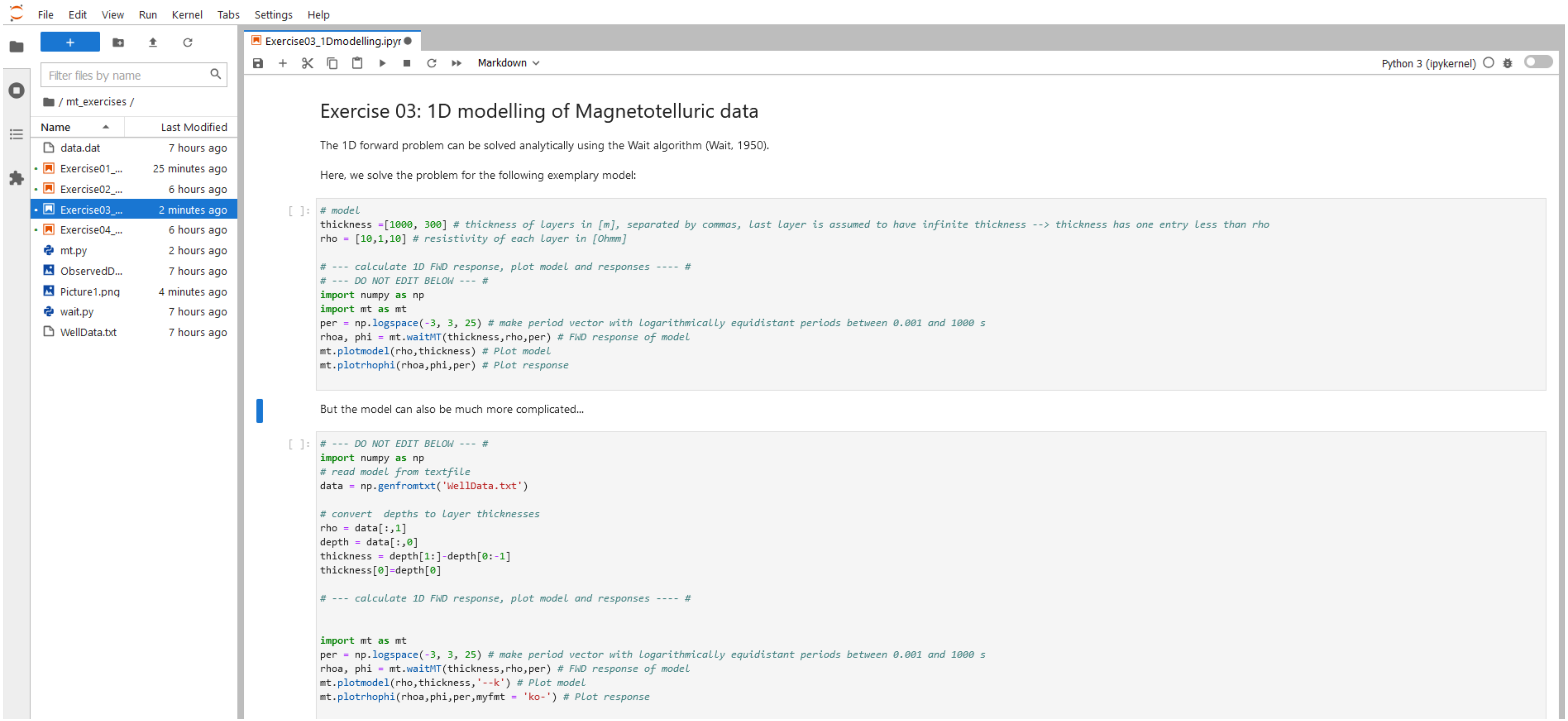

Python exercise 04: Find a suitable 1D model

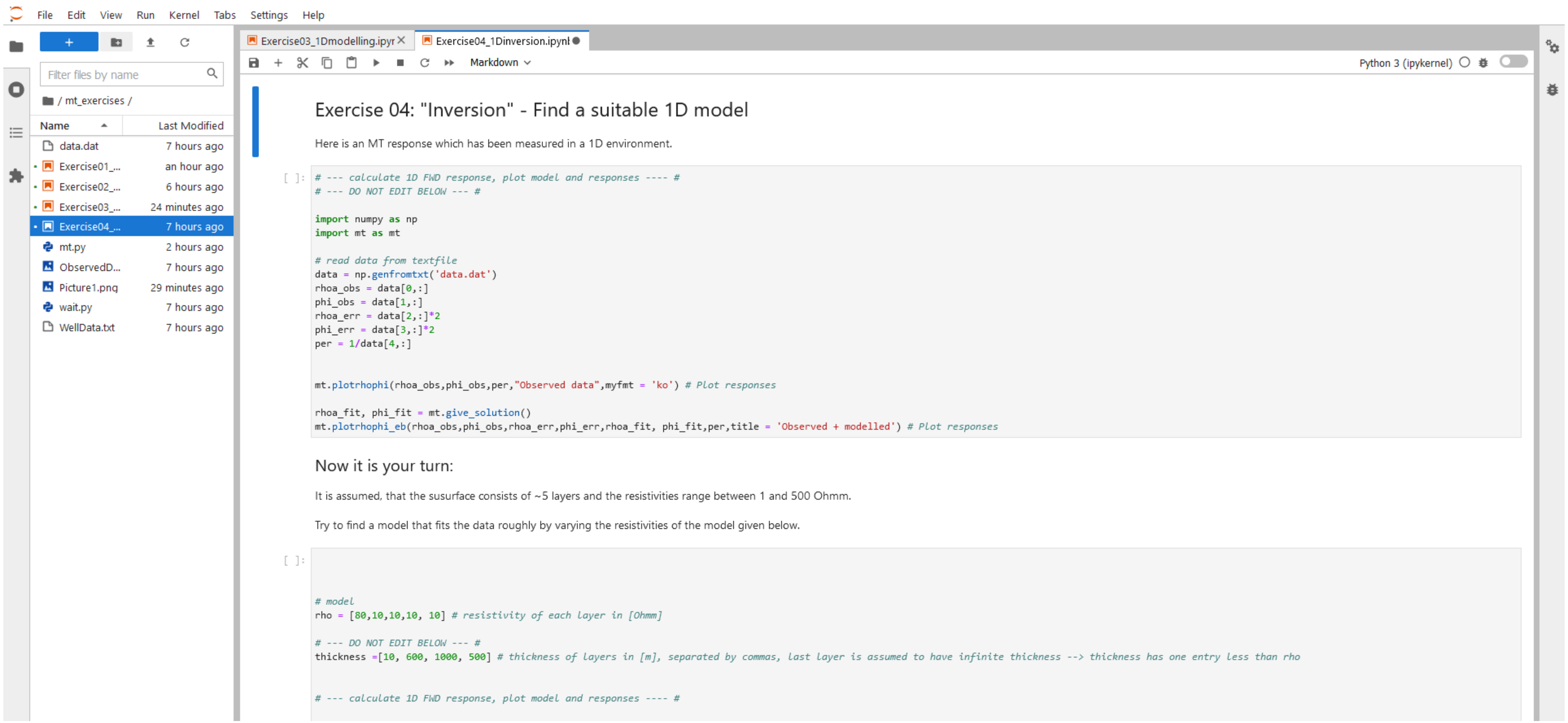

Exercise 04: "Inversion" - Find a suitable 1D model

Here is an MT response which has been measured in a 1D environment.

```python
# --- calculate 1D FWD response, plot model and responses ---- #
# --- DO NOT EDIT BELOW --- #

import numpy as np
import mt as mt

# read data from textfile
data = np.genfromtxt('data.dat')
rhoa_obs = data[0,:]
phi_obs = data[1,:]
rhoa_err = data[2,:]*2
phi_err = data[3,:]*2
per = 1/data[4,:]


mt.plotrhophi(rhoa_obs,phi_obs,per,"Observed data",myfmt = 'ko') # Plot responses

rhoa_fit, phi_fit = mt.give_solution()
mt.plotrhophi_eb(rhoa_obs,phi_obs,rhoa_err,phi_err,rhoa_fit, phi_fit,per,title = 'Observed + modelled') # Plot responses
```

Now it is your turn:

It is assumed, that the susurface consists of ~5 layers and the resistivities range between 1 and 500 Ohmm.

Try to find a model that fits the data roughly by varying the resistivities of the model given below.

```python
# model
rho = [80,10,10,10, 10] # resistivity of each layer in [Ohmm]

# --- DO NOT EDIT BELOW --- #
thickness =[10, 600, 1000, 500] # thickness of layers in [m], separated by commas, last layer is assumed to have infinite thickness --> thickness has one entry less than rho


# --- calculate 1D FWD response, plot model and responses ---- #
```

Summary

- MT problem is highly non-linear.
- Modelling/inversion of MT data requires a numerical, iterative approach.
- Finite difference / finite element approaches both exist, have their advantages and disadvantages.
- The inverse problem is non-unique! There is more than one model that fits the data within the uncertainties.
- A lot of thought has to be put in the set up of inversions, several sets of inversion parameters should be used.
- Doing this (+ adding information from other disciplines, if available), a reliable "preferred" model can be obtained.

MT case studies:
Constraints on the lithosphere from MT

Main expertise of magnetotellurics (may be incomplete)

Today's examples

Geologic reconnaissance

- Continental Arrays - understanding entire continents down into the asthenosphere — AusLAMP
- Cratons, stable continents — AusLAMP
- Plate boundaries — San Andreas fault** — Tibetan Plateau
- Marine studies**

Hazards

- Earthquake potential — San Andreas fault**
- Geomagnetically induced currents (GIC) (3D, 4D) — AusLAMP
- Volcanic system (3D, 4D)

Resources

- Groundwater
- Mineral exploration — Olympic Dam IOCG-U deposit**
- Geothermal systems (3D, 4D) — Rotokawa geothermal field

San Andreas fault

LETTER

doi:10.1038/nature10609

Correlation between deep fluids, tremor and creep along the central San Andreas fault

Michael Becken[1,2]†, Oliver Ritter[1], Paul A. Bedrosian[3] & Ute Weckmann[1,2]

San Andreas fault in the context of major tectonic plates

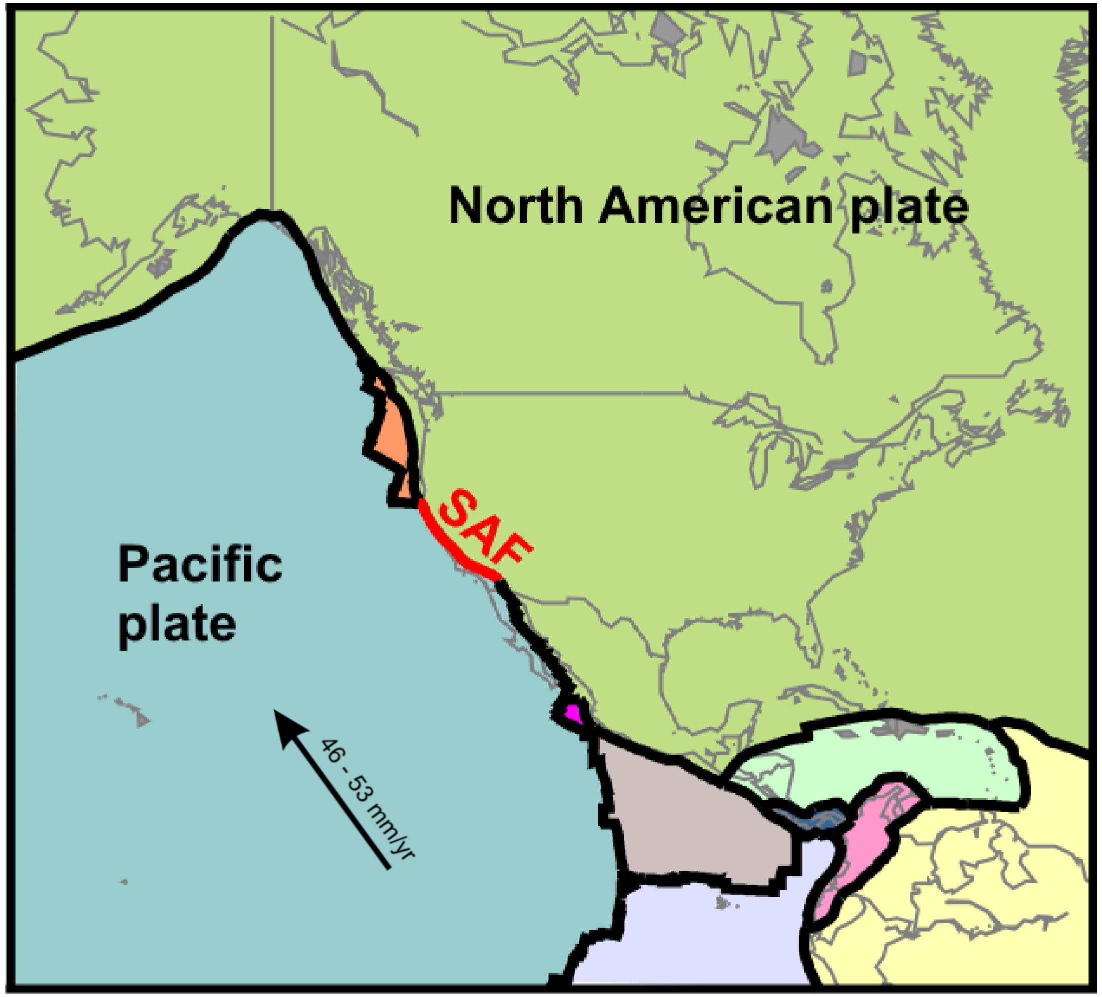

SAF San Andreas fault

PB2002 (Bird, 2003)

Plate movement
e.g., Argus & Gordon (2001), DeMets et al. (1990), Ward (1990)

San Andreas fault system

San Andreas fault

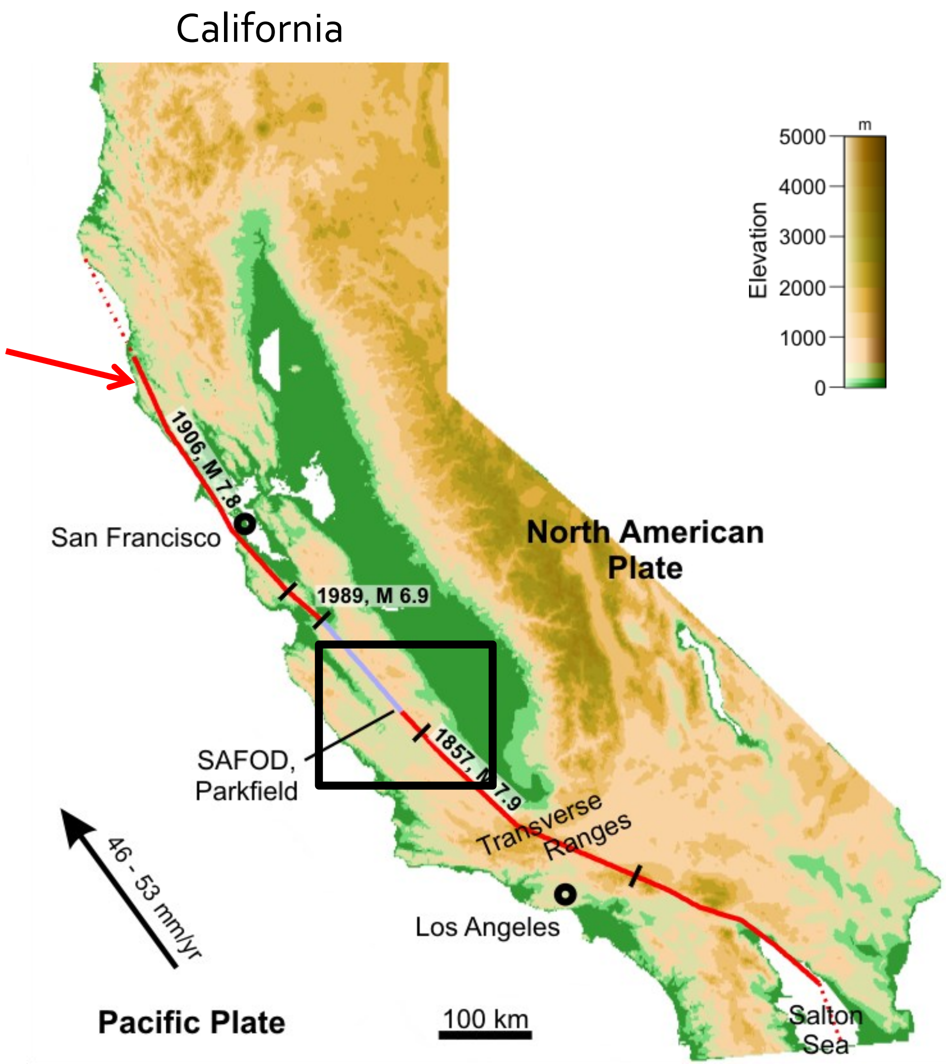

Plate movement
e.g., Argus & Gordon (2001);
DeMets et al. (1990); Ward (1990)

Parkfield-Cholame region

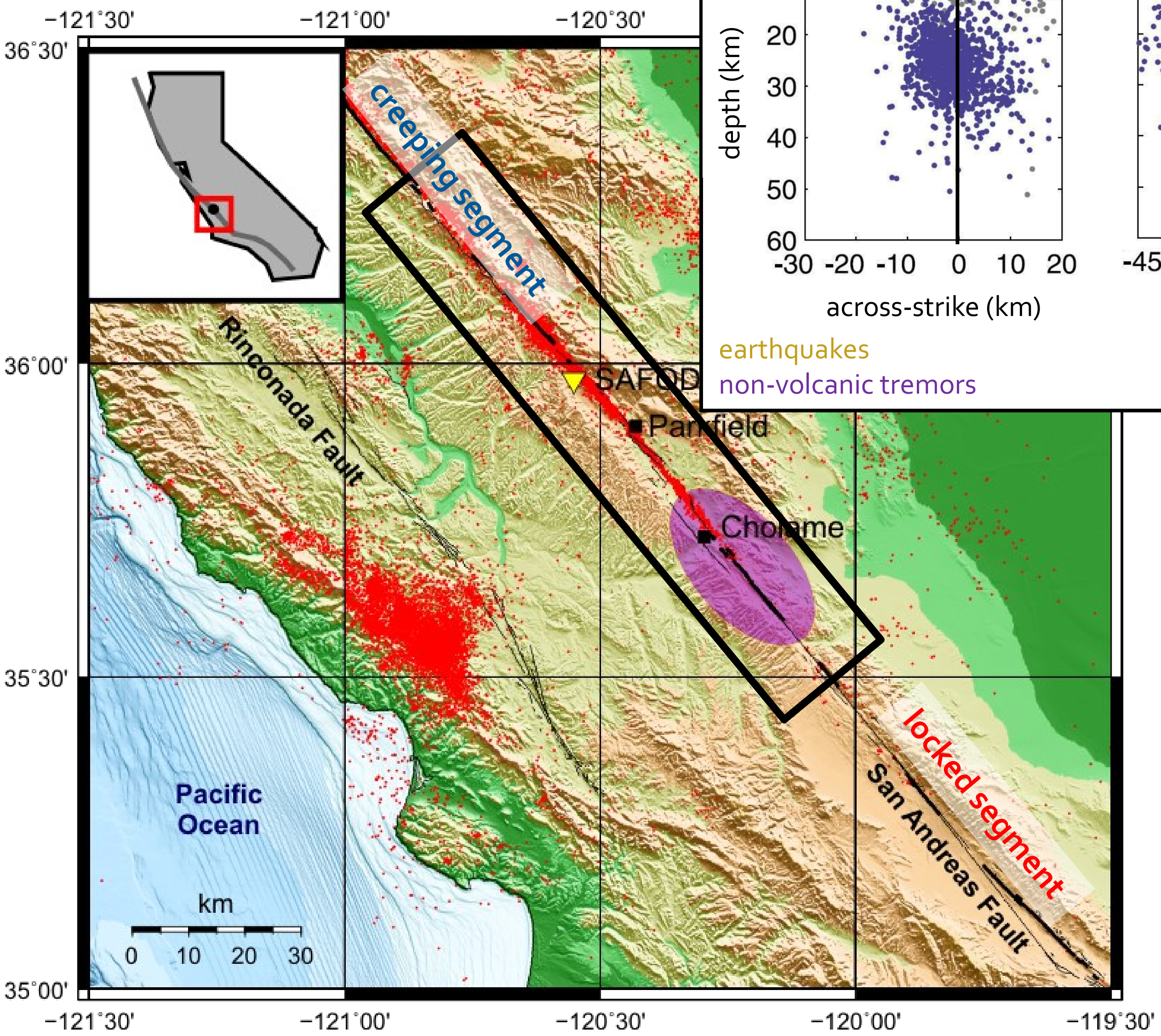

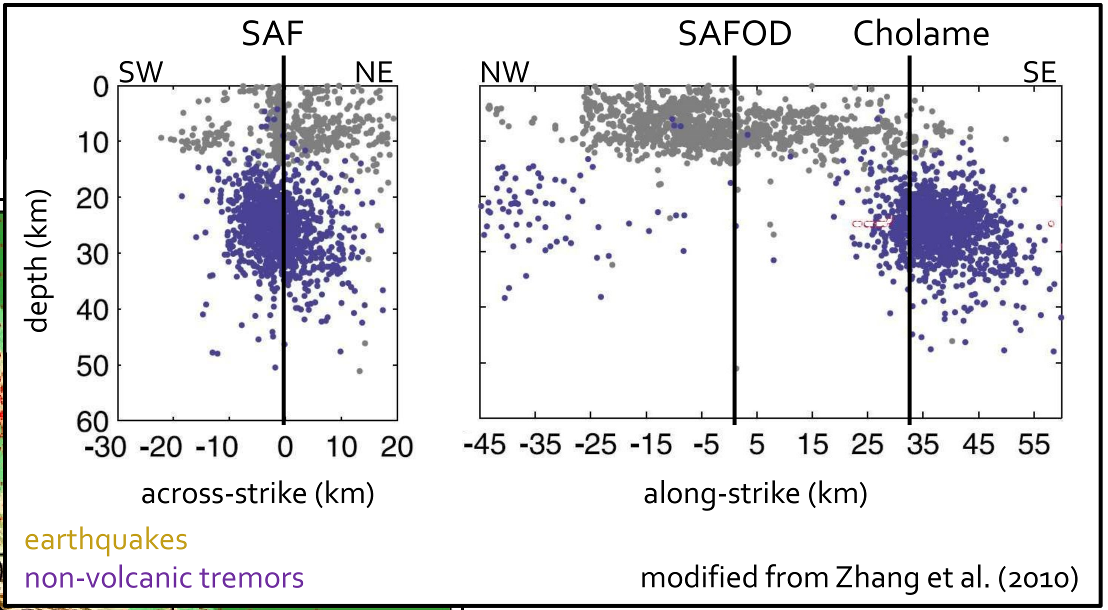

Seismicity $M > 1.0$ (NCDEC 2002-2011)

Non-volcanic tremor (e.g., Nadeau & Dolenc, 2005; Zhang et al., 2010)

Fluids in the SAF system

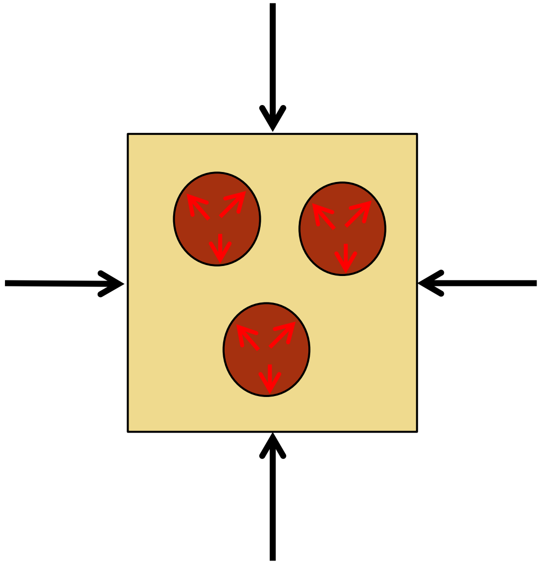

Fluids can reduce rock strength

- Mechanical weakening: elevated pore-fluid pressure
- Chemical weakening: production of weak mineral phases

Origin of fluids in the SAF system

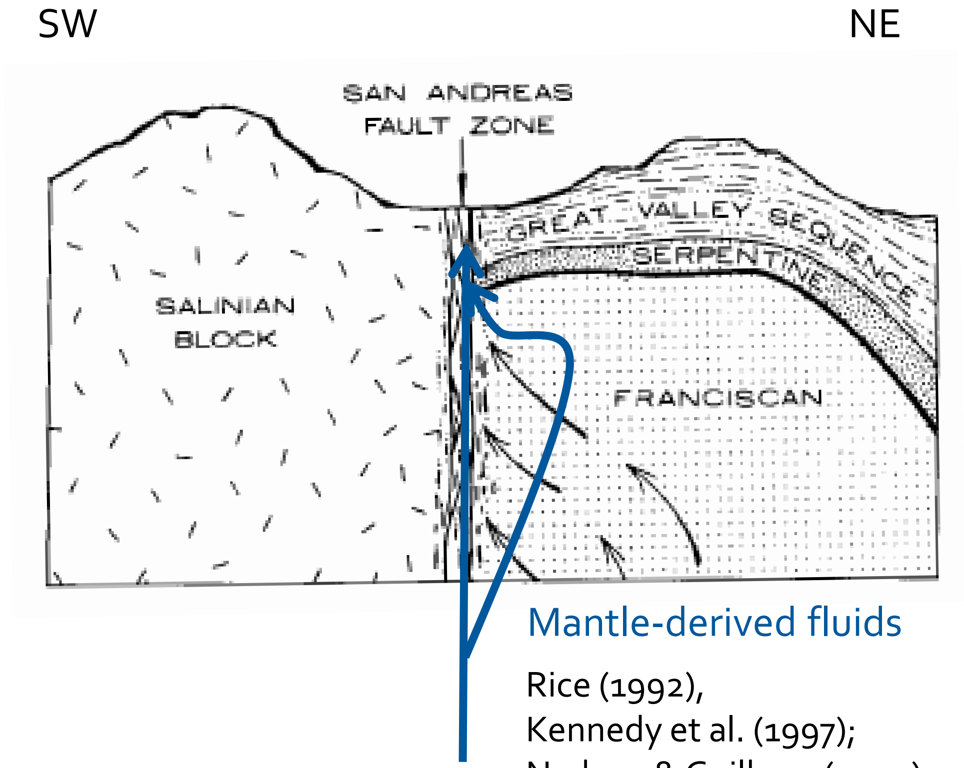

Crustal, metamorphic fluids

Irwin & Barnes (1975)

Mantle-derived fluids

Rice (1992),
Kennedy et al. (1997);
Nadeau & Guilhem (2009)

Parkfield MT array

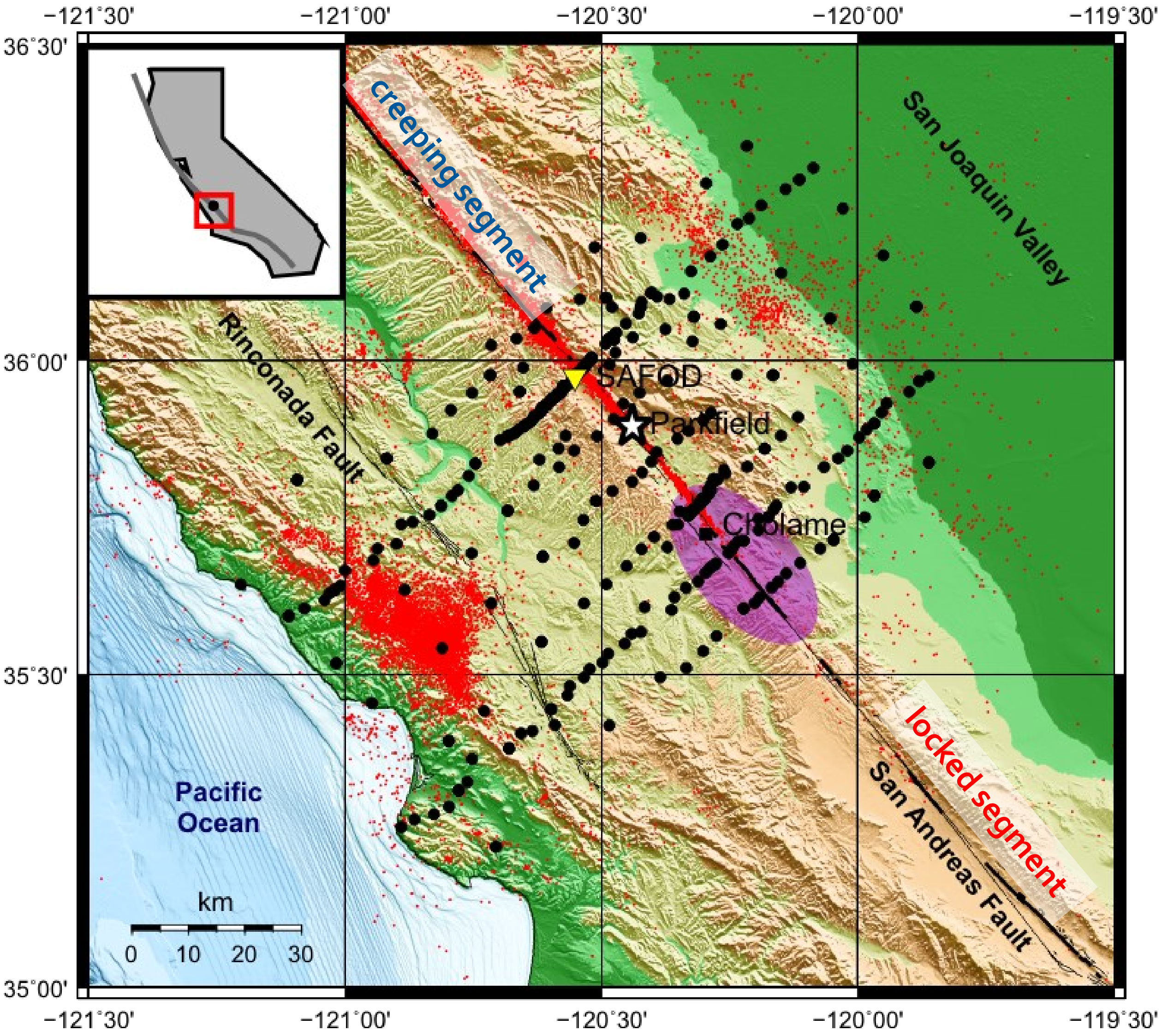

SAFOD
San Andreas Fault
Observatory at Depth

Seismicity $M > 1.0$
(NCDEC 2002-2011)

Non-volcanic tremor
(e.g., Nadeau & Dolenc, 2005;
Zhang et al., 2010)

Compilation of 2D conductivity models

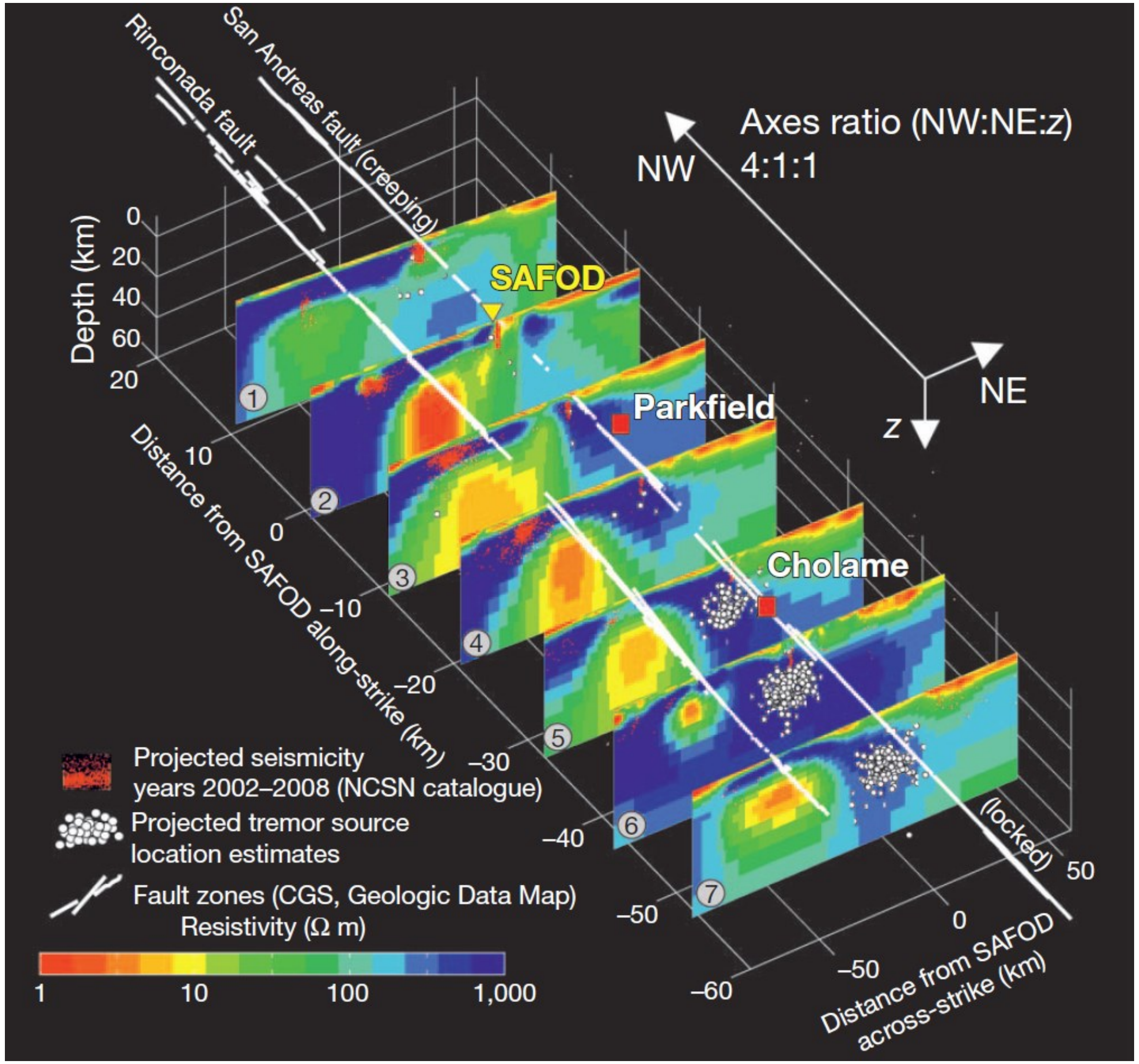

Along-strike variations of electrical conductivity structure:

- Creeping segment: conductive channel from deep crust / upper mantle to SAF
- Locked segment: conductive zone isolated from SAF

Becken et al., *Nature* (2011)

Resistivity cross-section at SAFOD (profile 2), creeping segment

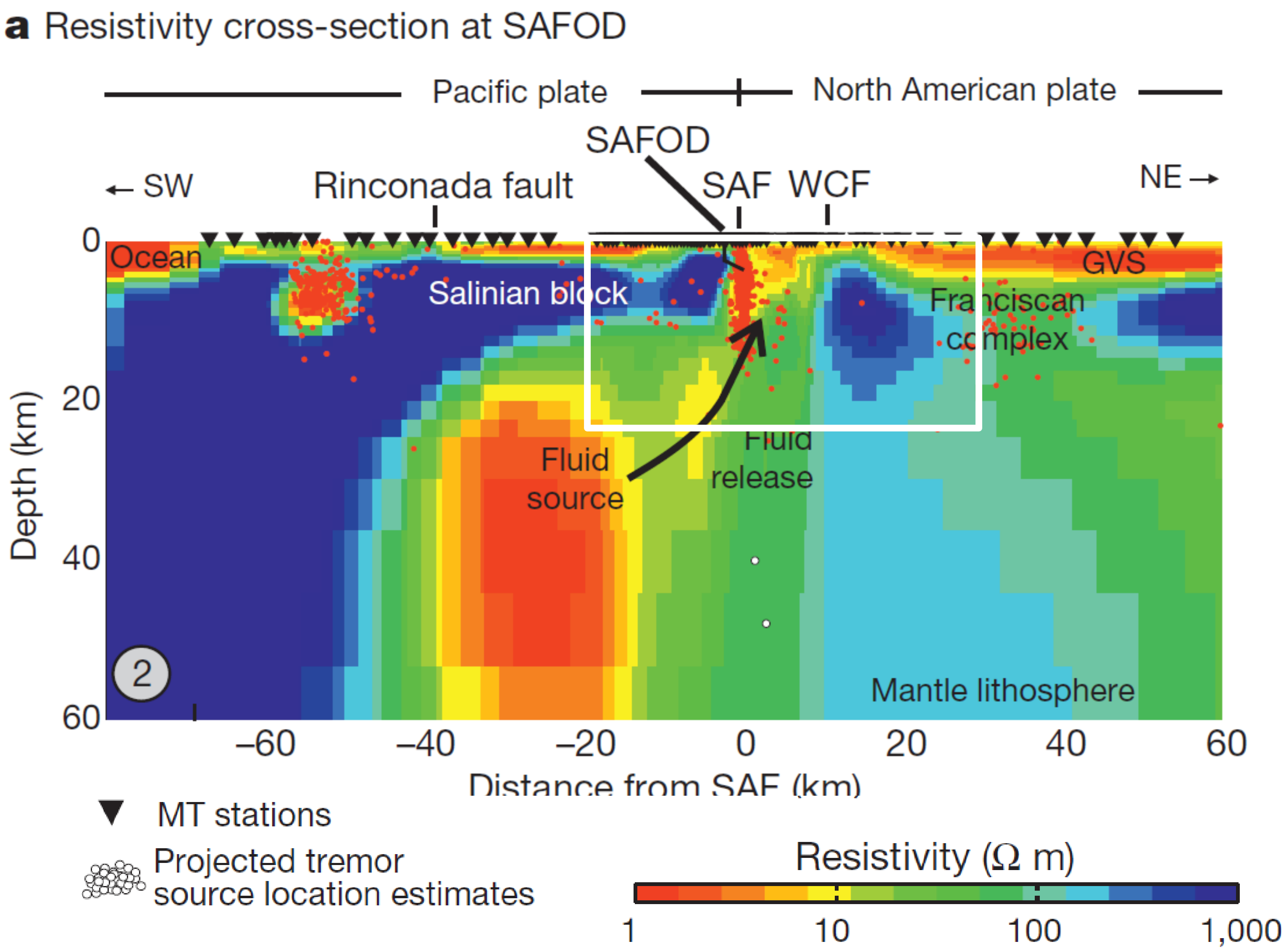

Becken et al., *Nature* (2011)

Resistivity cross-section at SAFOD (profile 2), creeping segment

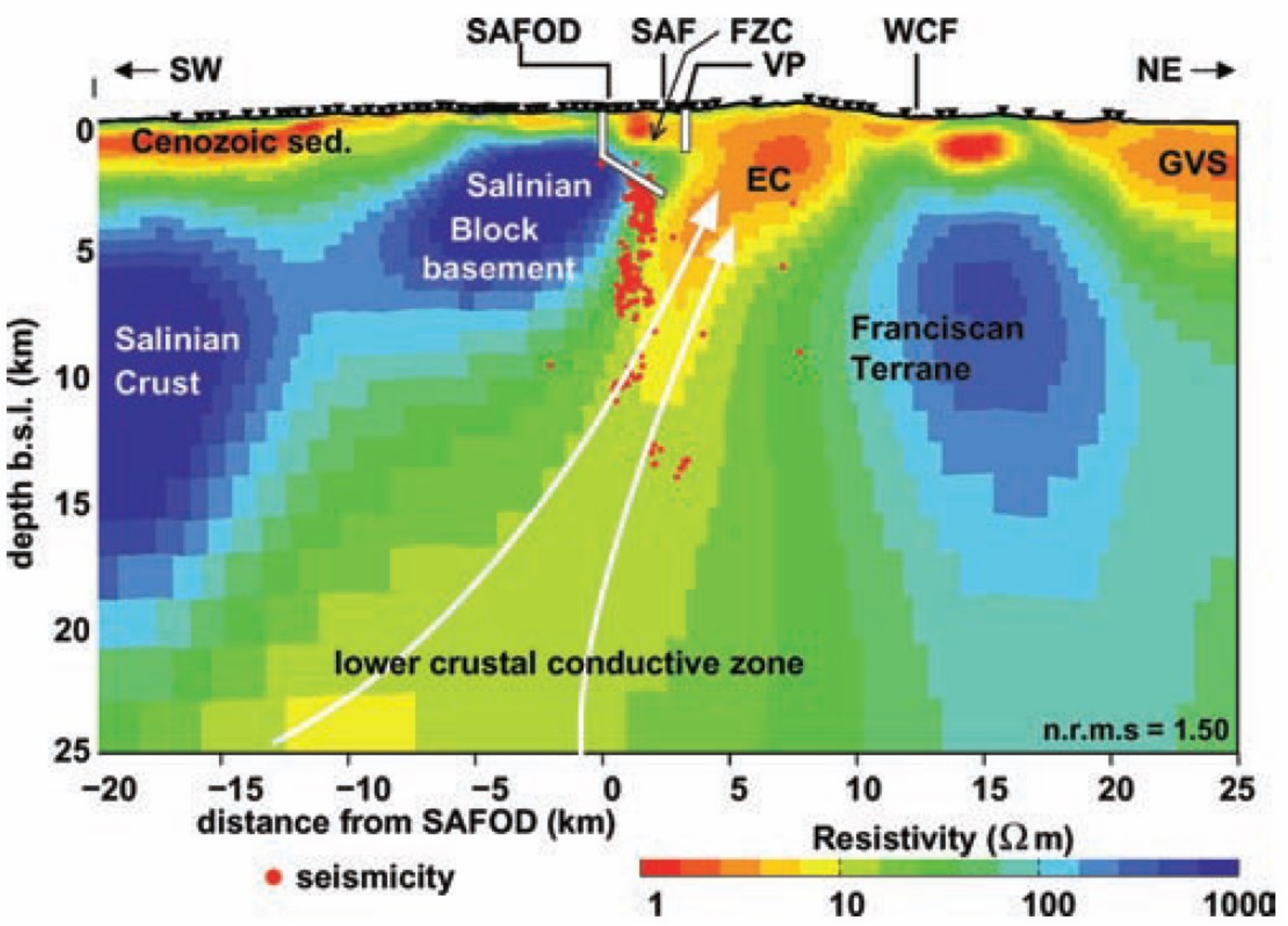

Becken et al. (2008)

Locked segment: Sensitivity study

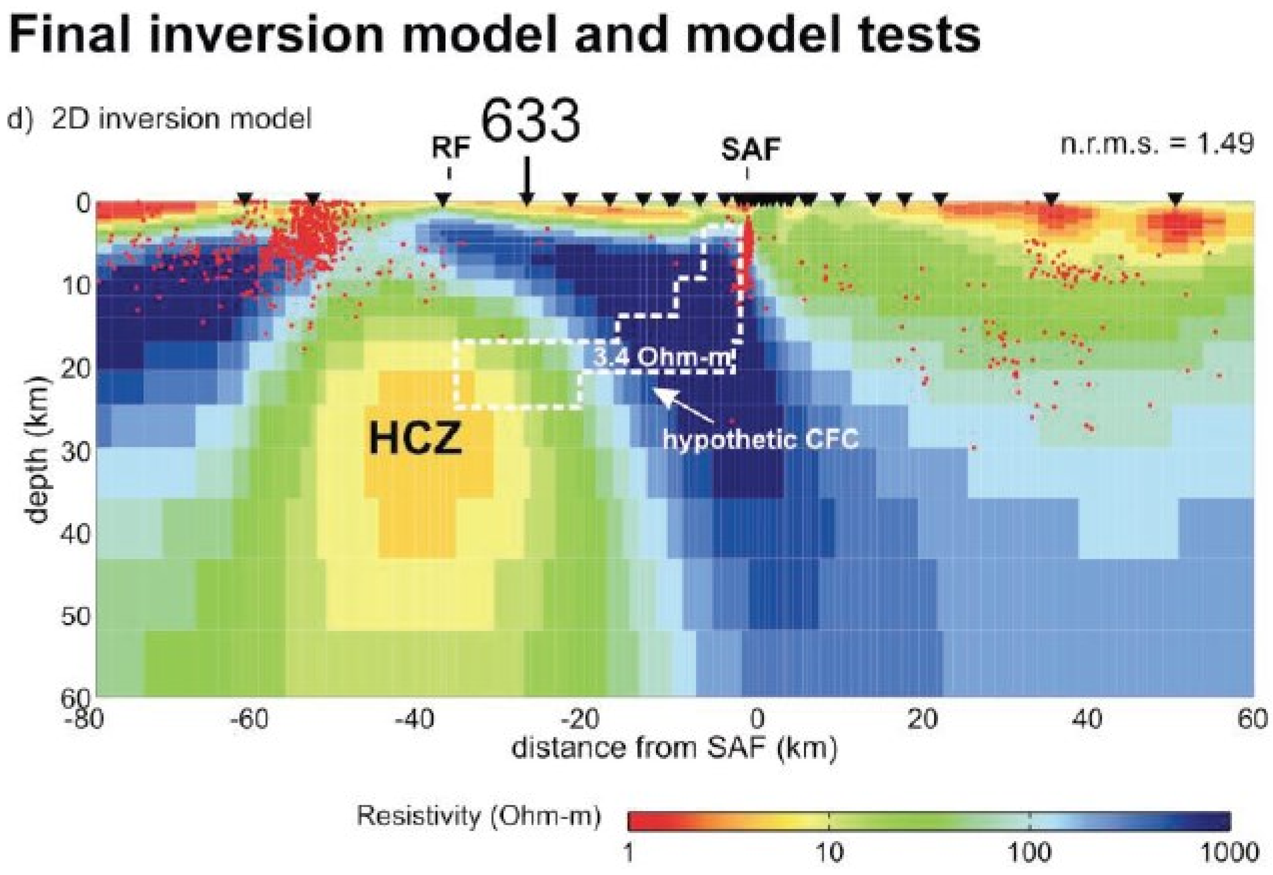

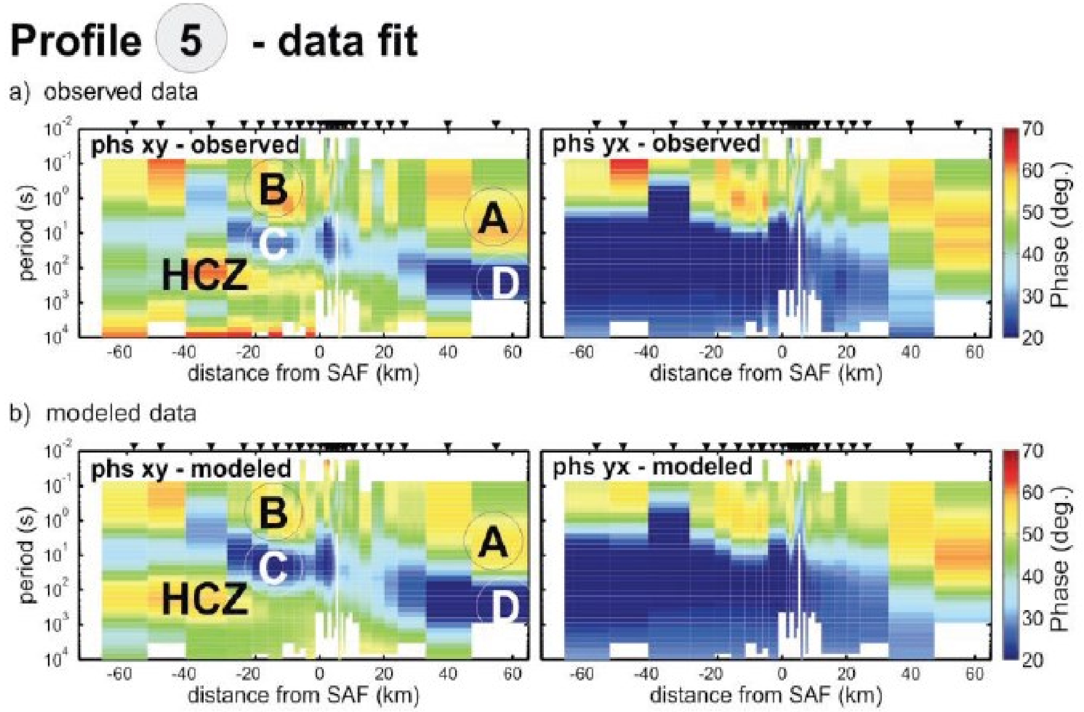

Becken et al.,
Nature (2011)

Locked segment: Sensitivity study

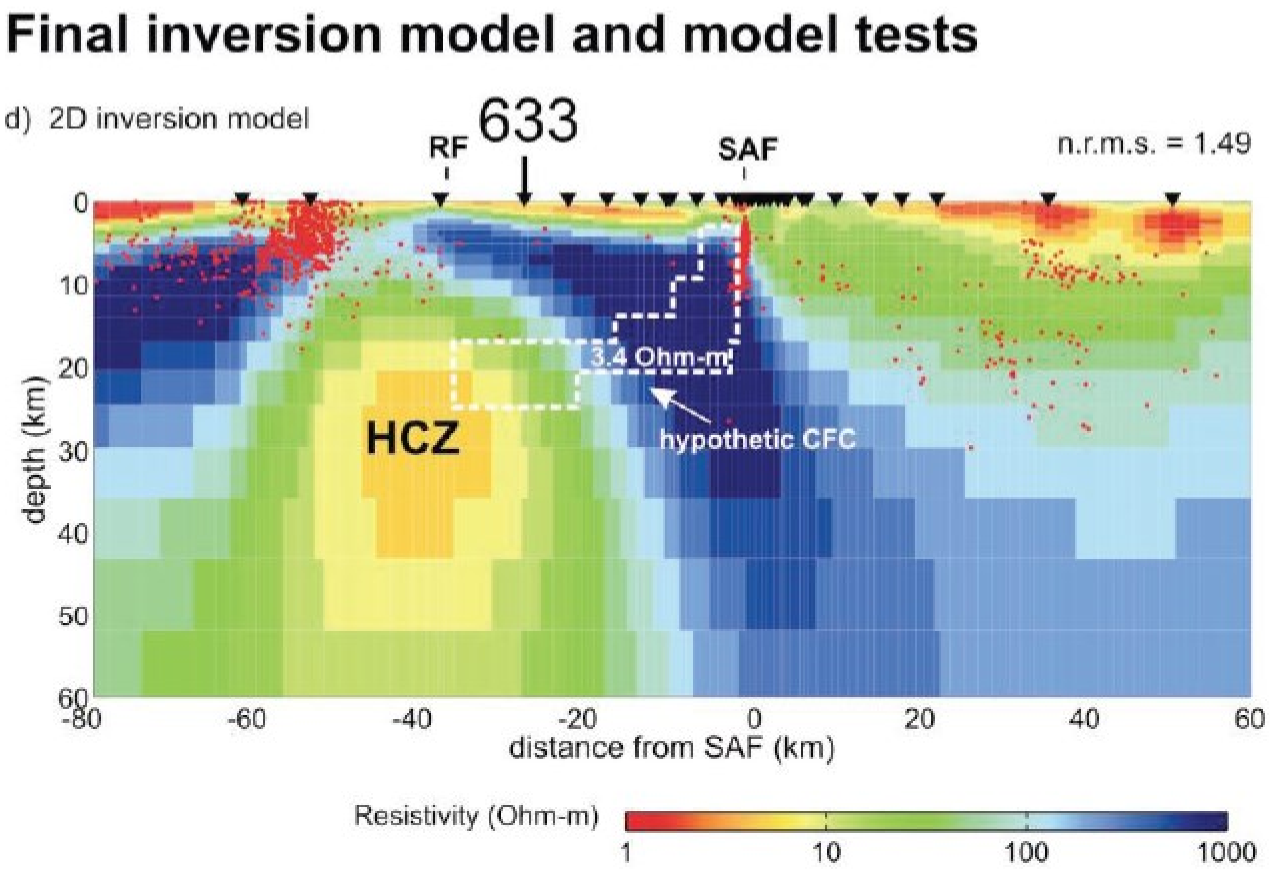

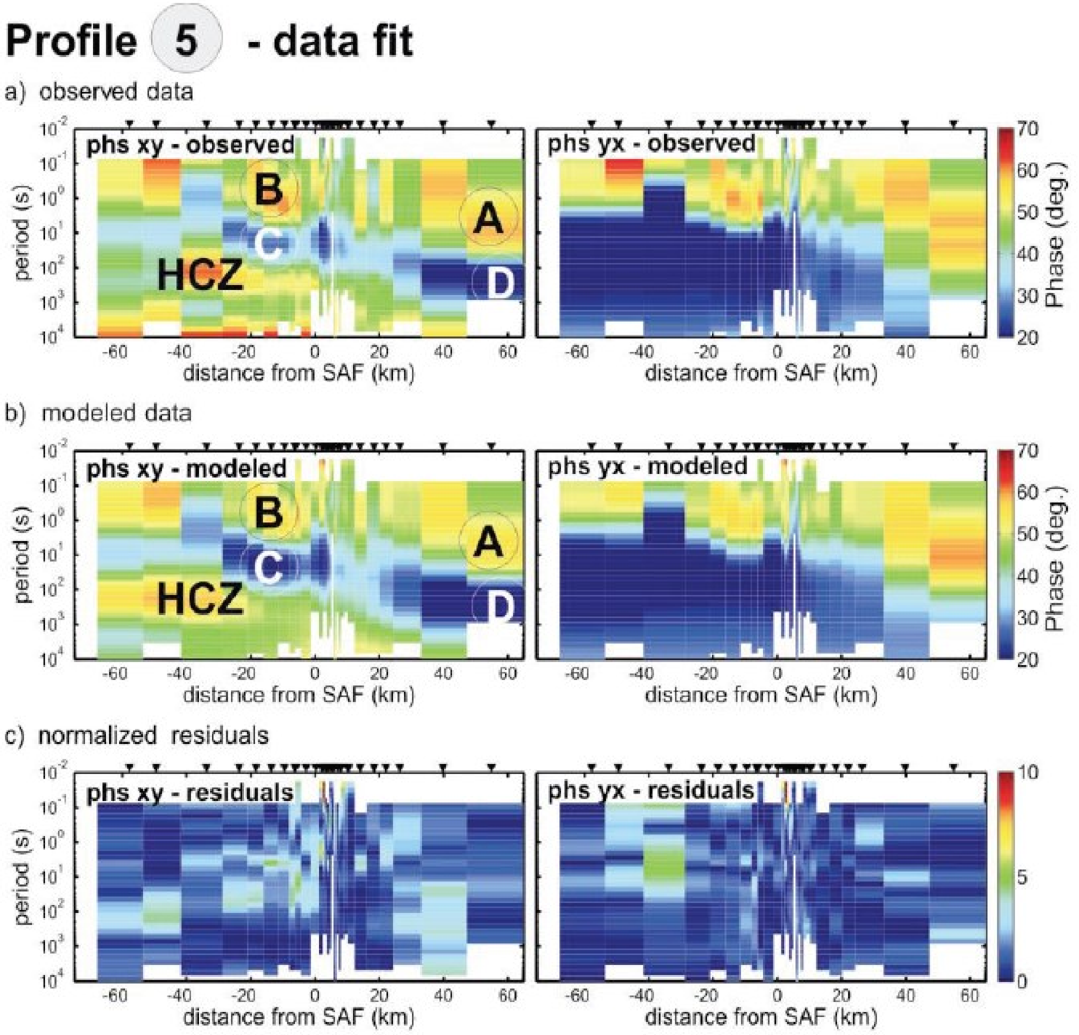

Becken et al., *Nature* (2011)

Locked segment: Sensitivity study

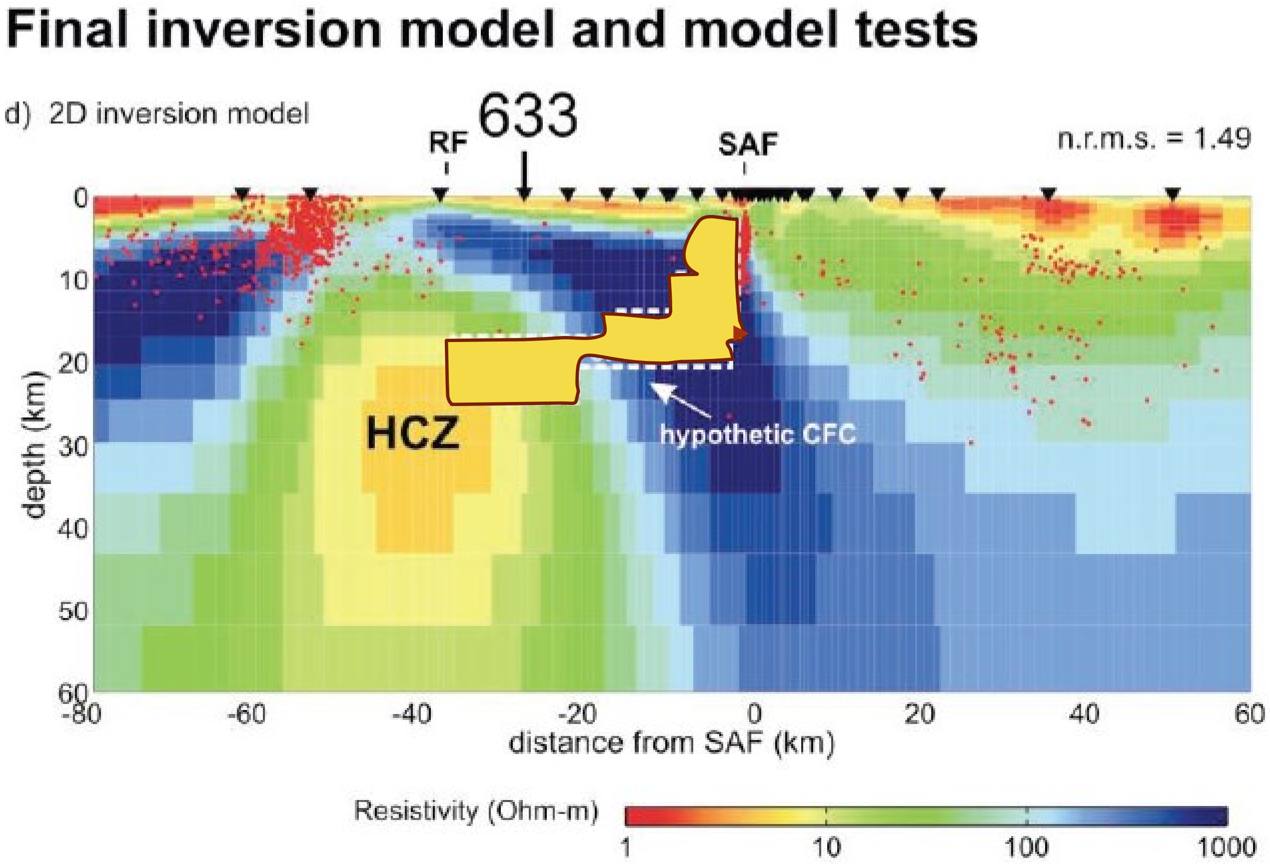

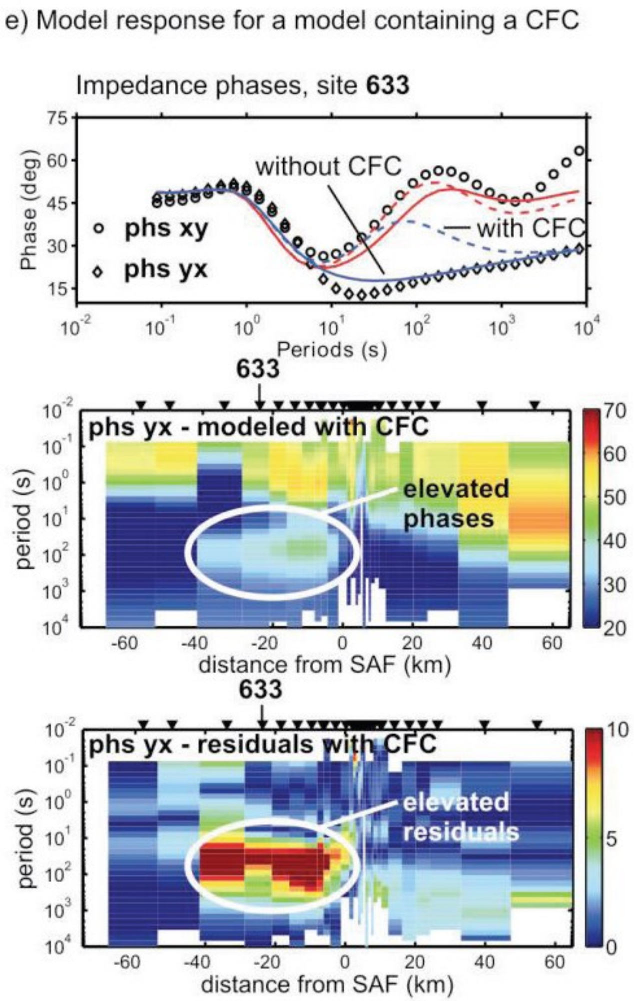

Becken et al., *Nature* (2011)

Summary

- MT imaged along strike variations of the San Andreas fault system
- Sensitivity tests: Simulation of alternative models

Creeping fault

- **MT**: Electrically conductive channel connects conductive zone (fluid reservoir) at mantle depths to SAF
- **Interpretation**: Mantle-derived fluids can enter the SAF system, reduce shear strenght, earthquakes < M6.0

Locked fault

- **MT**: Electrically conductive conductive zone (fluid reservoir) at mantle depths separated by resistive material from SAF
- **Interpretation:**
  - Fluids are trapped at lower crustal to upper mantle depths, no fluids in fault zone, strong fault → earthquakes with M > 6.0 possible.
  - Non-volcanic tremors are located at boundaries of fluid reservoir.
    Tremors are probably result of episodic fluid release caused by episodic stress changes such as teleseismic events etc.

Himalaya, Tibetan Plateau

nature Vol 438|3 November 2005|**doi:10.1038/nature04154**

LETTERS

Crustal rheology of the Himalaya and Southern Tibet inferred from magnetotelluric data

M. J. Unsworth[1], A. G. Jones[2], W. Wei[3], G. Marquis[4], S. G. Gokarn[5], J. E. Spratt[2] & the INDEPTH-MT team*

Map of the Tibetan Plateau and MT survey lines

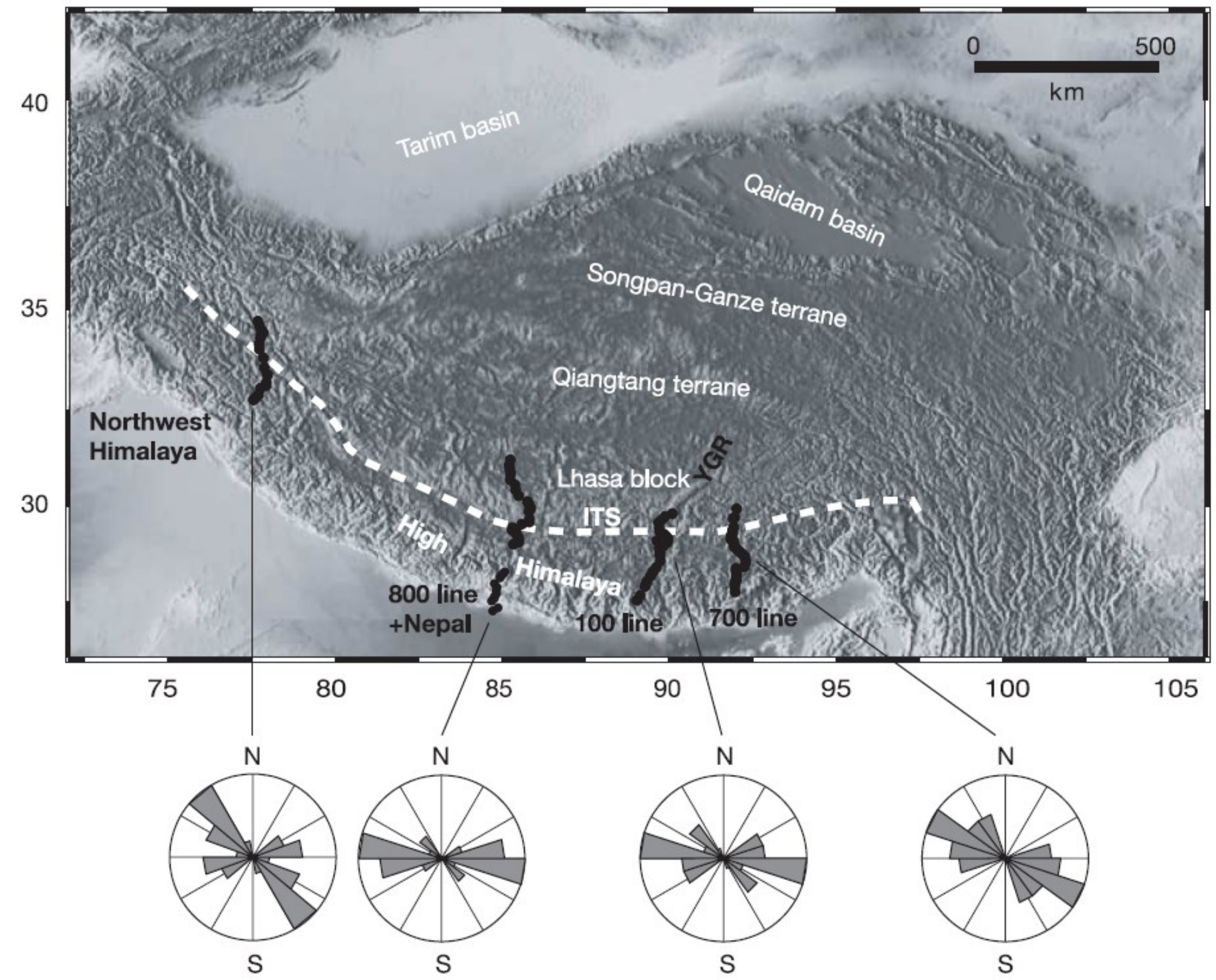

2D resistivity models

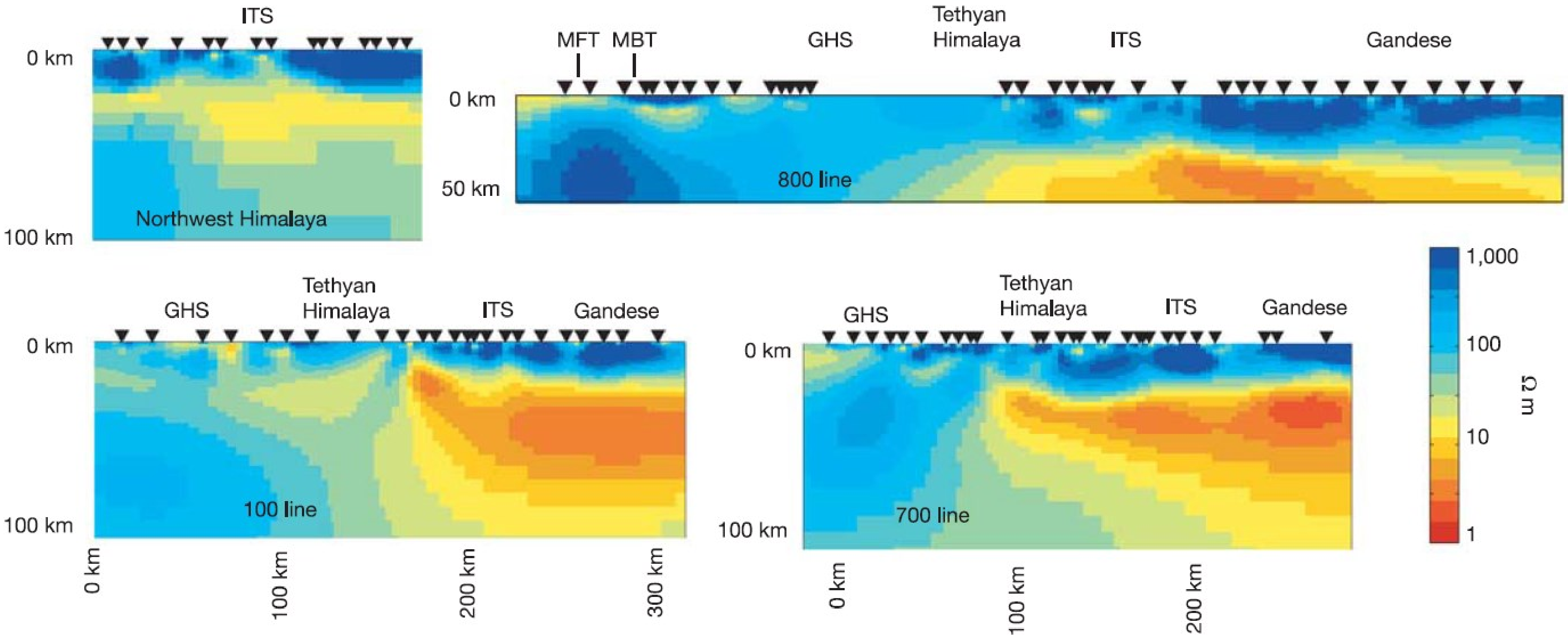

Figure 2 | Resistivity models for the four profiles derived from inversions of the MT data. The control parameters were varied to ensure that the final models were well defined. The MT data are fitted to a root-mean-square (r.m.s.) misfit in the range 1.5 and 2.5, which is statistically acceptable. Static shifts were removed from the data by allowing the inversion algorithm to estimate the coefficients. Other approaches were used and gave consistent results. Inverted triangles denote the locations of the MT stations. MFT, Main Frontal Thrust, MBT, Main Boundary Thrust; GHS, Greater Himalayan Sequence.

Electric resistivity and seismic reflecitivity

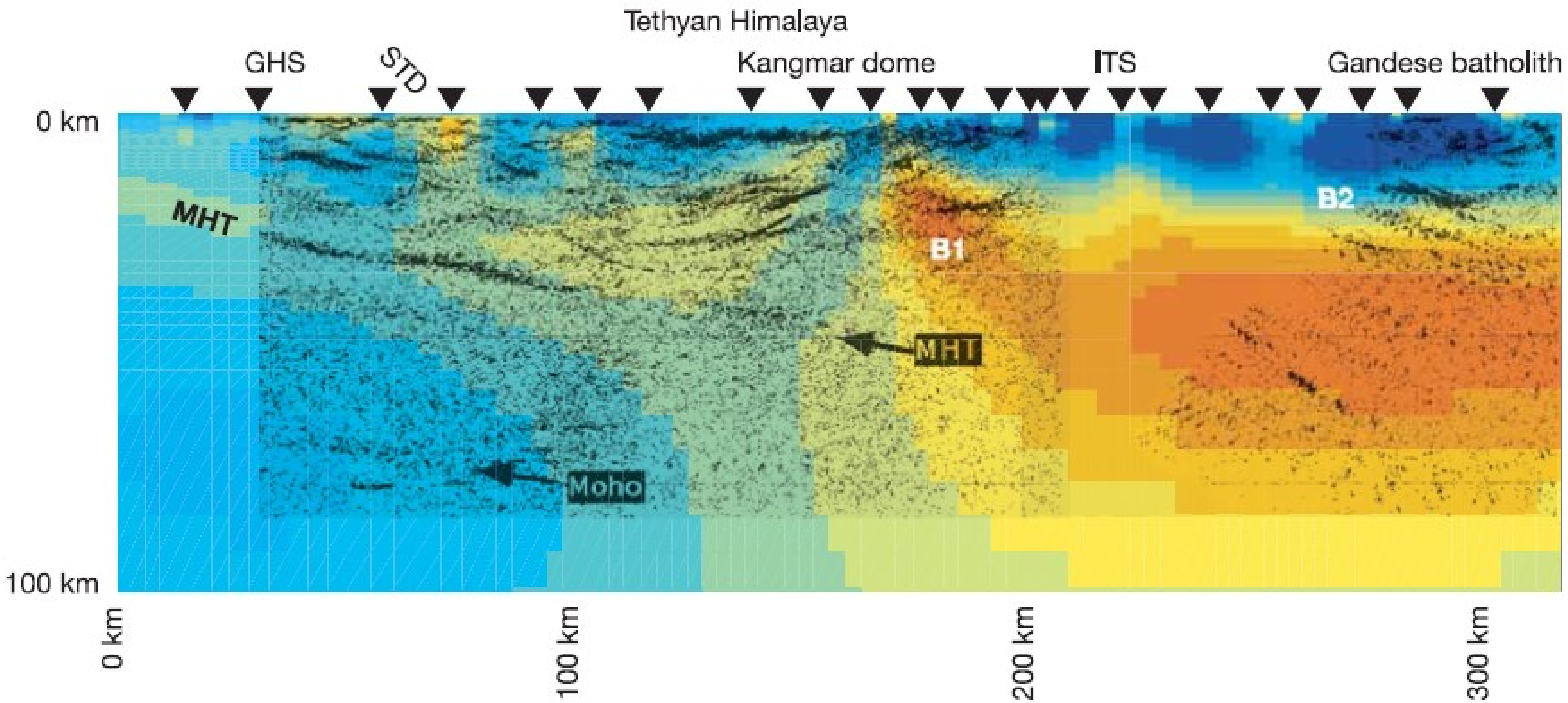

Figure 3 | Comparison of 100-line resistivity model and the INDEPTH common mid-point reflection profile. B1 and B2 are seismic bright spots that indicate zones with high fluid content. MHT, Main Himalayan Thrust; STD, Southern Tibetan detachment. Moho, Mohorovic discontinuity.

Electric resitivity → melt fraction → viscosity

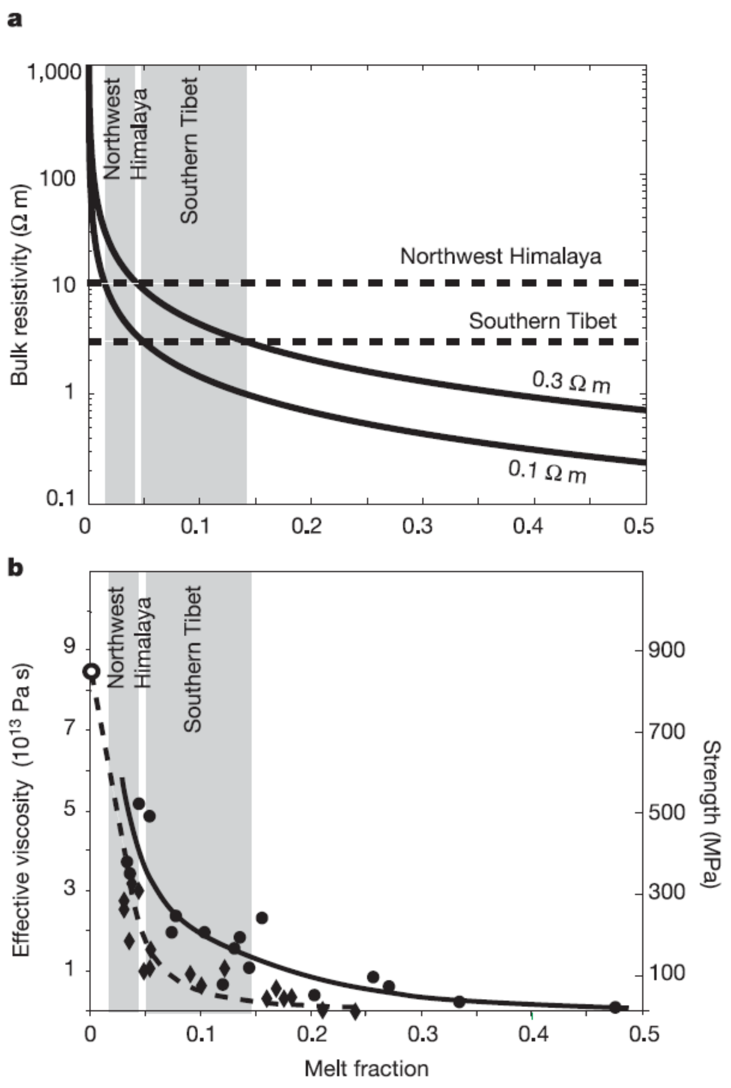

Figure 4 | Summary of laboratory measurements of the electrical resistivity and mechanical properties of a partially molten rock. a, Bulk electrical resistivity of partial melts as a function of melt fraction for melt resistivities of 0.1 and 0.3 Ω m; **b**, effective viscosity and strength of Westerly granite (circles) and aplite (diamonds) as a function of melt fraction[27]. Error bars are not shown, and solid and dashed lines show best-fitting trends for Westerly granite[28] and aplite[29]. The strength was computed for a strain rate of $10^{-5}\,s^{-1}$.

LETTERS
PUBLISHED ONLINE: 11 APRIL 2010 | DOI: 10.1038/NGEO830
nature geoscience

Crustal deformation of the eastern Tibetan plateau revealed by magnetotelluric imaging

Denghai Bai[1]*, Martyn J. Unsworth[2], Max A. Meju[3], Xiaobing Ma[1], Jiwen Teng[1], Xiangru Kong[1], Yi Sun[4], Jie Sun[5], Lifeng Wang[5], Chaosong Jiang[6], Ciping Zhao[6], Pengfei Xiao[1] and Mei Liu[1]

Survey region and research questions

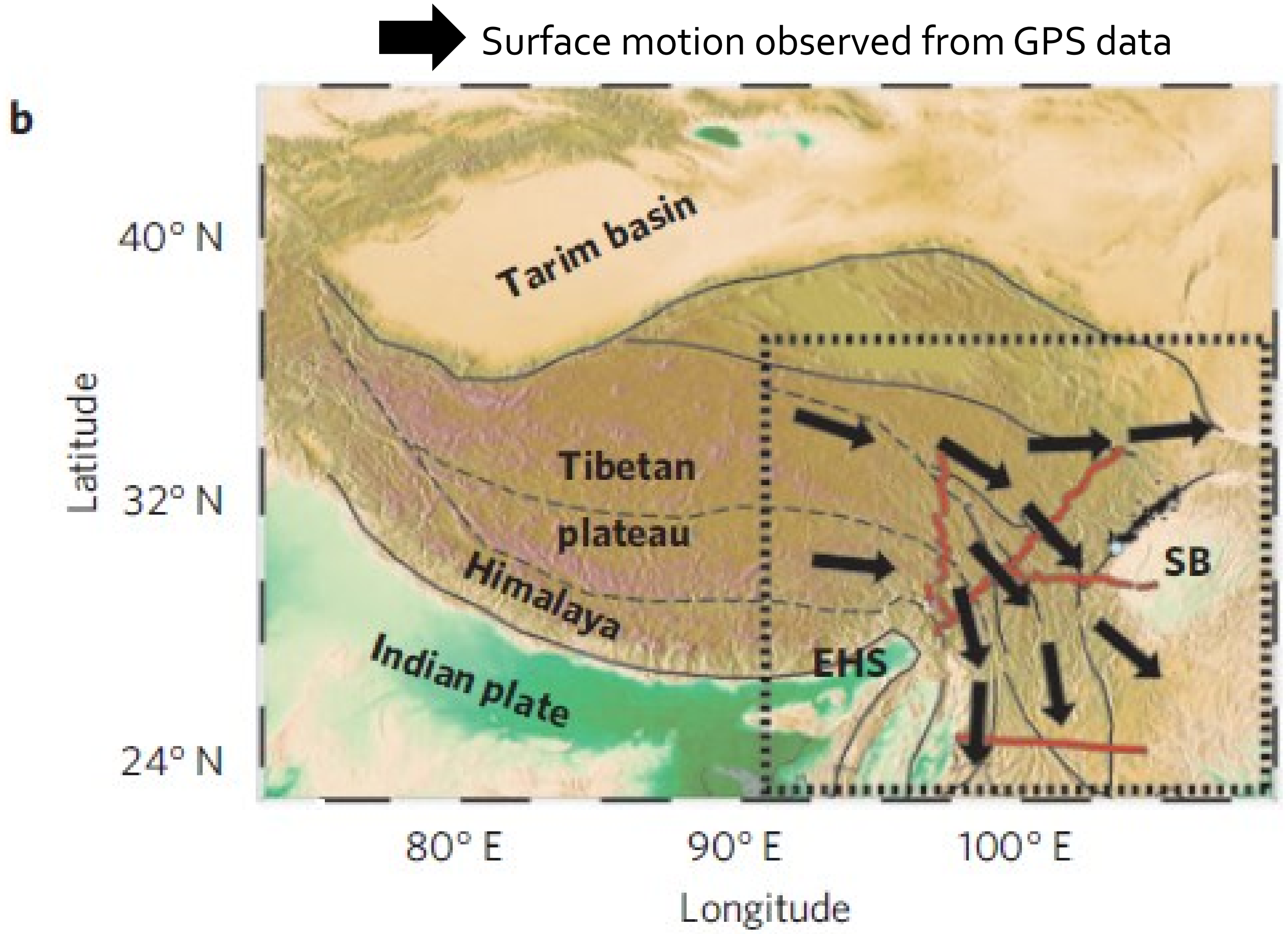

Research questions

- Which deformation processes are most significant at Indian-Asian collision zone including crustal thickening, delamination, flow in a weakened crust?
- Nature of surface motion?

MT parameters

- 4 profiles, 600 – 900 km long
- perpendicular to major geologic boundaries and flow
- 325 sites in total

Location of MT profiles and strike analysis

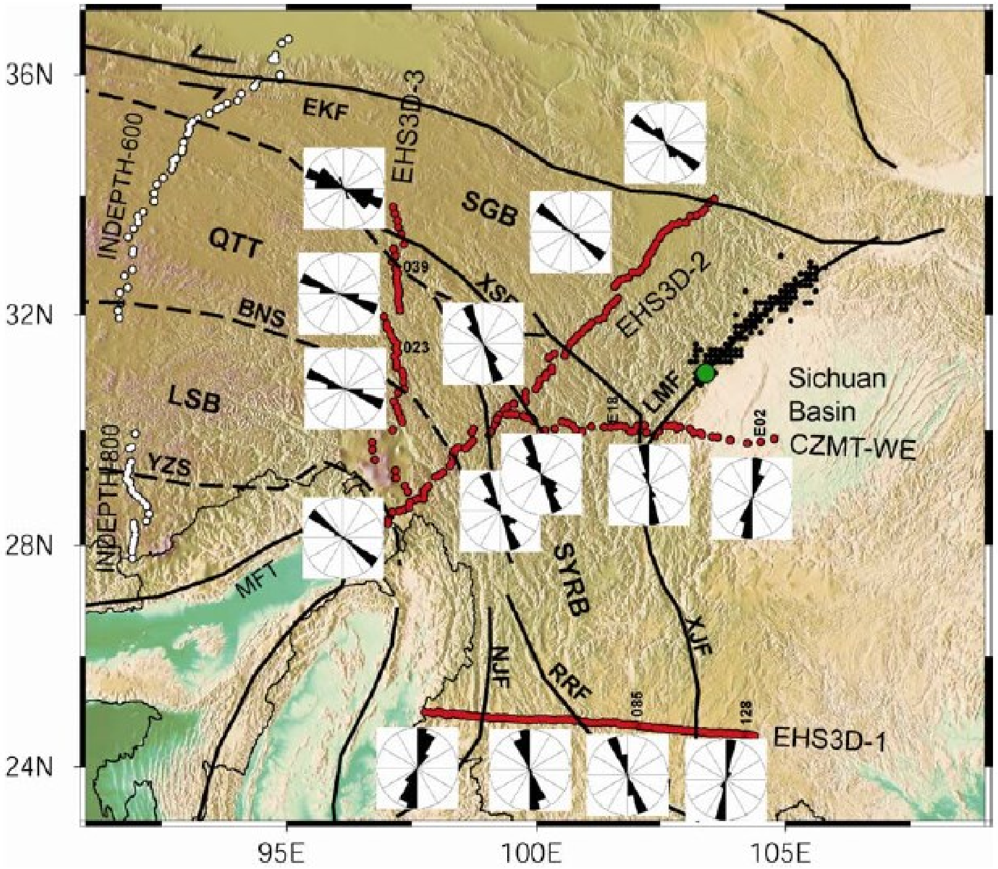

Figure S1: Rose diagrams showing geoelectric strike direction from tensor decomposition. The rose diagrams are for a single MT station that was representative of that section of each profile. Geological labels are the same as in Figure 1. Locations of stations plotted in Figures S2-S4 are labelled.

2D resistivity models and conductance

Cell height

Conductivity of model cell

Conductance $S = \sum h_i \sigma_i$

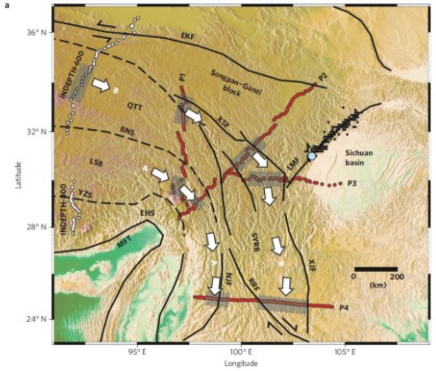

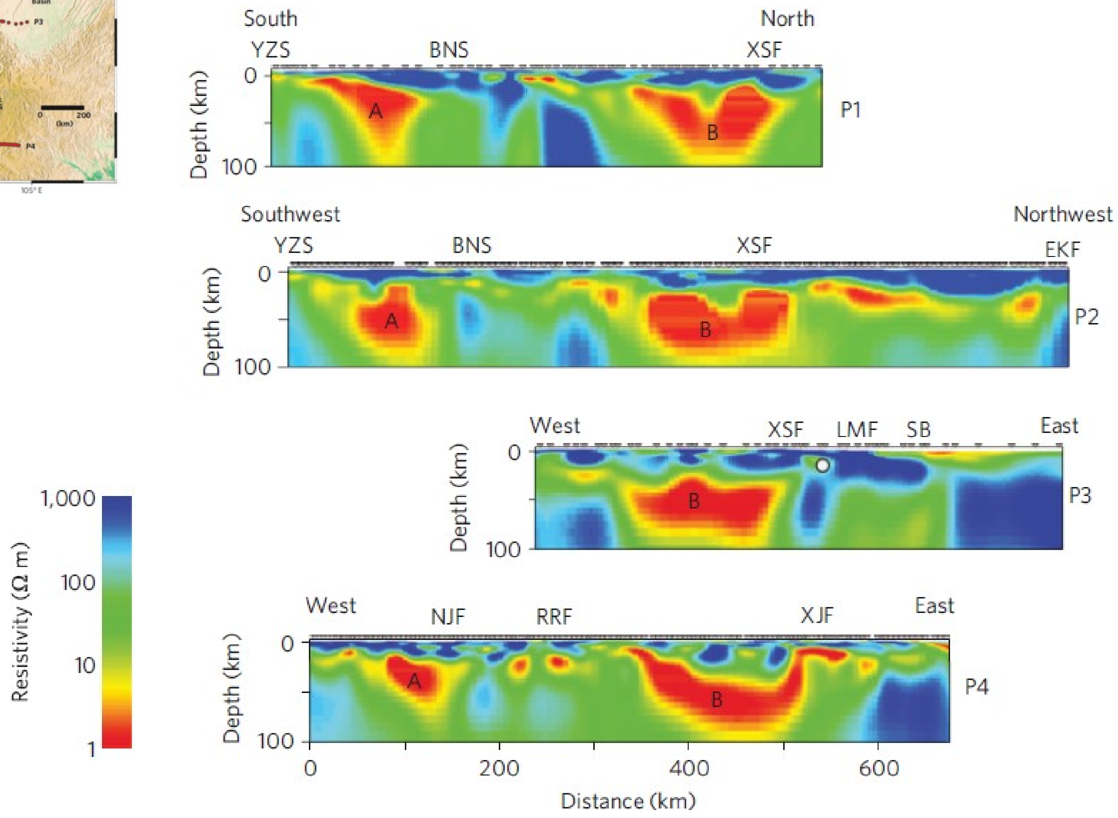

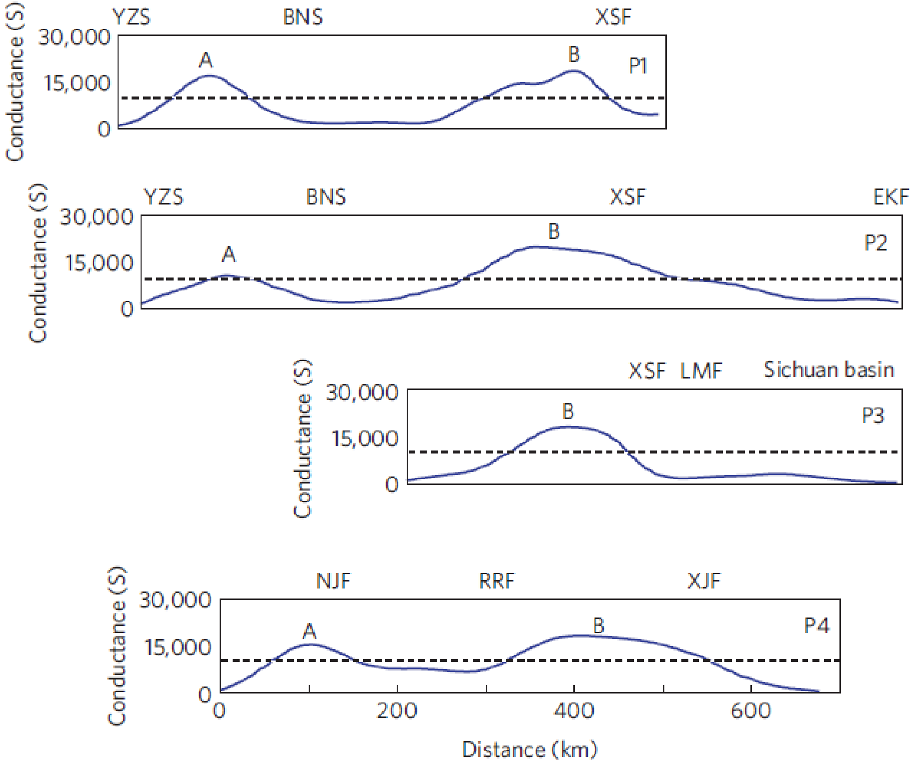

Conductance of stable crust: 200 – 500 S.

Tibet 1-2 orders of magnitude higher

2 correlated zones A and B

Estimation of fluid content for crustal conductors

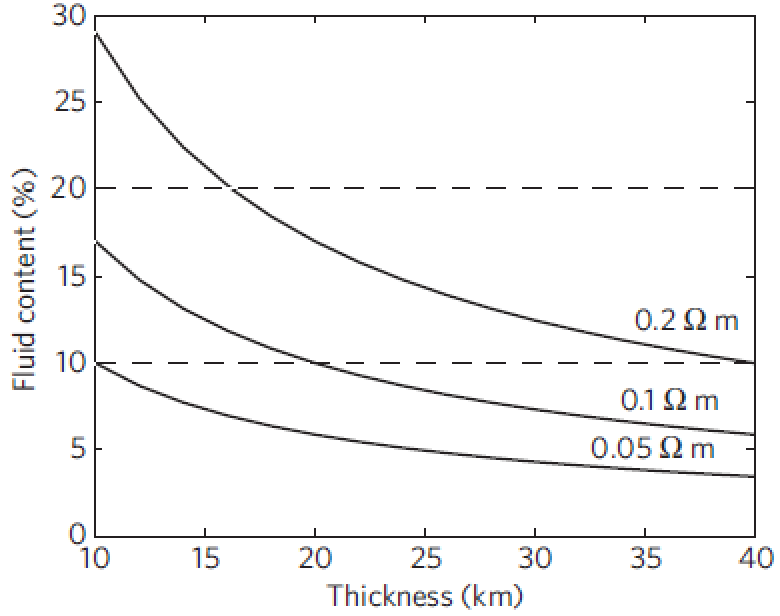

Figure 3 | Variation of thickness and fluid content (porosity) for a crustal layer with a conductance of 10,000 S. The three curves used values of resistivity for a fluid phase of 0.05, 0.1 and 0.2 Ω m. The fluid is assumed to be relatively well interconnected and the bulk resistivity is estimated with Archie's Law.

Recall:

Archie's Law

$$\rho_{ROCK} = \rho_{FLUID}\ A\ \phi^{-m}$$

Well connected porosity

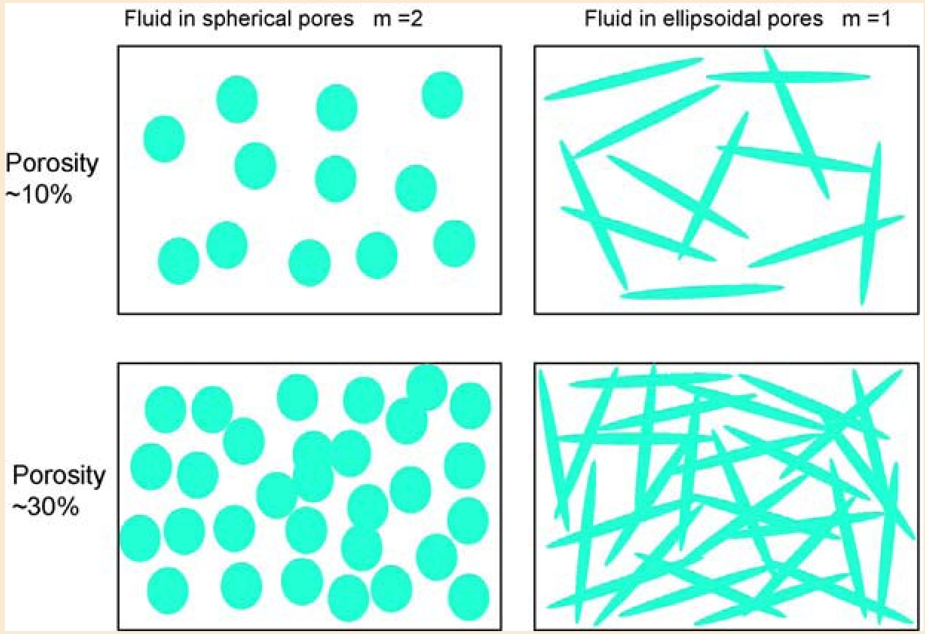

Estimation of fluid content for crustal conductors

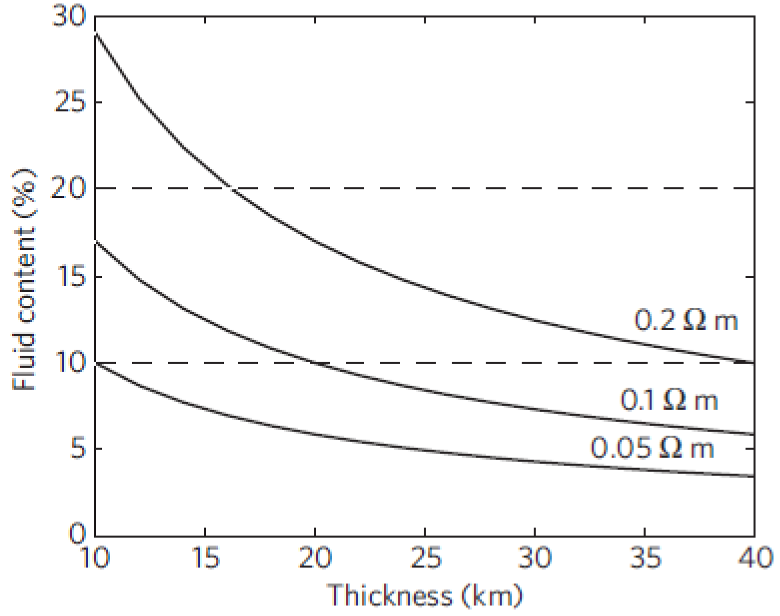

Figure 3 | Variation of thickness and fluid content (porosity) for a crustal layer with a conductance of 10,000 S. The three curves used values of resistivity for a fluid phase of 0.05, 0.1 and 0.2 Ω m. The fluid is assumed to be relatively well interconnected and the bulk resistivity is estimated with Archie's Law.

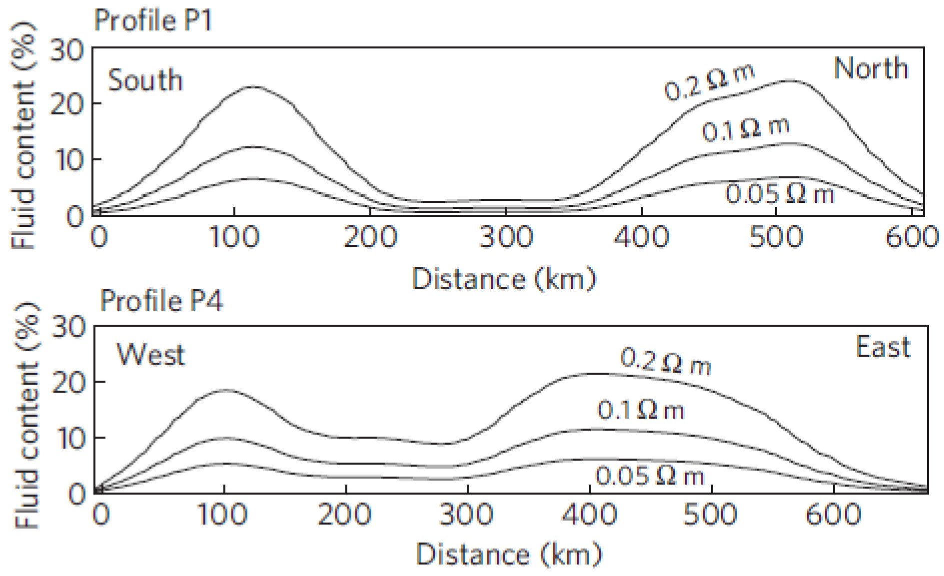

Figure 4 | Fluid content (porosity) of a 20-km-thick mid-crustal layer required to account for the conductance of profiles P1 and P4. The three curves use values of resistivity for the pure fluid phase of 0.05, 0.1 and 0.2 Ω m respectively. The fluid is assumed to be well interconnected and the bulk resistivity is estimated with Archie's Law.

A fluid content greater than 5% is sufficient to produce a factor of 10 strength reduction compared with the surrounding material with the same composition.

Summary

MT

- MT: 2 conductive channels imaged which correlate spatially with highest crustal flow rates.
- MT-derived: Fluid content of 5-20 % is required to explain the MT models.
- Additional info:
  A fluid content greater than 5% is sufficient to produce a factor of 10 strength reduction compared with the surrounding material with the same composition.
  Geodynamic modelling indicates that this strength contrast is sufficient for crustal flow to occur.
  Seismics: Crust and upper mantle are mechanically coupled and deform coherently.
- Together these arguments suggest that zones A and B could also act as shear zones that permit the relative motion of lithospheric blocks.

Continental scale arrays

EarthScope Transportable USArray, as of 2021

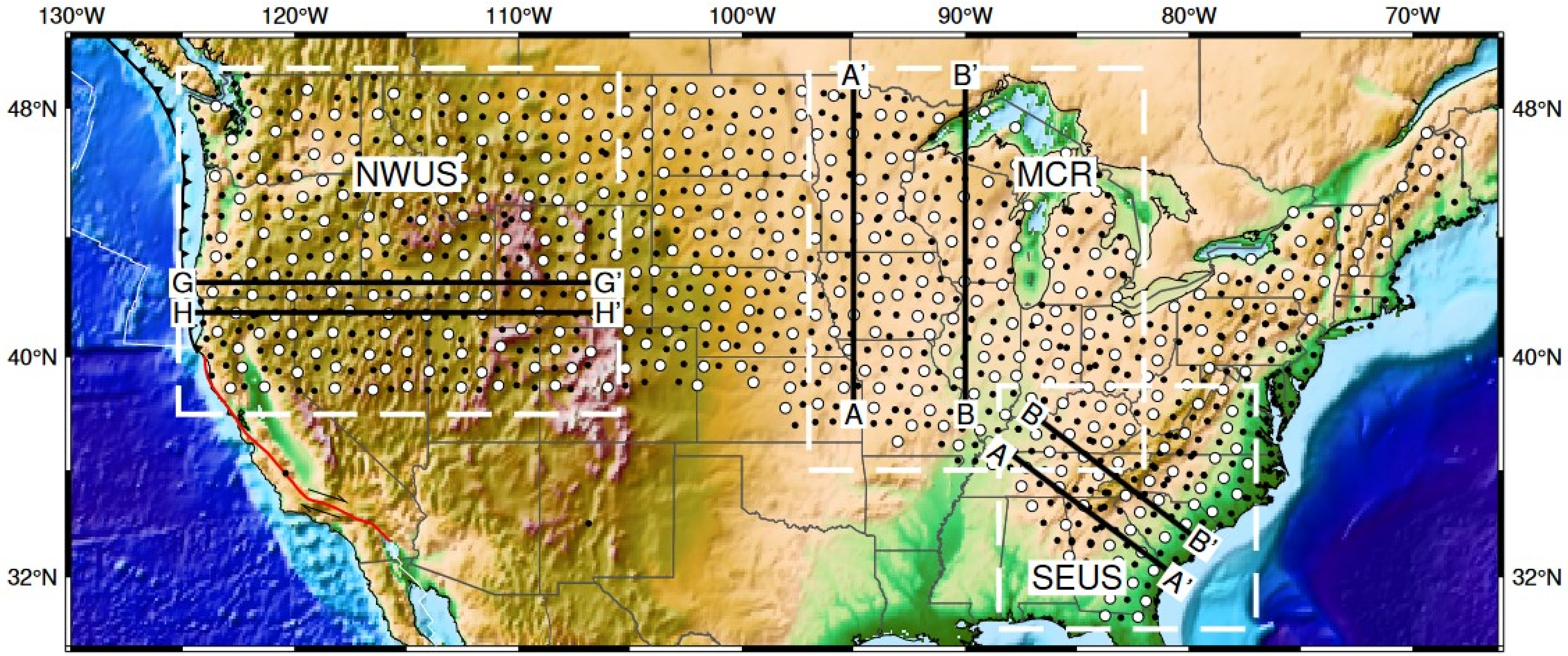

Yang et al. 2021

The Australian Lithospheric Architecture Magnetotelluric Project (AusLAMP)

- MT stations at 0.5 degree spacing (~55 km)
  → ~ 3000 sites in total

AusLAMP assists with
- understanding the geological make up of Australia
- understanding how geological processes work
- geological hazard mapping such as earthquake risk
- analysing risks to Australia's electricity infrastructure
- helping to identify potential mineral and energy resources at a broad regional scale, not at a local property scale

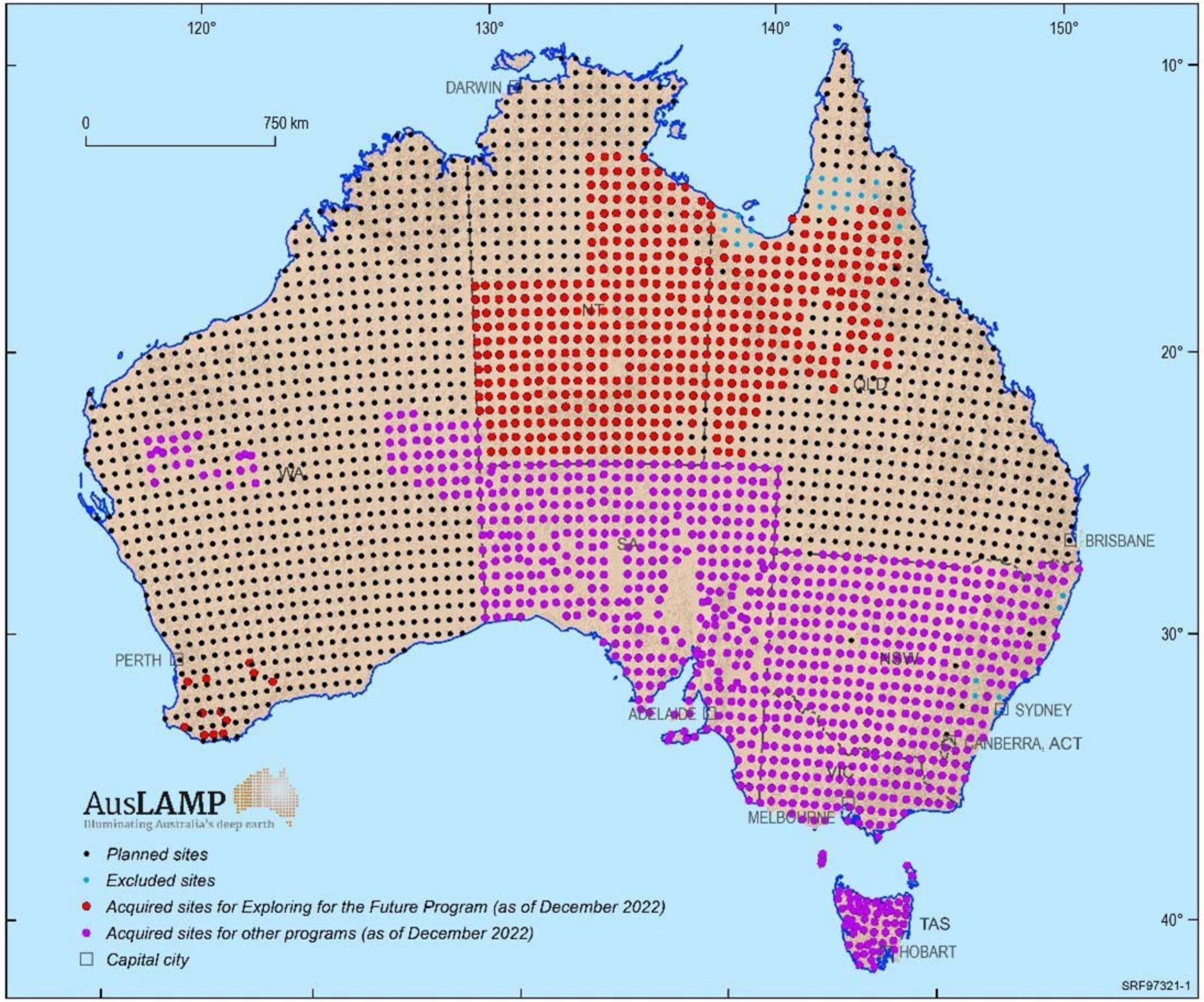

https://www.ga.gov.au/about/projects/resources/auslamp

MT case studies: (3) Continental scale arrays – really multipurpose

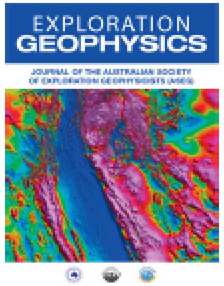

Taylor & Francis

Exploration Geophysics

ISSN: (Print) (Online) Journal homepage: https://www.tandfonline.com/loi/texg20

Comparative 3D inversion of magnetotelluric phase tensors and impedances reveals electrically anisotropic base of Gawler Craton, South Australia

Kristina Tietze, Stephan Thiel, Kate Brand & Graham Heinson

To cite this article: Kristina Tietze, Stephan Thiel, Kate Brand & Graham Heinson (20 Nov 2023): Comparative 3D inversion of magnetotelluric phase tensors and impedances reveals electrically anisotropic base of Gawler Craton, South Australia, Exploration Geophysics, DOI: 10.1080/08123985.2023.2281615

To link to this article: https://doi.org/10.1080/08123985.2023.2281615

MT study on the Gawler Craton in South Australia: How deep can we go?

Location of survey area in Australia

AusLAMP - Australian Lithospheric Architecture Magnetotelluric Project

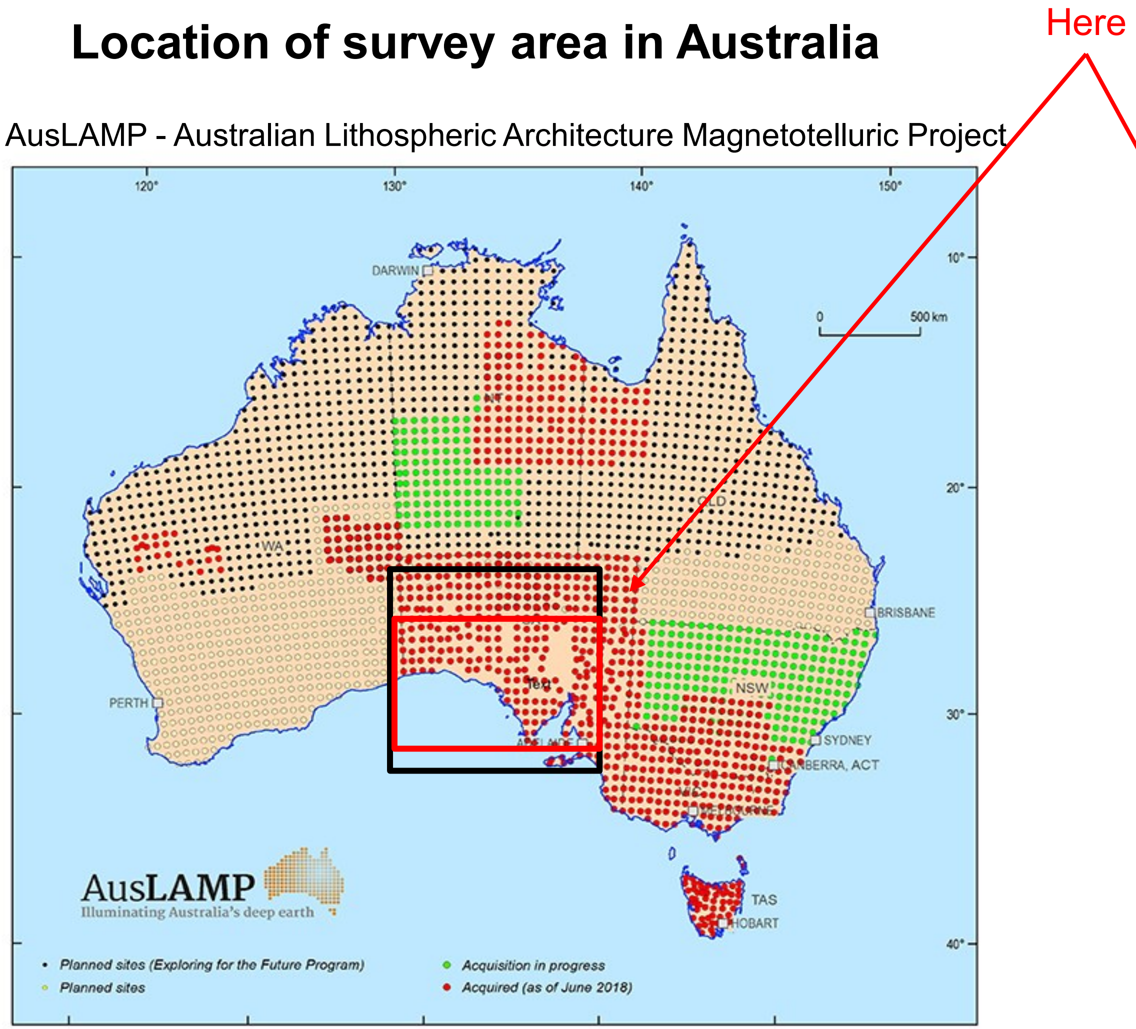

Geoscience Australia 2020

Topography and major geologic units

282 stations

24 periods

10 - 14,000 s

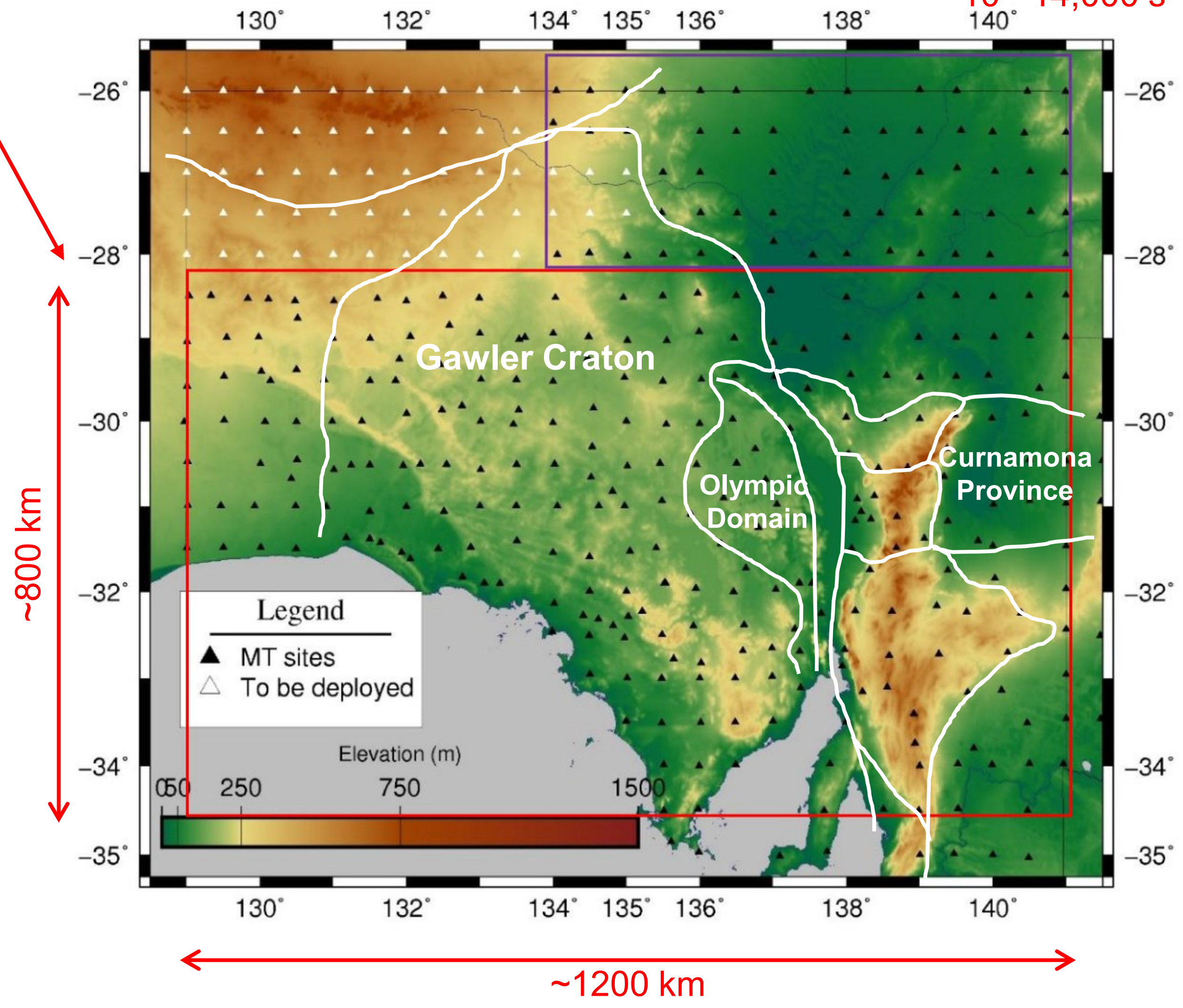

Modified from Robertson et al. 2018

Real part of induction vectors, Wiese convention.

282 stations

24 periods
10 - 14,000 s

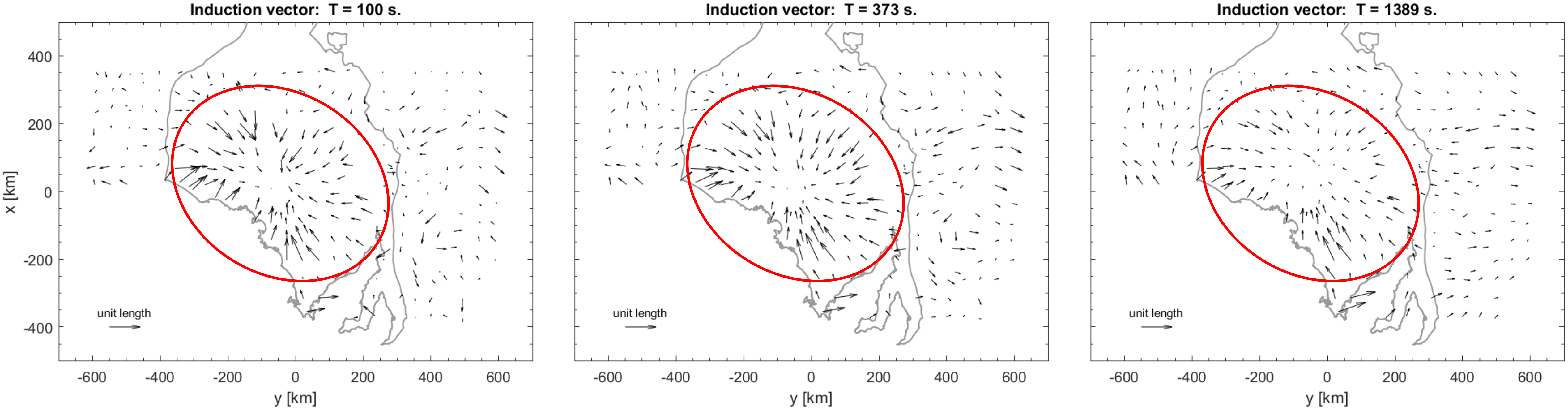

Induction arrows point away from craton edges.
Induction arrows (in Wiese convention) point away from conductors
→ …

MT data set – phase tensors

282 stations

24 periods
10 - 14,000 s

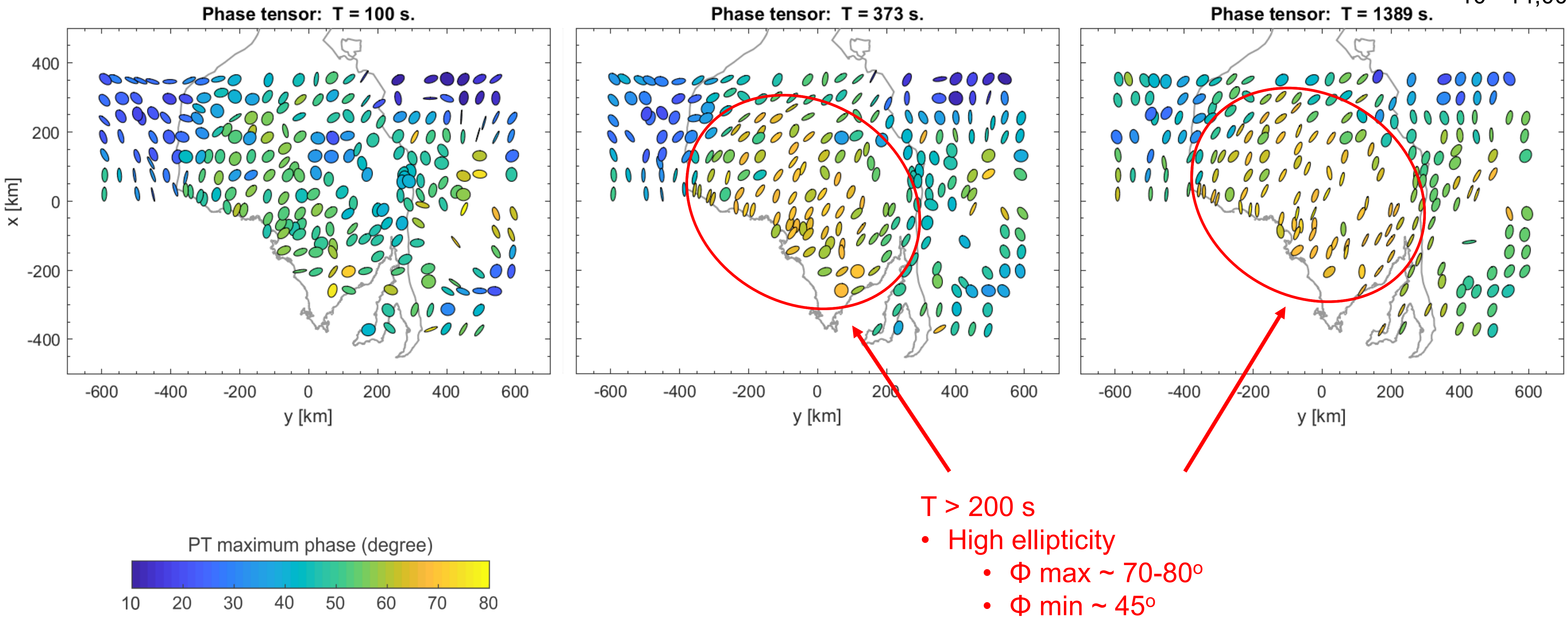

T > 200 s

- High ellipticity
  - Φ max ~ 70-80°
  - Φ min ~ 45°
- Major axes aligned ~ N23°E

3D resistivity structures, 0-70 km

Details and geologic interpretation see Thiel et al. (*in rev.*)

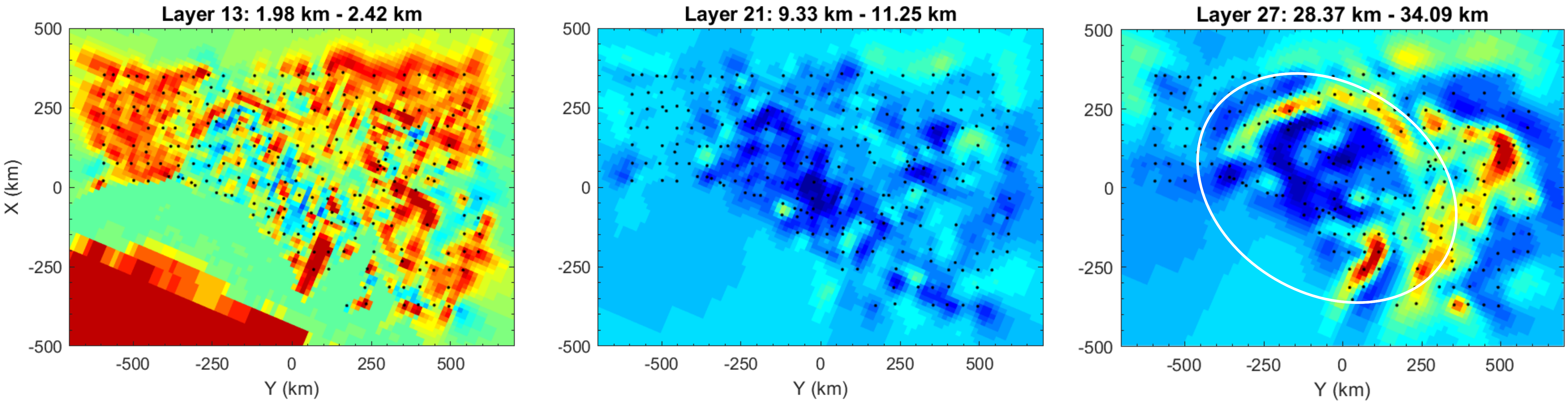

Induction arrows point away from craton edges.
Induction arrows (in Wiese convention) point away from conductors
A lot of conductive material along the egde of the Gawler Craton

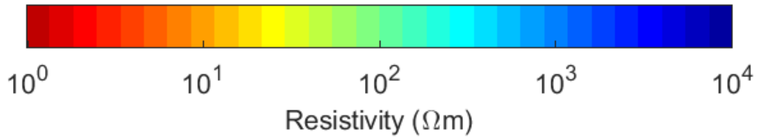

3D resistivity structures, 0-70 km

Details and geologic interpretation see Thiel et al. (*in rev.*)

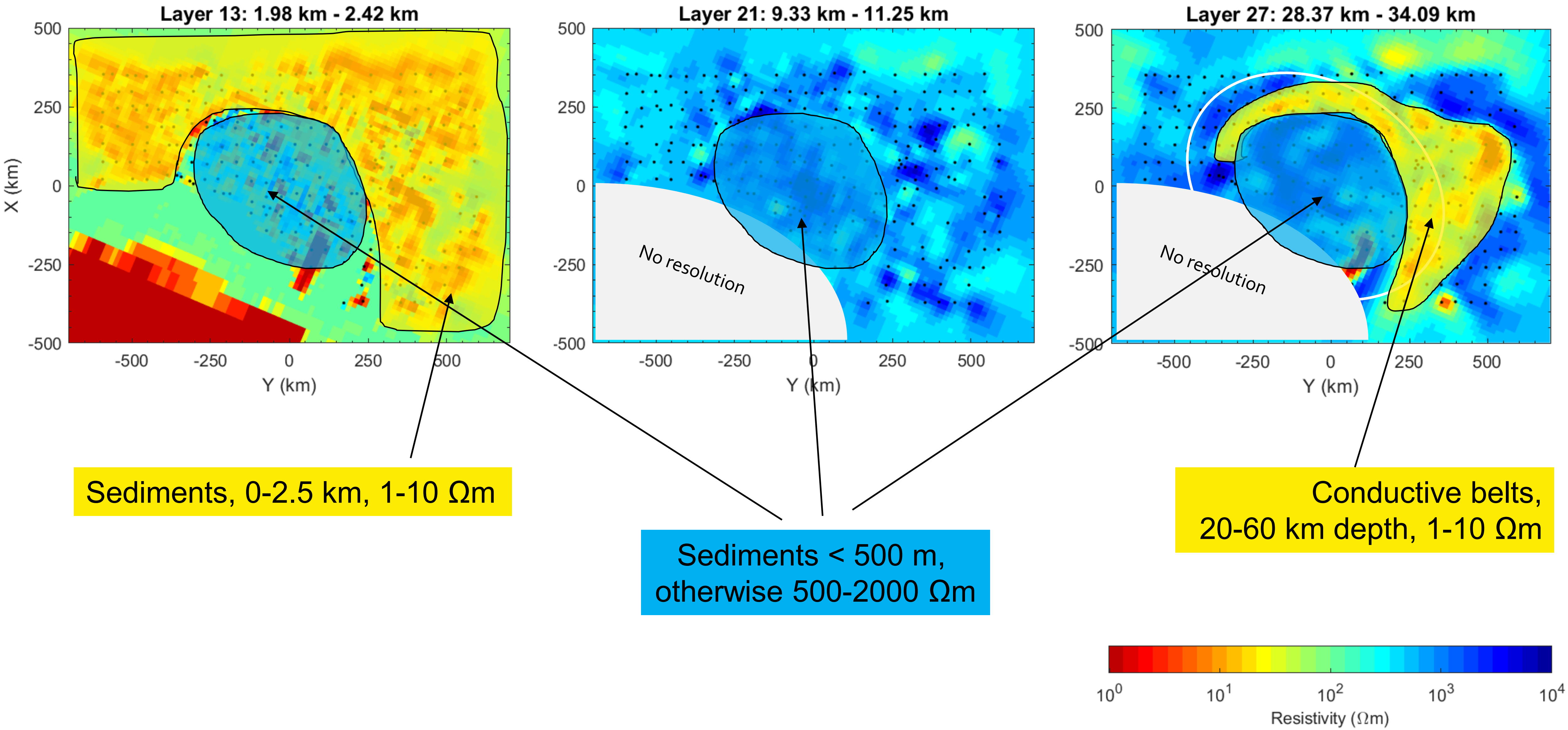

3D resistivity structures, 0-70 km

Sensitivity to 70(-100) km depth

Sensitivity to > 200 km depth

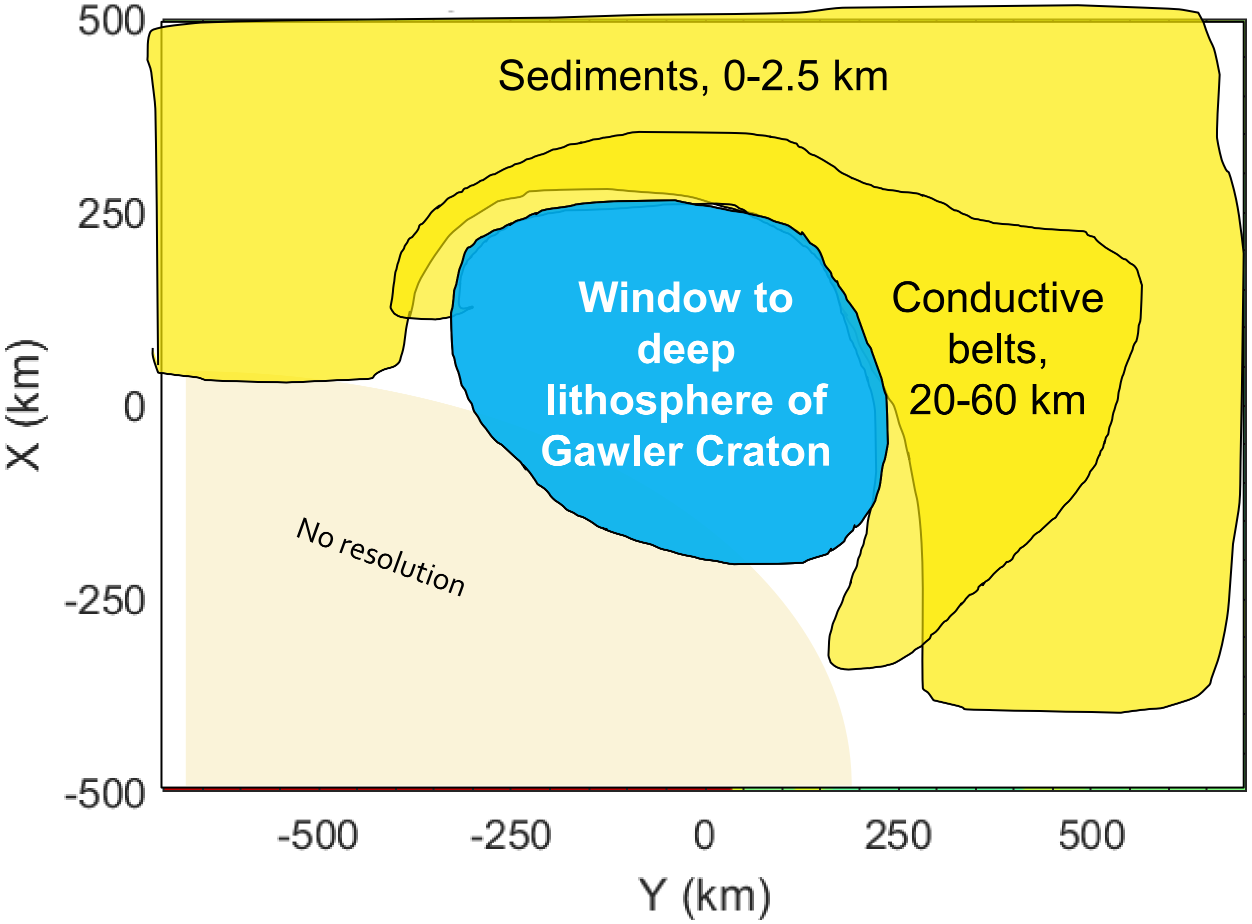

Depth of Lithosphere – Asthenosphere boundary

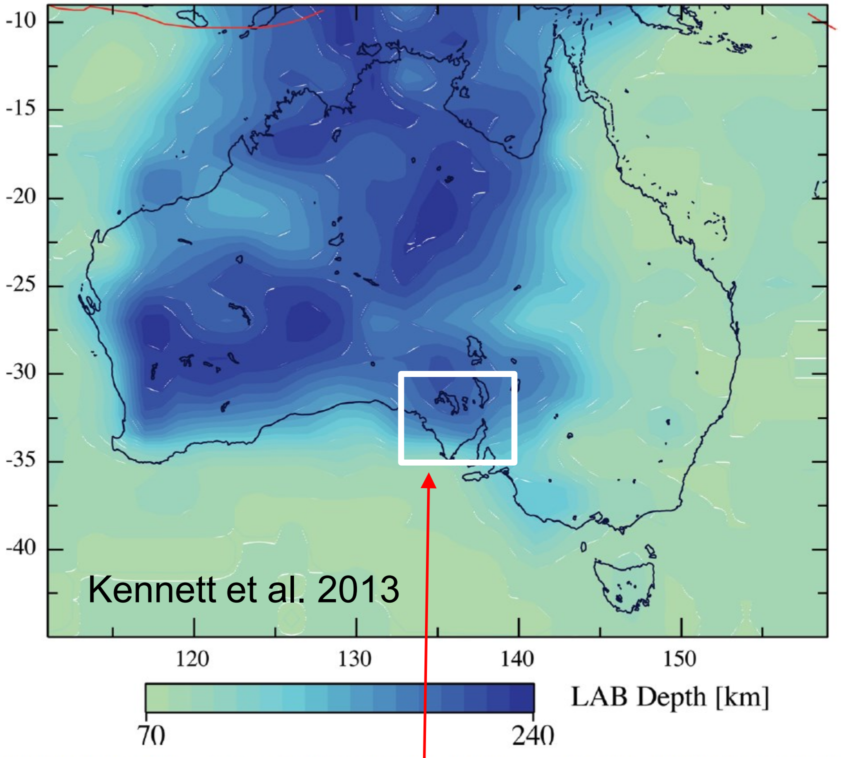

Depth of LAB in survey area up to 250 km

Electric anisotropy at the base of the Gawer Craton (base of the lithosphere)

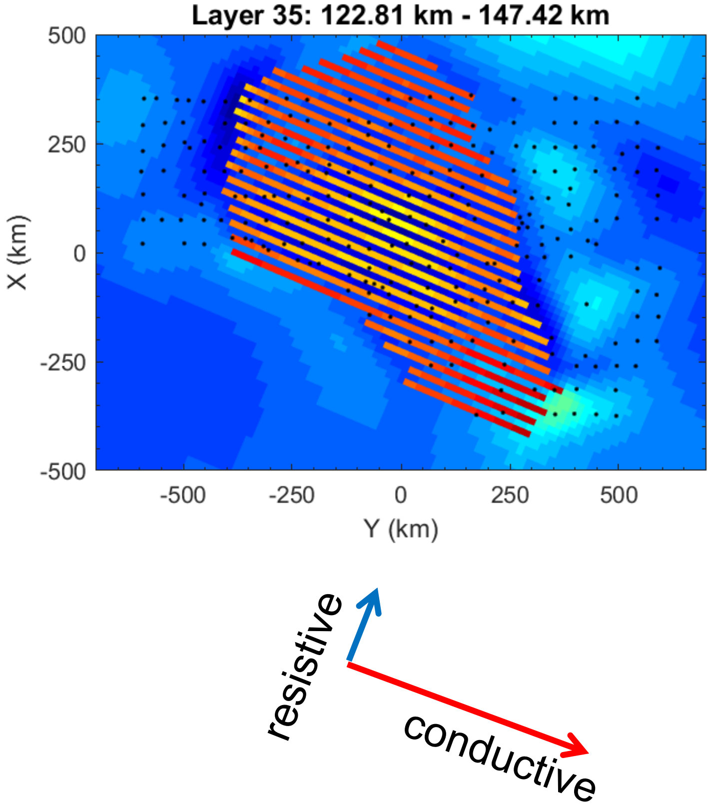

Anomalous shear wave velocities (modified from Simons et al. 2002)

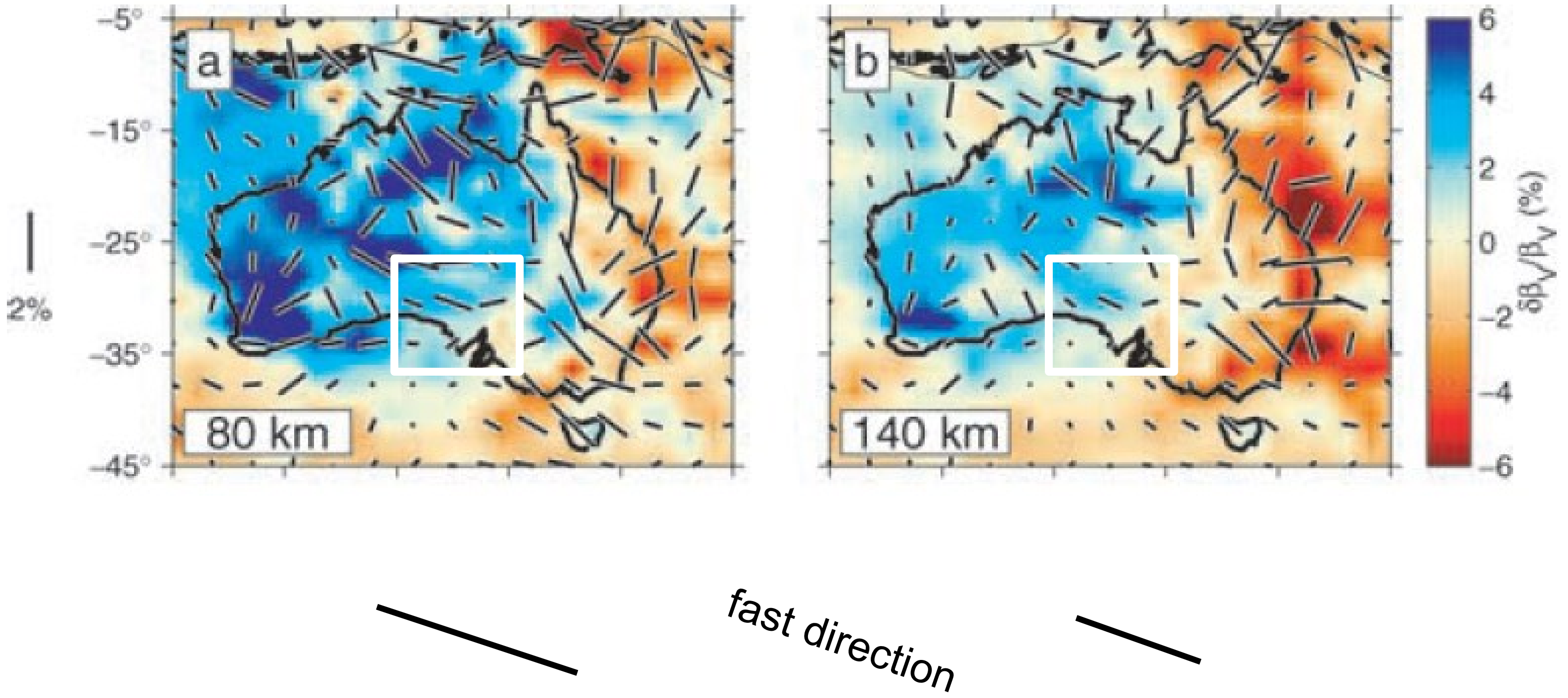

Electrically conductive direction
parallel to fast direction of shear waves.
☺

Slice on electrical anisotropy

Origin of the electric anisotropy

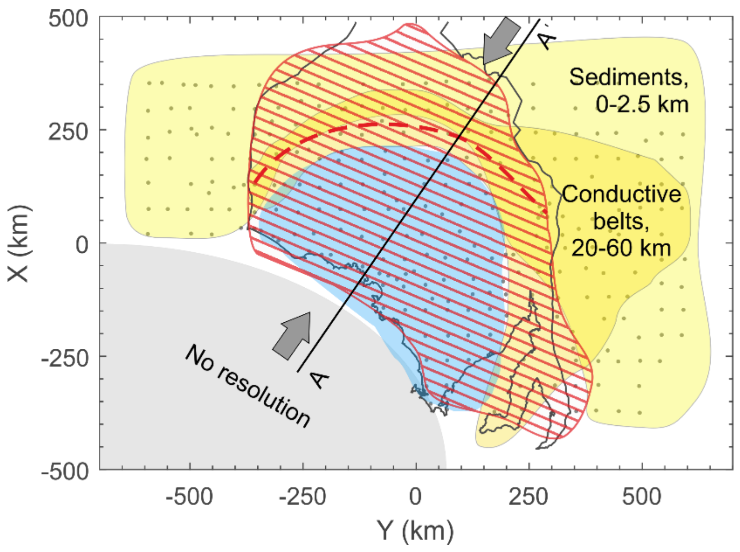

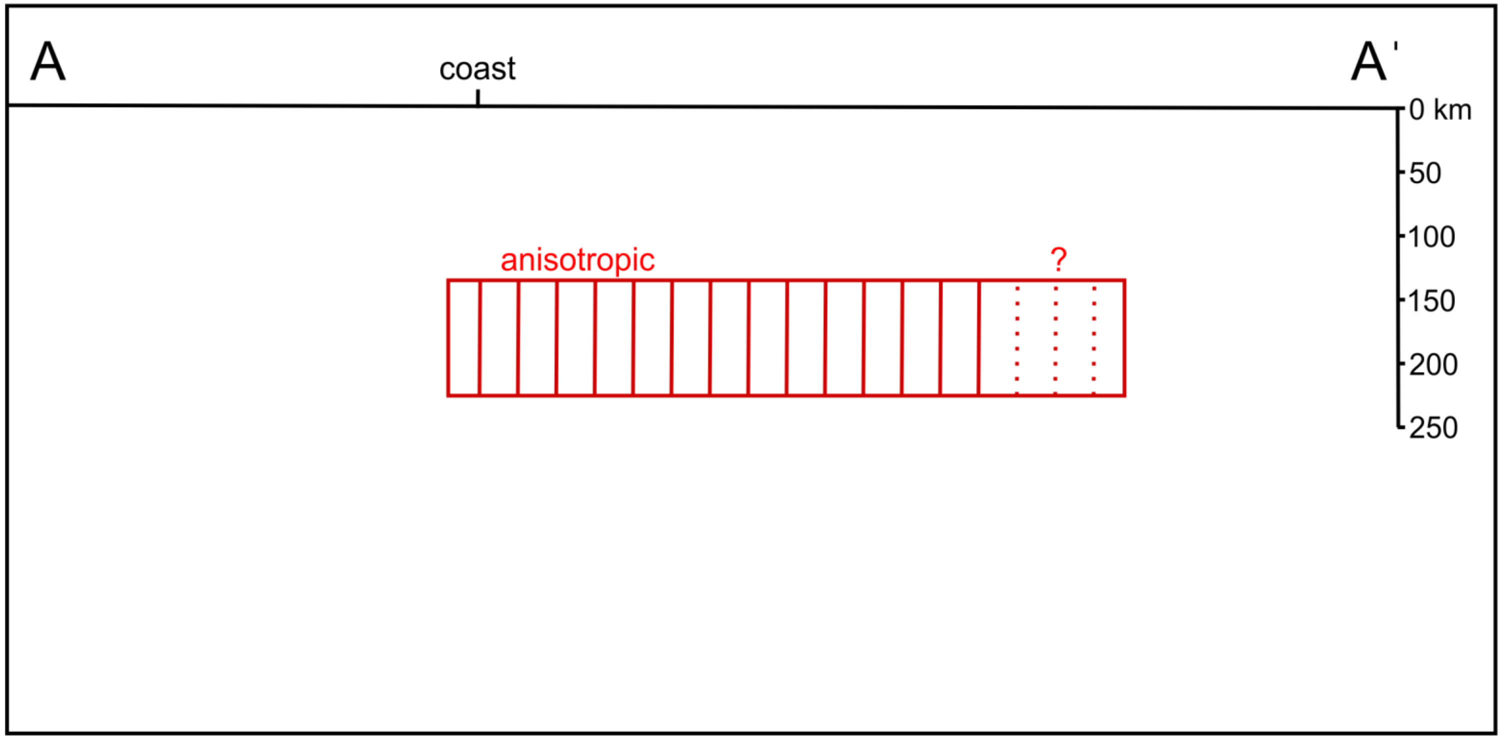

Origin of the electric anisotropy

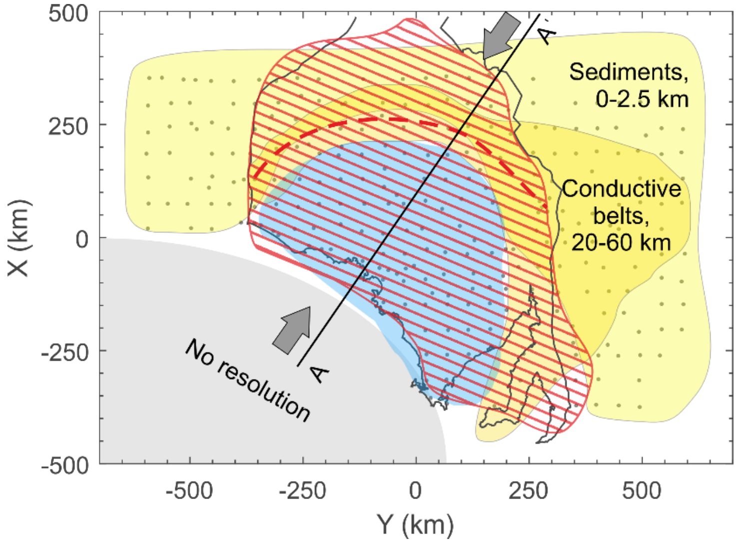

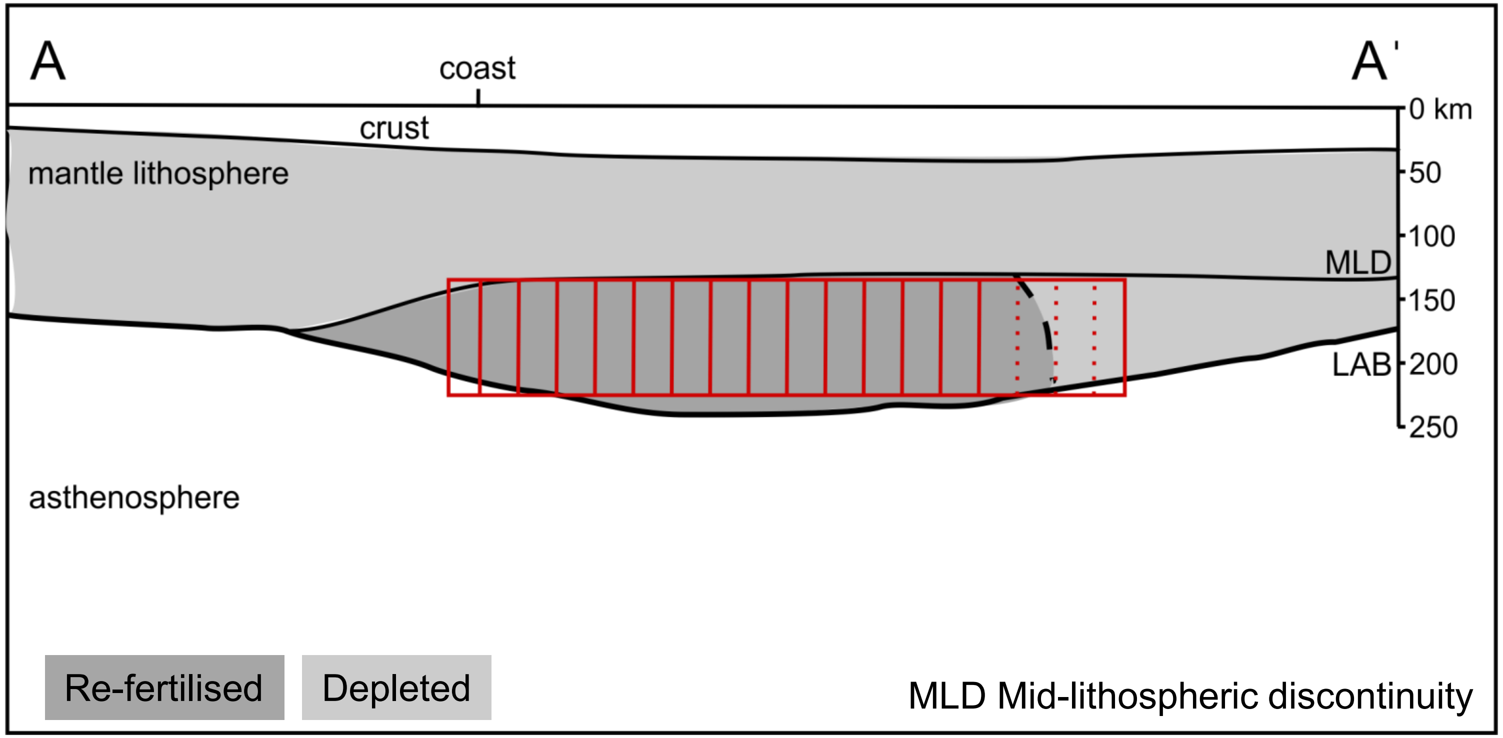

Interpretation based on Skirrow et al. (2018)

3) Implications for deep lithosphere of the Gawler Craton?

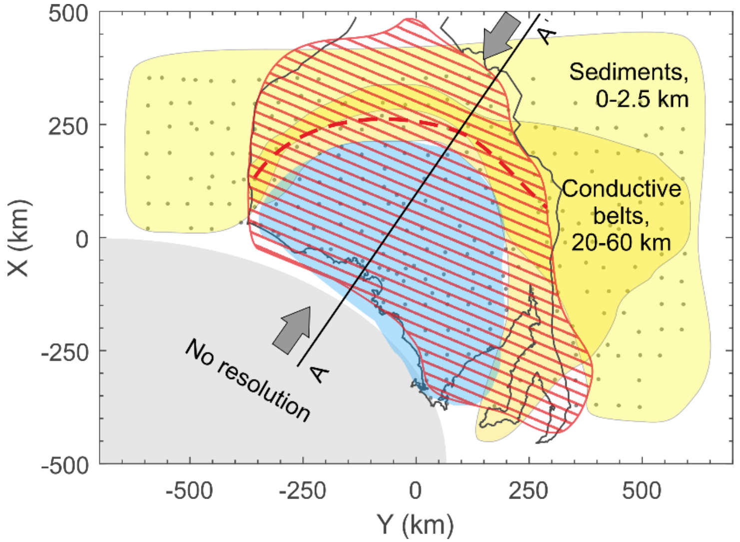

Lattice-preferred orientation of olivine, max. anisotropy 1:10

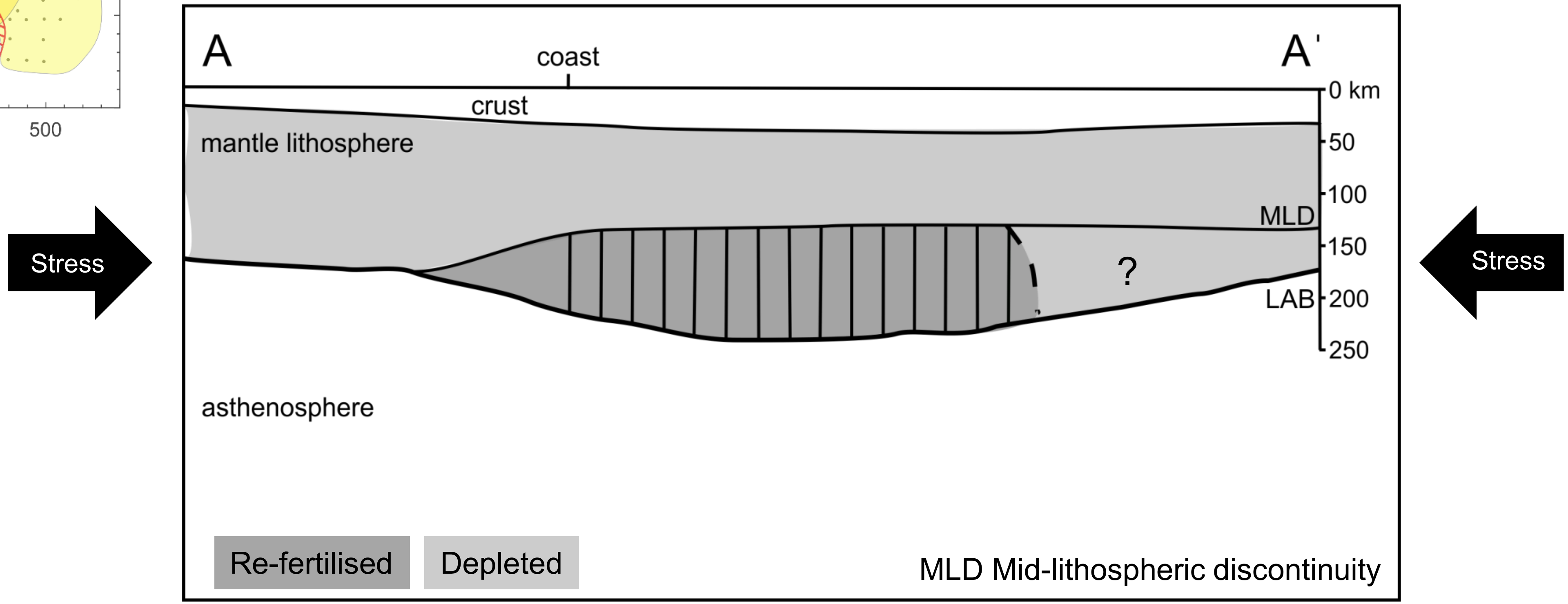

Interpretation based on Skirrow et al. (2018)

Origin of the electric anisotropy

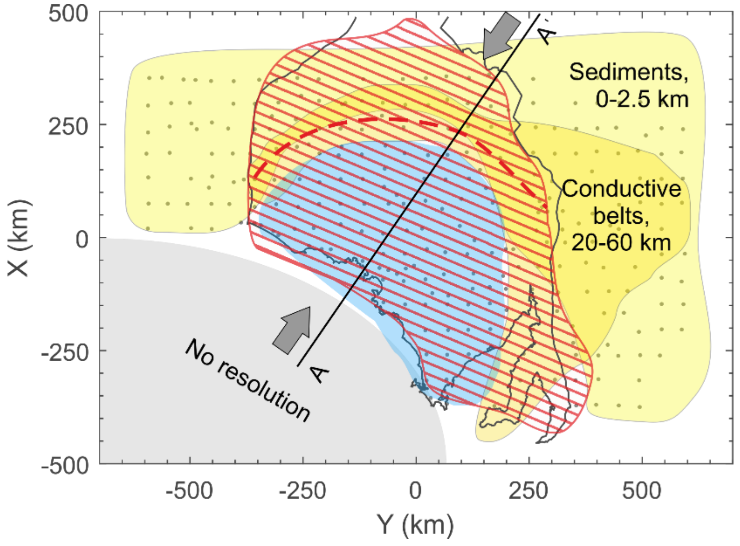

Lattice preferred orientation of olivine, max. anisotropy 1:10

+ Subduction-related metasomatism, preferentially along aligned cracks

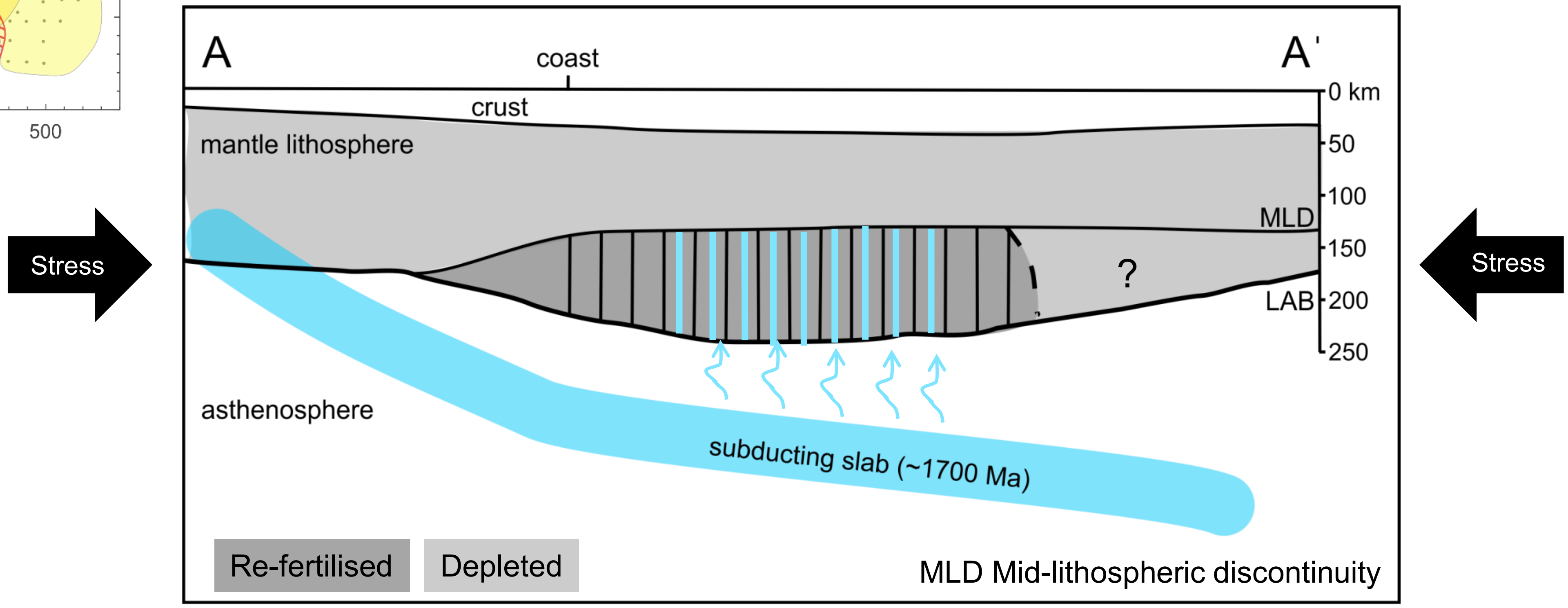

Interpretation based on Skirrow et al. (2018)

Summary

Gawler Craton

- Electrically anisotropic base of Gawler Craton
- Origin: Metasomatism along aligned cracks
  (+ lattice-preferred orientation of olivine crystals)

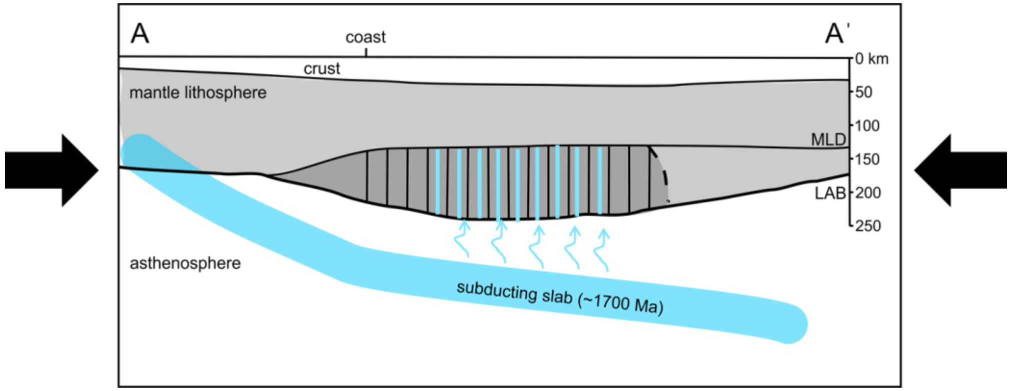

MT

- can be able to look into the deepest parts of the lithosphere (which can be ~300 km in cratonic areas)
- conductivity can be anisotropic,
  probably required in 10-20 % of cases, but this probably also depends on whom you ask
- BUT: MT **cannot** discriminate between macroscopic and intrinsic anisotropy, way beyond resolution

Mineral exploration,

Imaging mineral systems from source to sink

SCIENTIFIC REPORTS

OPEN

The crustal geophysical signature of a world-class magmatic mineral system

Received: 29 January 2018
Accepted: 2 July 2018
Published online: 13 July 2018

Graham Heinson[1], Yohannes Didana[1], Paul Soeffky[1], Stephan Thiel[1,2] & Tom Wise[2]

World-class magmatic mineral systems are characterised by fluid/melt originating in the deep crust and mantle. However, processes that entrain and focus fluids from a deep-source region to a kilometre-scale deposit through the crust are unclear. A magnetotelluric (MT) and reflection seismic program across the margin of the Gawler Craton, Australia yield a distinct signature for a 1590 Ma event associated with emplacement of iron-oxide copper gold uranium (IOCG-U) deposits. Two- and three-dimensional MT modelling images a 50 km wide lower-crustal region of resistivity $<10\,\Omega$m along an accreted Proterozoic belt. The least resistive (~1 Ωm) part terminates at the brittle-ductile transition at ~15 km, directly beneath a rifted sedimentary basin. Above the brittle-ductile transition, three narrow low-resistivity zones (~100 Ωm) branch to the surface. The least resistive zone is remarkably aligned with the world-class IOCG-U Olympic Dam deposit and the other two with significant known IOCG-U mineral occurrences. These zones are spatially correlated with narrow regions of low seismic reflectivity in the upper crust, and the deeper lower-crust conductor is almost seismically transparent. We argue this whole-of-crust imaging encapsulates deep mineral system and maps pathways of metalliferous fluids from crust and mantle sources to emplacement at discrete locations.

Overview of geology and MT site layout

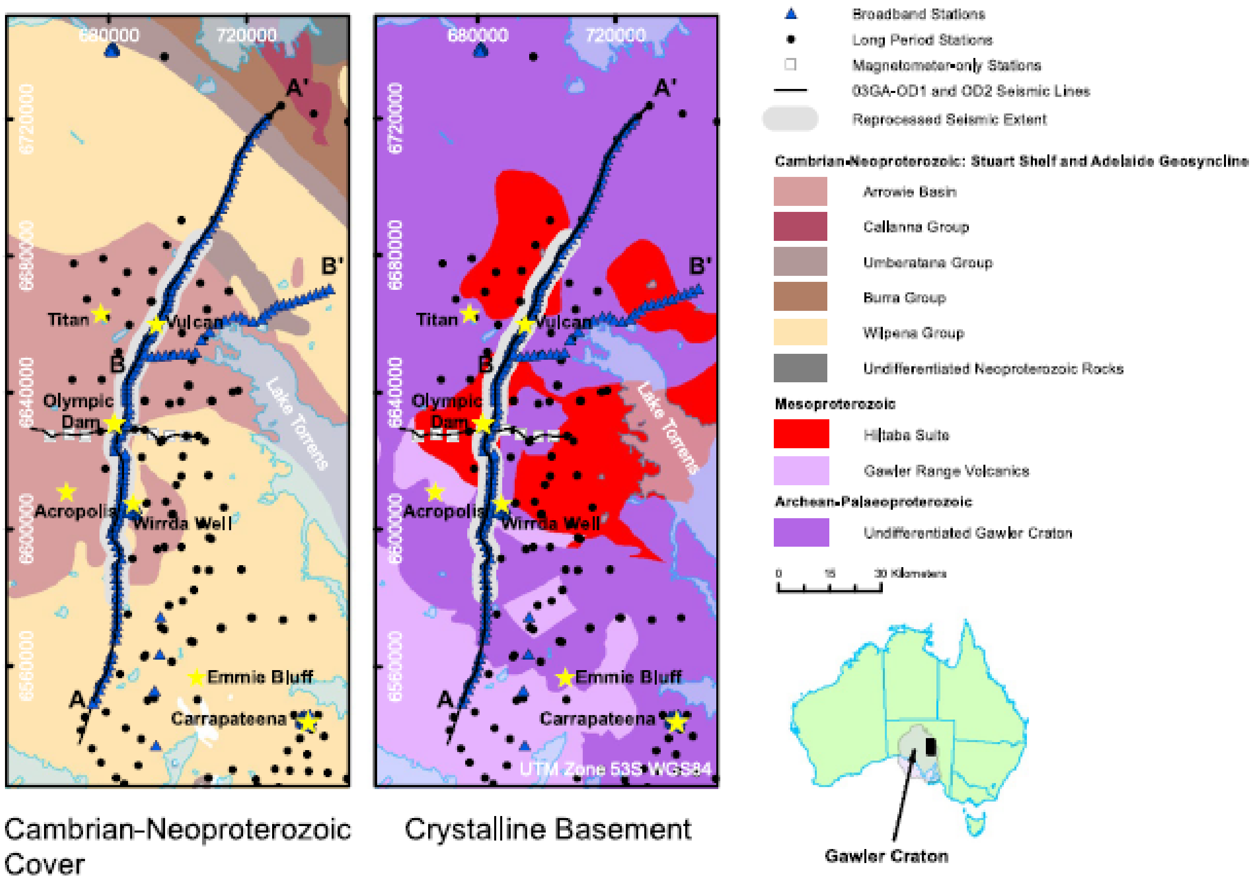

Figure 1. Location map of the survey area showing Neoproterozoic-Cambrian sedimentary cover (left hand side); crystalline basement geology (right hand side). Yellow stars are major mines and mineral occurrences: most notable along the transect are Acropolis-Wirrda Well; Olympic Dam; and Vulcan-Titan. Carapateena is a major IOCG-U mineral deposit under development as a new mine. Blue triangles show broadband MT sites; black circles show long period MT sites; and white squares show magnetometer-only sites. The black lines (03GA-OD1 and OD2) are the original seismic reflection transects[16], and the reprocessed section is shown by the wider grey band[17]. Figure 1 maps were created using ArcGIS 10.3.1 software (https://www.esri.com/arcgis/about-arcgis).

Research questions

World-class magmatic ore systems are often characterised by fluids/melts that are derived from deep lithosphere, mostly located at the margins of ancient craton.

There is, however, debate about the source of metals, and how they migrate from deep crust and upper mantle to focus as kilometre-scale deposits in the upper crust.

MT parameters

- 200 km long transect centred at Olympic dam
- 5/10 km site spacing
- Periods of 10^{-3} to 10^{3} s

Electrical resistivity model (2D)

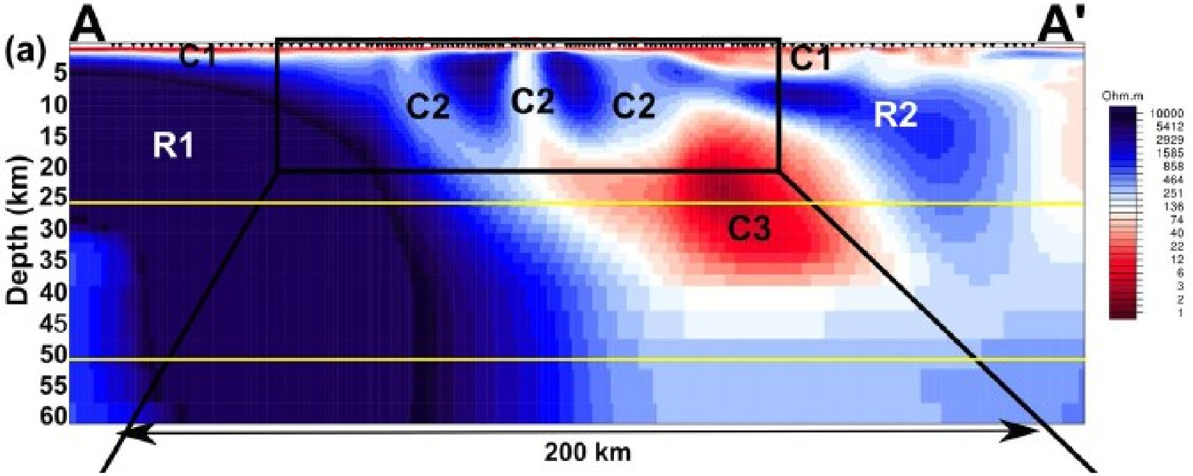

Figure 2. (**a**) 2D resistivity model of Profile A-A' to a depth of 60 km. (**b**) The central part of the profile is expanded to a depth of 20 km. The Archean Gawler Craton on the left-hand side, and Proterozoic mobile belt on the right-hand side are characterized by very high resistivity (blue colour, R1 and R2) to a depth of more than 60 km. A striking high conductivity structure (C3) is situated at the margins of the Archean Gawler Craton at a depth 15–40 km in the mid to lower crust. In addition, three narrow low-resistivity pathways (C2) extend from conductor C3 to the surface, which link the lower crust with major IOCG-U mineral deposits. (**c**) 2D Seismic depth converted image[17] showing zones of reduced reflectivity (C2 and C3) under all major mineral deposits. WW, OD and VC denote the major occurrences at Wirrda Well, Olympic Dam and Vulcan, respectively as shown in Fig. 1.

Electrical resistivity model (2D)

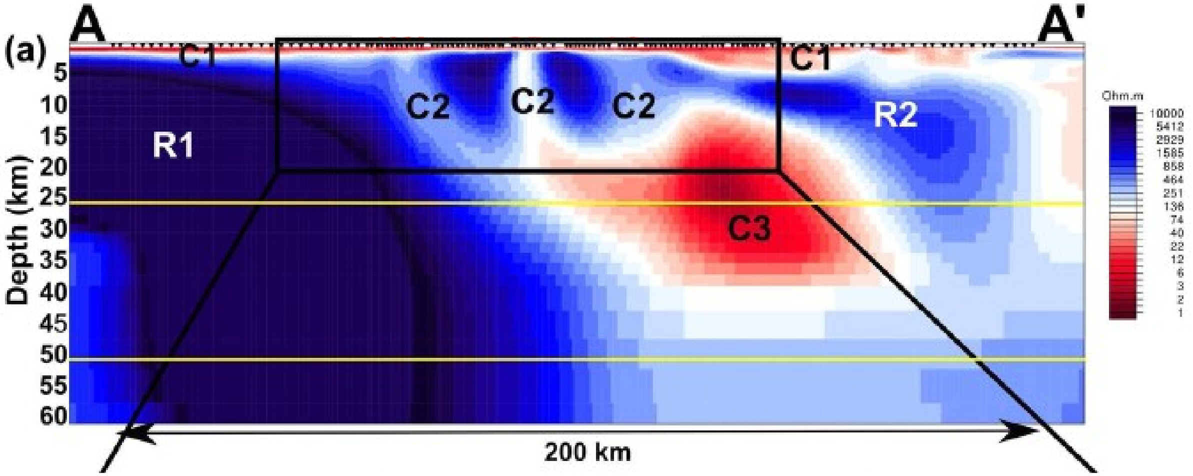

- C1: conductive surface layer = sediments
- R1/R2: resistive craton / crust
- C3: coincident with low seismic reflectance → rheologically weak
- C2: three narrow, low-resistive (well conductive) pathways extending from top of conductor to the base of C1
  - remarkable correlation with major IOCG-U deposits
  - not spacially aligned with significant mapped crustal faults
  - = paths of crustal fluids from a lower-crustal source

Figure 2. (**a**) 2D resistivity model of Profile A-A' to a depth of 60 km. (**b**) The central part of the profile is expanded to a depth of 20 km. The Archean Gawler Craton on the left-hand side, and Proterozoic mobile belt on the right-hand side are characterized by very high resistivity (blue colour, R1 and R2) to a depth of more than 60 km. A striking high conductivity structure (C3) is situated at the margins of the Archean Gawler Craton at a depth 15–40 km in the mid to lower crust. In addition, three narrow low-resistivity pathways (C2) extend from conductor C3 to the surface, which link the lower crust with major IOCG-U mineral deposits. (**c**) 2D Seismic depth converted image[17] showing zones of reduced reflectivity (C2 and C3) under all major mineral deposits. WW, OD and VC denote the major occurrences at Wirrda Well, Olympic Dam and Vulcan, respectively as shown in Fig. 1.

Electrical resistivity model (2D)

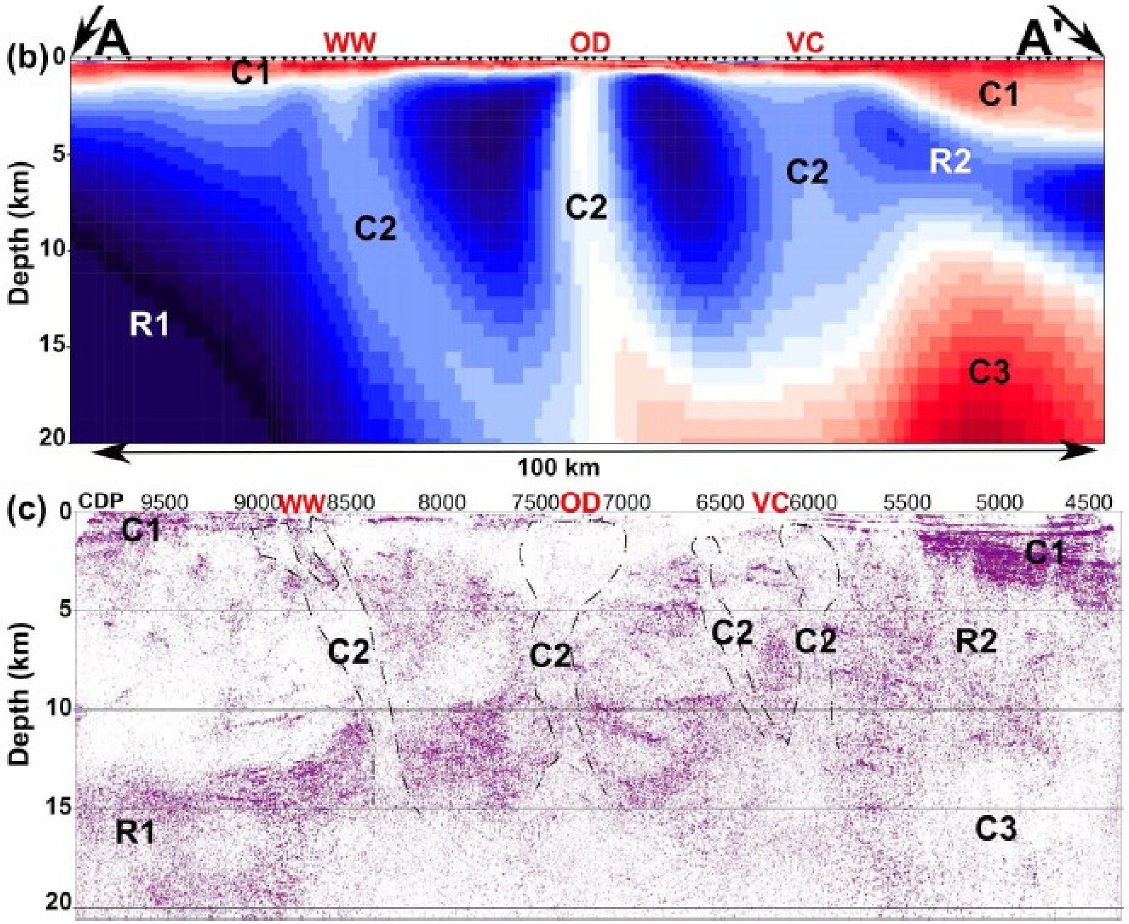

- C1: conductive surface layer = sediments
- R1/R2: resistive craton / crust
- C3: coincident with low seismic reflectance → rheologically weak
- C2: three narrow, low-resistive (well conductive) pathways extending from top of conductor to the base of C1, remarkable correlation with major IOCG-U deposits

Electric resistivity model (3D)

- To complete the study, 3D modelling was performed on an array like MT data set across the Olympic Dam deposit.
- C3 is imaged consistently with the 2D model.
- → 2D interpretation confirmed (no distortion because 2D approach was applied to 3D subsurface)
- → C3 limited horizontally and vertically

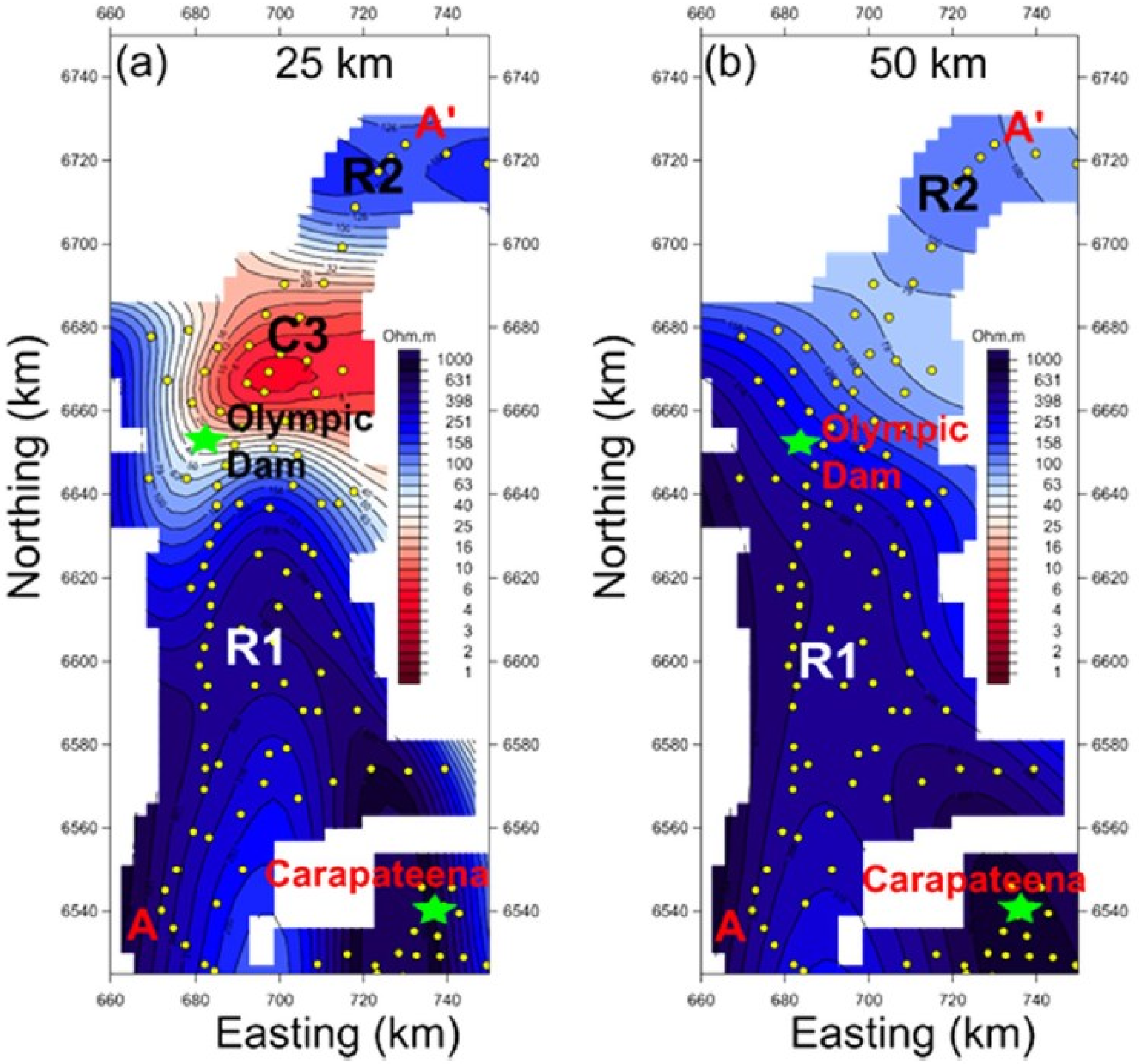

Figure 3. 3D resistivity maps at depths of (a) 25 km (b) 50 km reveal that most of the Archean Gawler Craton in the south west is characterized by high resistivity structure in the lower crust. At 25 km depth, low resistivity is imaged to the north-east of the Olympic Dam deposit. C3 is a low resistivity zone and R1, R2 are high resistivity zones associated with the Archean Gawler Craton and Proterozoic mobile belt, as shown in Fig. 2.

Summary

- At Olympic Dam, MT imaged the pathways of fluids from lower crustal to deposit depth
- MT can be used to look for footprints of mineral systems to identify new potentials
- There is other studies where MT was used to map the actual deposit (e.g. in Canada), but that is much harder. Deposits have to be large enough etc. to be mapped with MT

Geothermal exploration

Geophys. J. Int. (2008) **173**, 740–750

doi: 10.1111/j.1365-246X.2008.03737.x

Three-dimensional modelling of magnetotelluric data from the Rotokawa geothermal field, Taupo Volcanic Zone, New Zealand

W. Heise, T. G. Caldwell, H. M. Bibby and S. C. Bannister

GNS Science, 1, Fairway Drive, PO Box 30368, *Lower Hutt, New Zealand. E-mail: w.heise@gns.cri.nz*

DC apparent resistivity maps and location

→ Spatial correlation between low resistivities at surface and high heatflow.

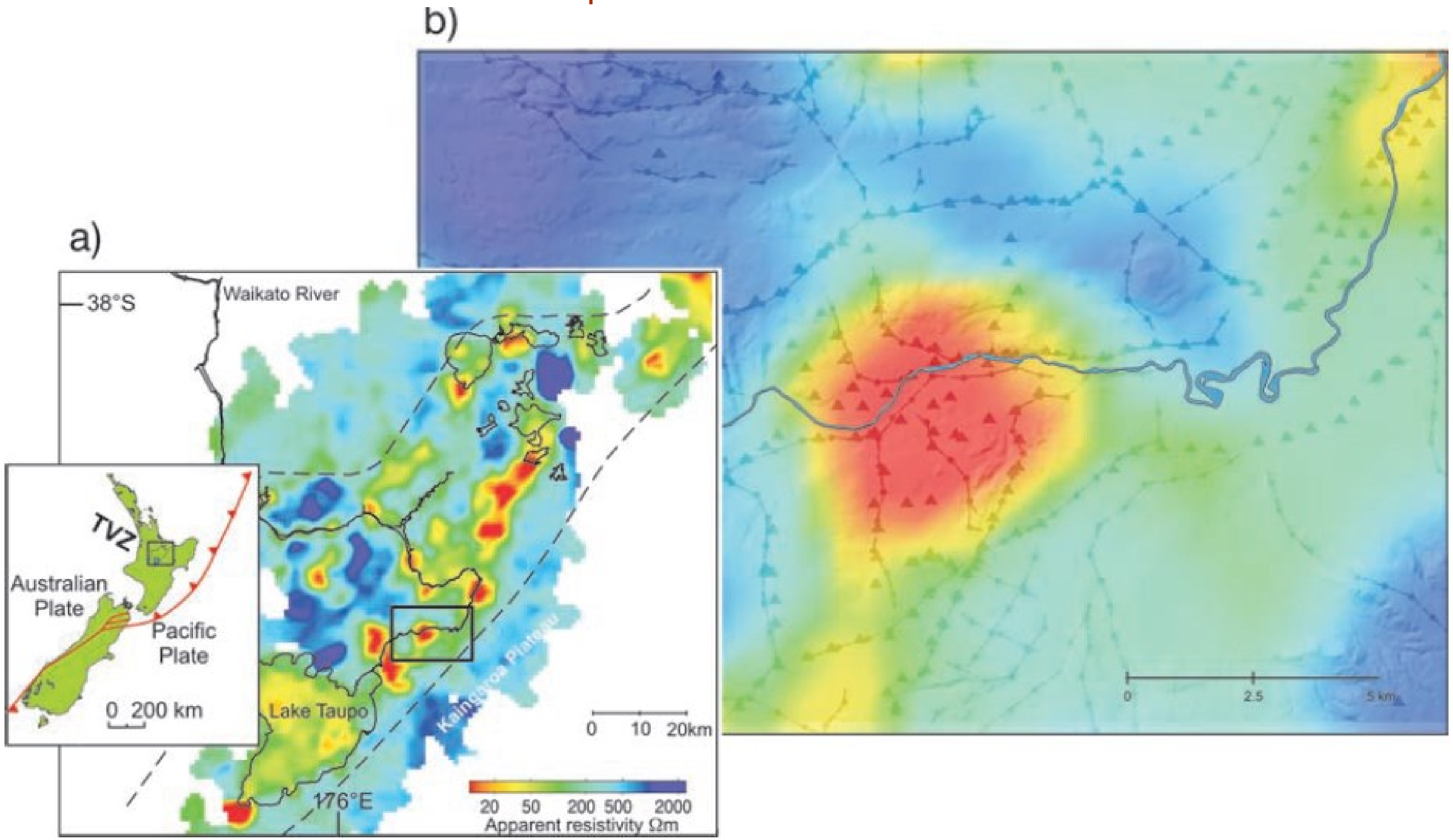

Figure 1. (a) DC apparent resistivity map from Bibby *et al.* (1995). Dashed lines show the approximate outline of the TVZ in the area containing (mainly rhyolitic) volcanism <2-Ma old. Conductive areas shown in red (<30 Ωm) mark the geothermal systems. (b) Schlumberger apparent resistivity map made with an electrode spacing of (AB/2) 500 m of the Rotokawa area. Background symbols show DC apparent resistivity measurement sites (Bibby 1988).

MT data and inversion response

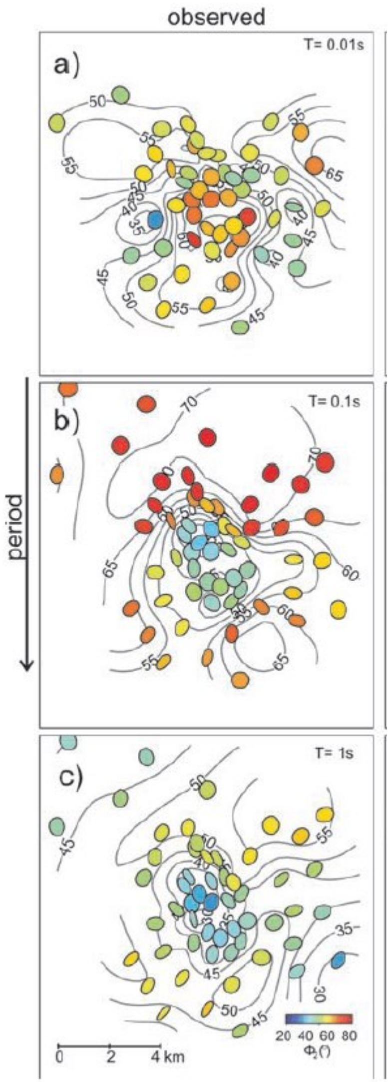

Vertical section through the resistivity model with thermal model

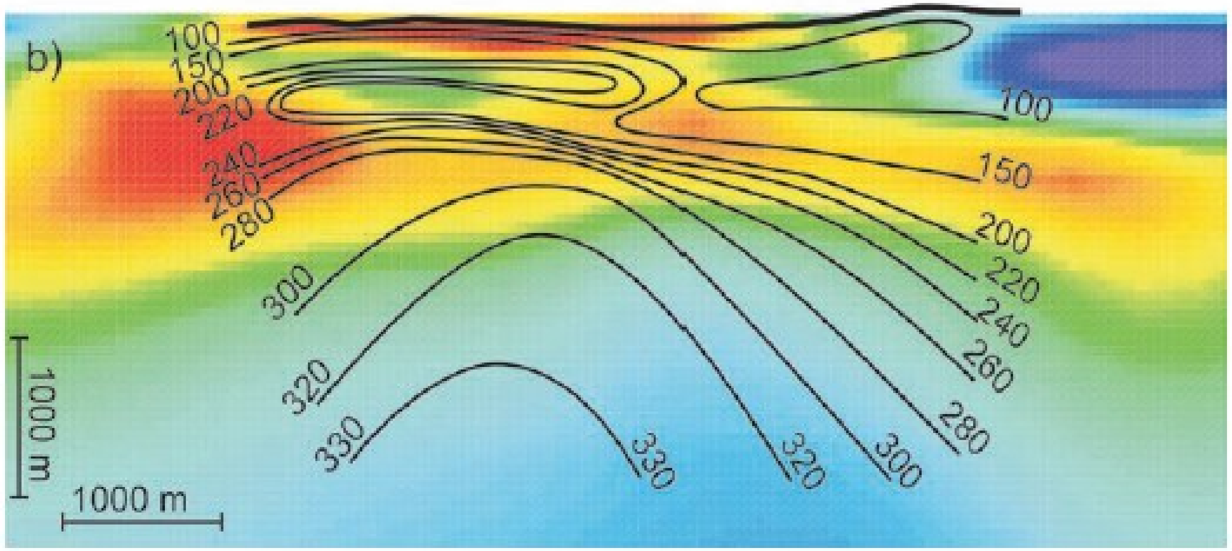

Figure 6. Resistivity section through the centre of the geothermal system (a) forward model; (b) inverse model. Isotherms, interpolated from wells measurements, show the temperature distribution inside the geothermal system. The complicated temperature structure of the near surface may partly reflect the reinjection of wastewater in the top 500 m. In the northern part the low temperatures (<100 °C) at ~500 m depth can be explained by an inflow of cold water from the resistive rhyolite dome north of the geothermal system. At depth the higher resistivity corresponds to temperatures >250 °C.

Colorbar missing!

Horizontal slices and 3D cube

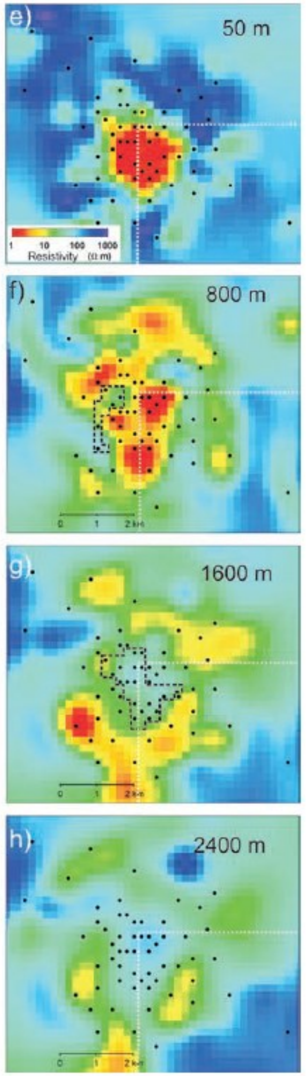

3D cube

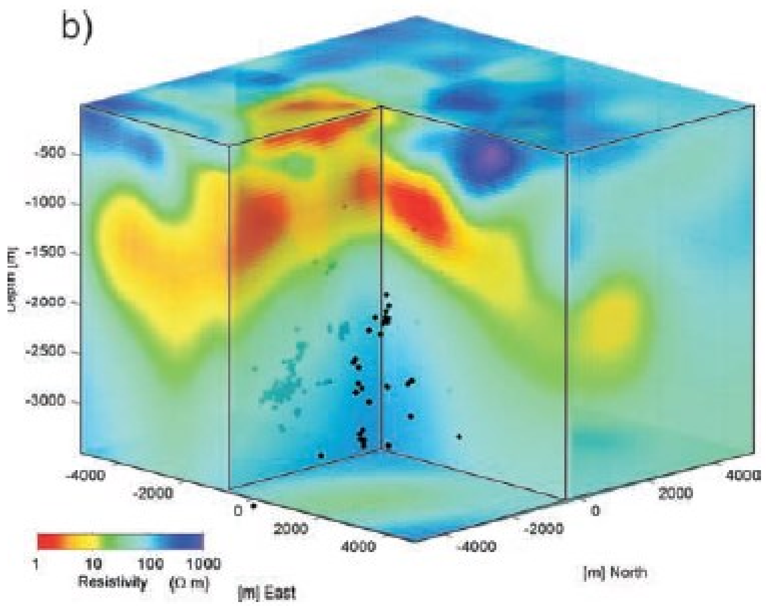

Interpretation and summary

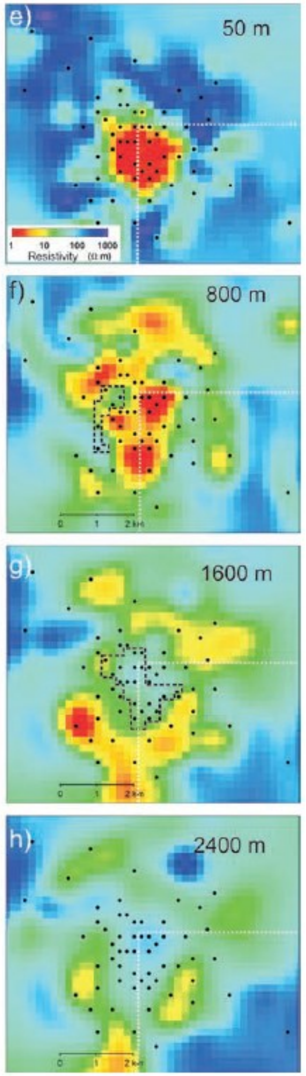

Inflow of fresh water

3D cube

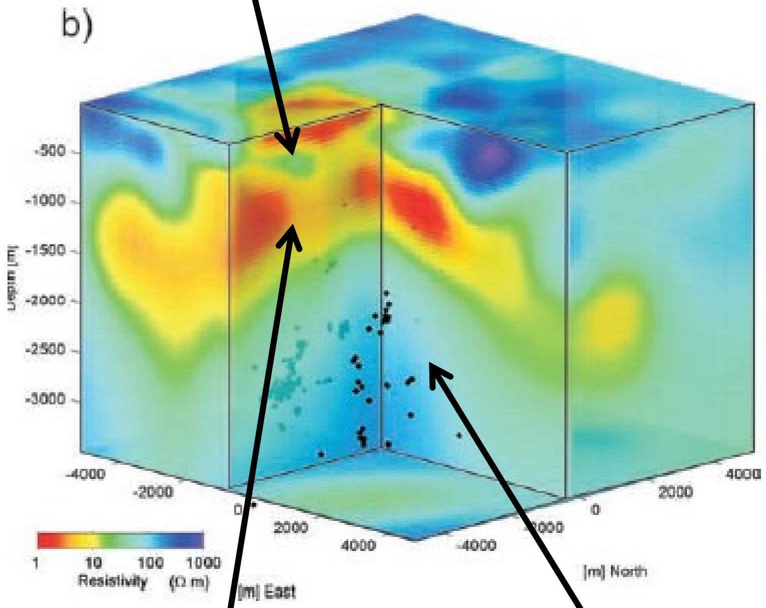

Low temperature (<250°C)
clay minerals (smectite)
+ high porosity
→ Low resistivities

High temperature (>250°C)
clay minerals (illite, chlorite)
+ lower porosity
→ High resistivities

Today’s journey

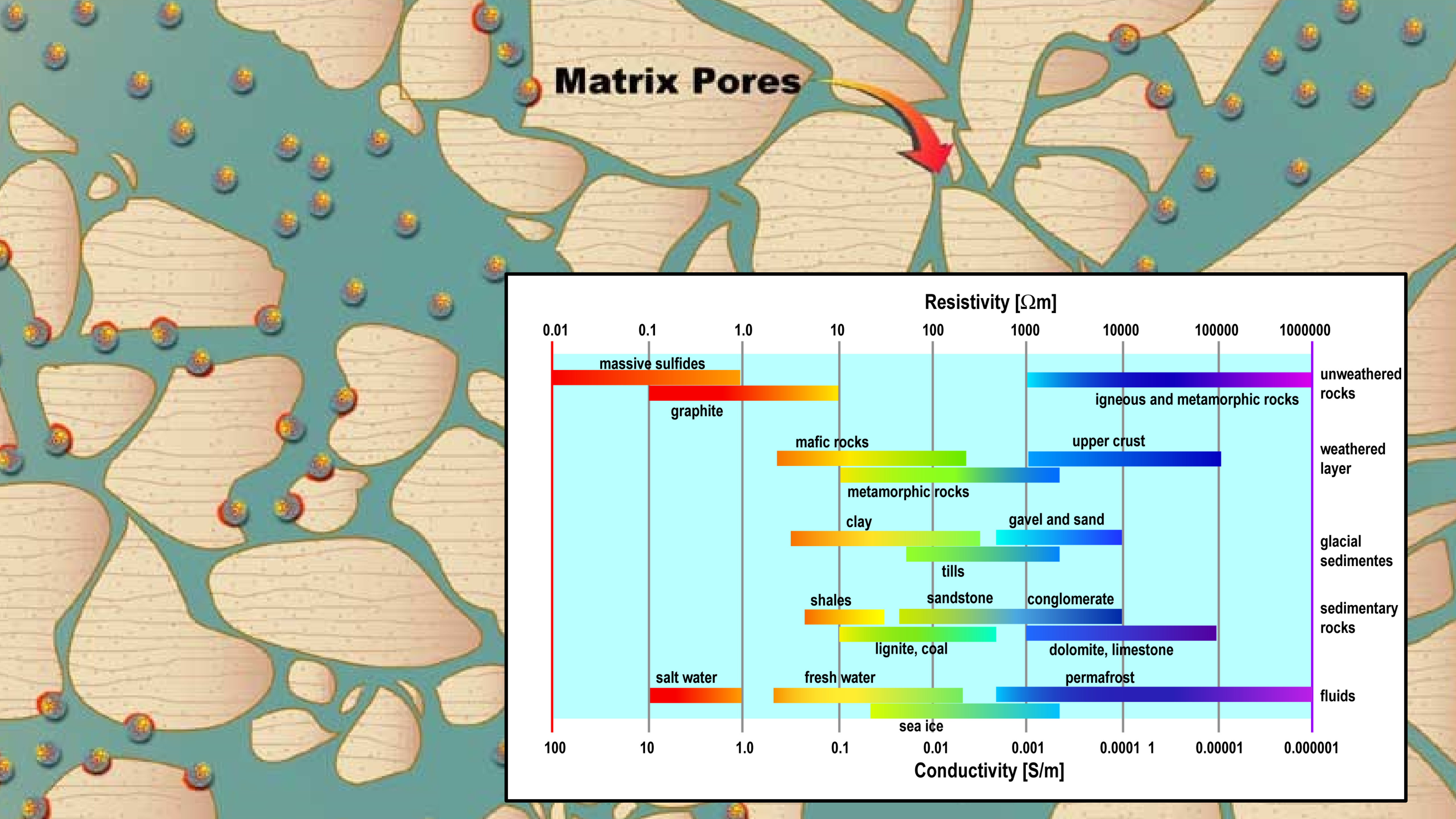
Matrix Pores
Resistivity [Ωm]
0.01
0.1
1.0
10
100
1000
10000
100000
1000000
massive sulfides
graphite
unweathered rocks
igneous and metamorphic rocks
mafic rocks
upper crust
weathered layer
metamorphic rocks
clay
gavel and sand
glacial sedimentes
tills
shales
sandstone
conglomerate
sedimentary rocks
lignite, coal
dolomite, limestone
salt water
fresh water
permafrost
fluids
sea ice
100
10
1.0
0.1
0.01
0.001
0.0001 1
0.00001
0.000001
Conductivity [S/m]

$$p = \sqrt{\frac{2}{\omega\mu_0\sigma}} \approx \frac{1}{2}\sqrt{\rho T}\ [km]$$

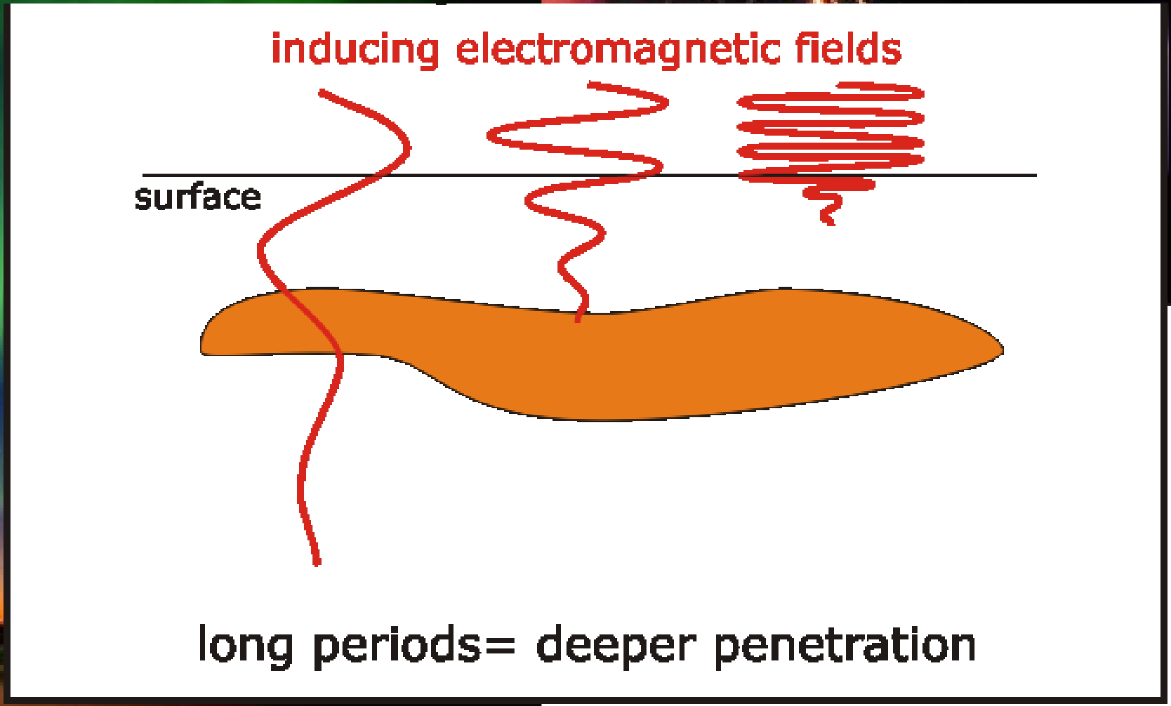

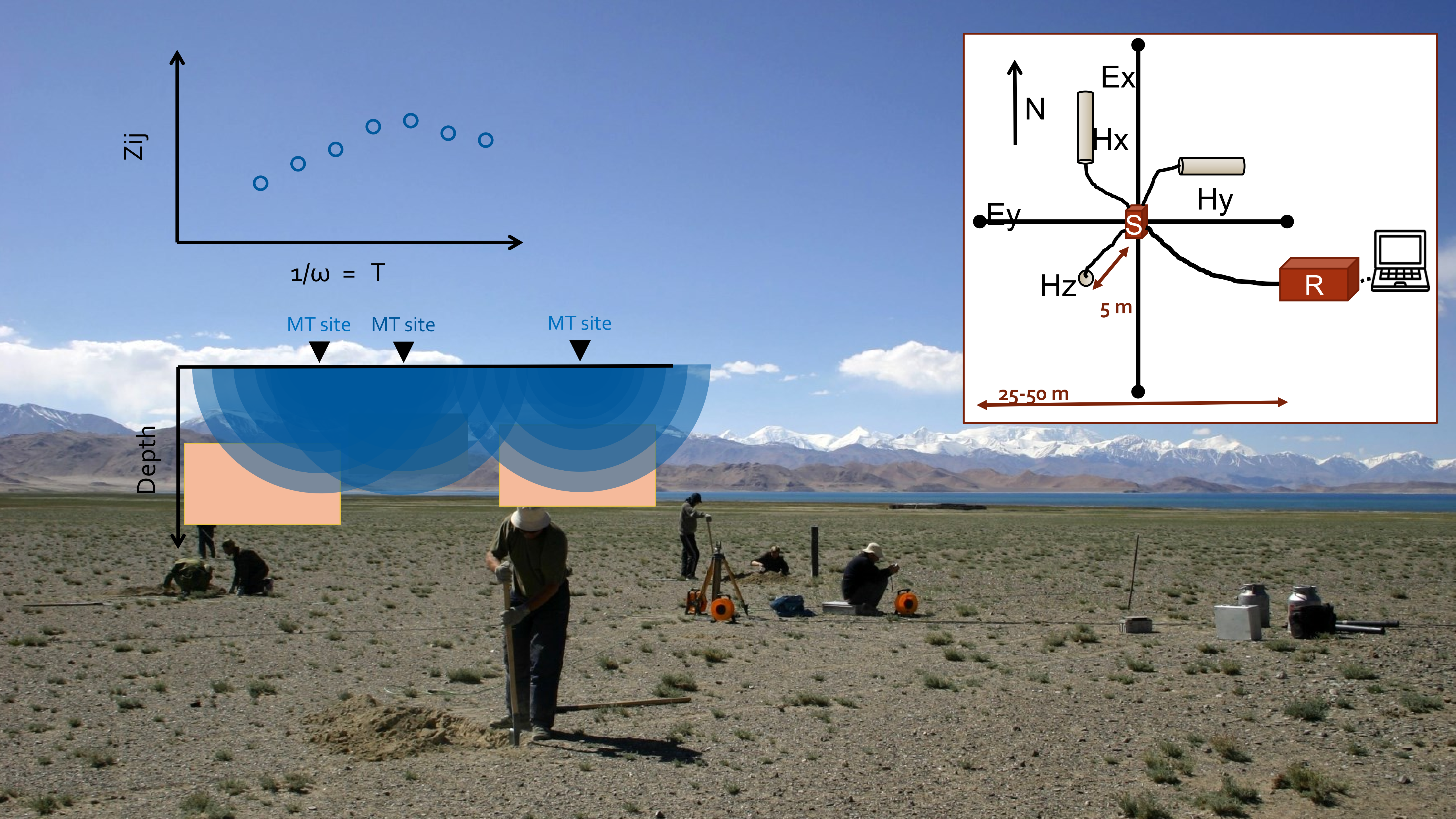
Zij
1/ω = T
MT site
MT site
MT site
Depth
N
Ex
Hx
Hy
Ey
S
Hz
5 m
R
25-50 m

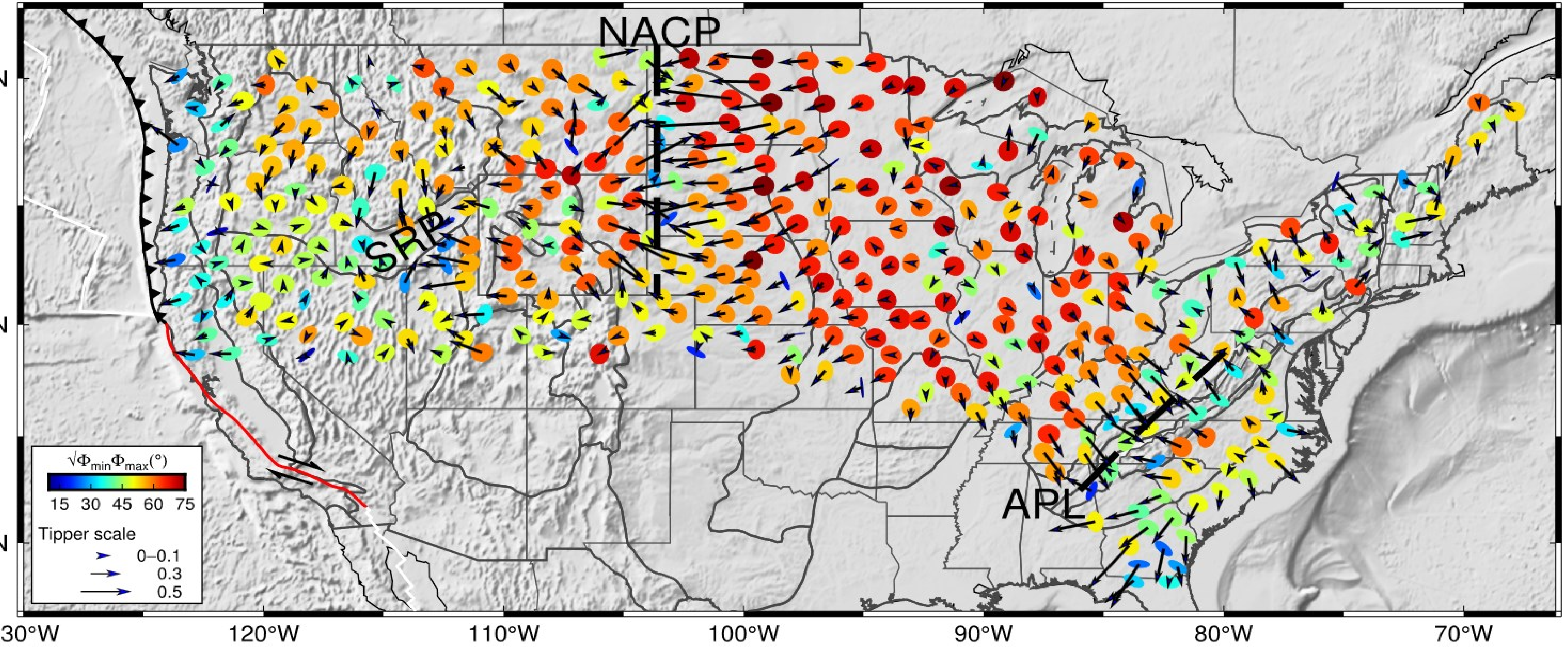

NACP
SRP
APL
48°N
40°N
32°N
130°W
120°W
110°W
100°W
90°W
80°W
70°W
$\sqrt{\Phi_{min}\Phi_{max}}(°)$
15 30 45 60 75
Tipper scale
0–0.1
0.3
0.5

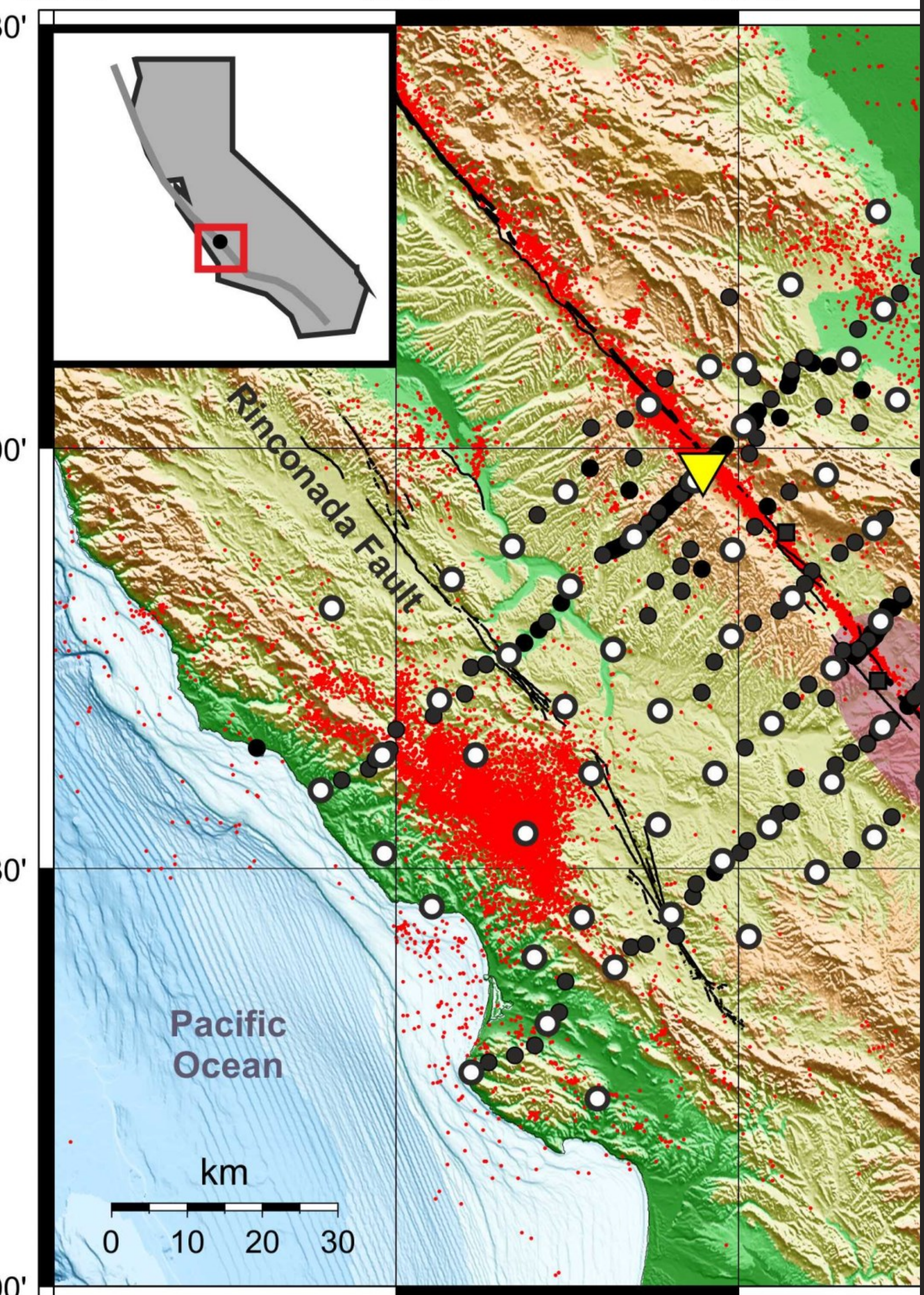
Rinconada Fault
Pacific Ocean
km
0 10 20 30

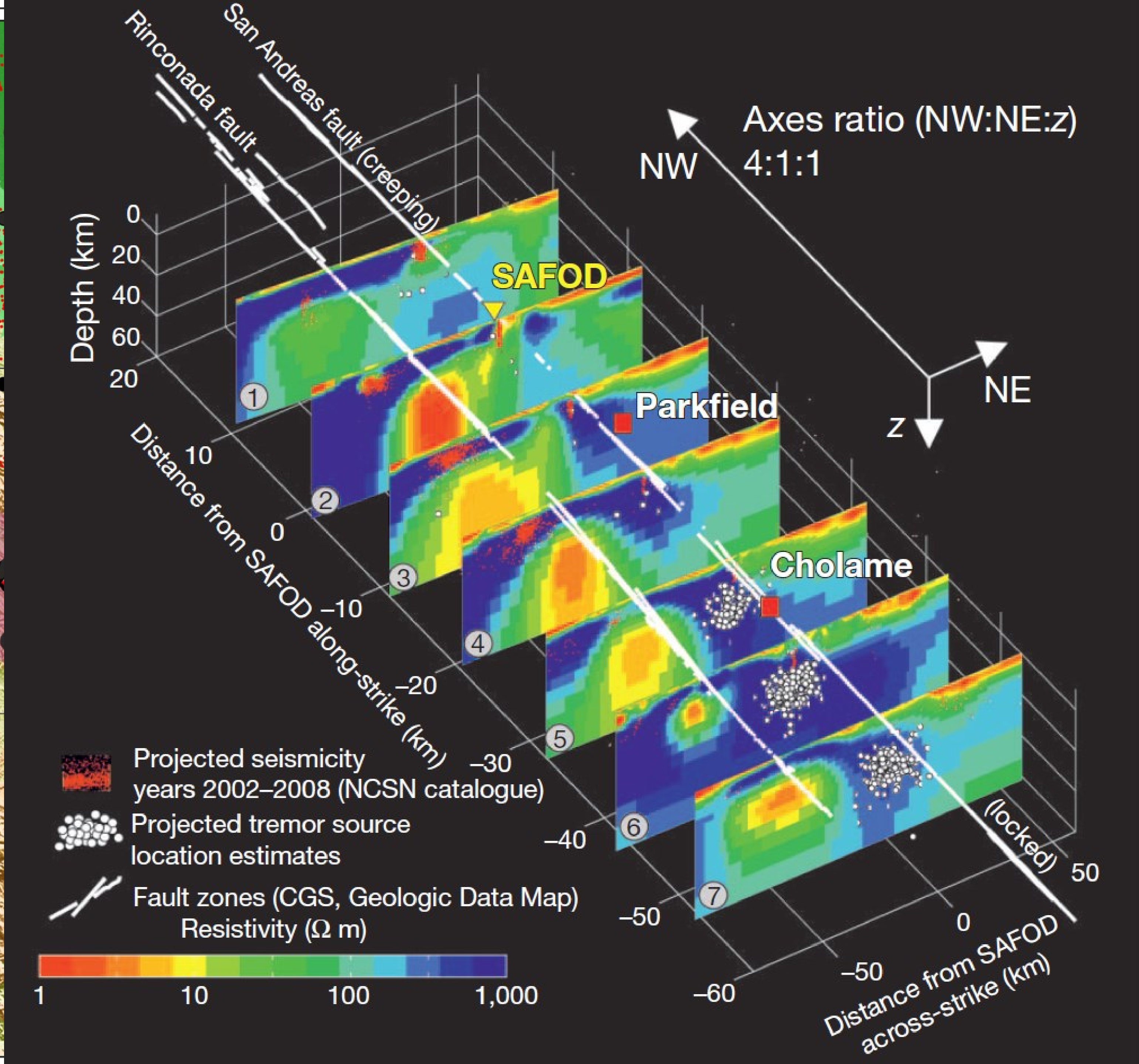
Rinconada fault
San Andreas fault (creeping)
Axes ratio (NW:NE:z)
4:1:1
NW
NE
z
Depth (km)
0
20
40
60
SAFOD
Parkfield
Cholame
(locked)
1
2
3
4
5
6
7
Distance from SAFOD along-strike (km)
20
10
0
−10
−20
−30
−40
−50
−60
Distance from SAFOD across-strike (km)
−50
0
50
Projected seismicity
years 2002–2008 (NCSN catalogue)
Projected tremor source
location estimates
Fault zones (CGS, Geologic Data Map)
Resistivity (Ω m)
1
10
100
1,000

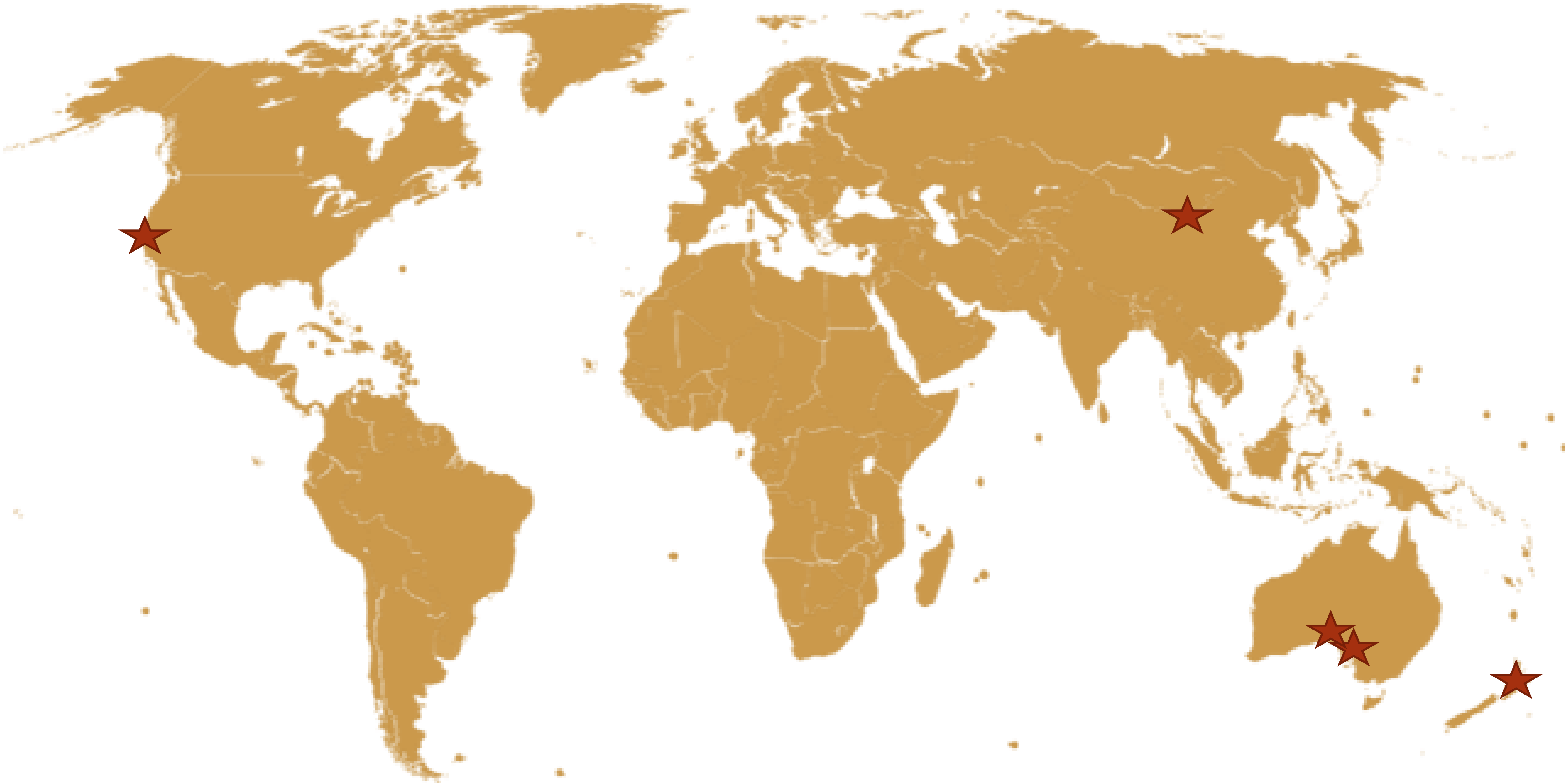

Magnetotellurics – what for?

- MT can be applied nearly everywhere on land and even in the sea
- MT works from near surface to the upper asthenosphere
- MT is best at imaging electrically conductive material
- Limitations:
  - Sensitive to conductance (thickness x conductivity)
  - Sensitive to high conductivities: MT probably won't miss conductive regions, but may miss particularly resistive regions.
  - Reality may be a bit less smooth than MT models (well, that's probably true for many methods)

- Which inferences can be made from MT models? What can MT provide for other methods?
  - Inferences on porosity, permeability, fluid fill, partial melt rate
  - Rheology, crustal strength
  - Imaging of fossil fluid pathways, mineralizations, hydrothermal alteration etc.

MT is best at imaging where fluids are and where they were.